

# **Using the OTIS Solute-Transport Model to Evaluate Remediation Scenarios in Cement Creek and the Upper Animas River**

By Katherine Walton-Day, Suzanne S. Paschke, Robert L. Runkel, and  
Briant A. Kimball

Chapter E24 of

**Integrated Investigations of Environmental Effects of Historical  
Mining in the Animas River Watershed, San Juan County, Colorado**

Edited by Stanley E. Church, Paul von Guerard, and Susan E. Finger

Prepared in cooperation with the  
U.S. Bureau of Land Management

Professional Paper 1651

**U.S. Department of the Interior  
U.S. Geological Survey**

# Contents

Abstract.....	979
Introduction.....	979
Purpose and Scope .....	980
Methods.....	982
Mass-Loading Studies .....	982
Solute-Transport Modeling with OTIS.....	982
Determination of Physical Parameters .....	983
Model Calibration for Conservative Solutes .....	984
Model Calibration for Reactive Solutes .....	984
Simulation of Remediation .....	985
OTIS Solute-Transport Modeling.....	985
Upper Cement Creek Subbasin .....	985
Determination of Physical Parameters and Boundary Conditions.....	987
Model Calibration for Simulation of the Bromide Tracer Profile.....	987
Model Calibration for Copper, Iron, and Zinc Simulations.....	988
Remediation Simulations .....	992
Lower Cement Creek Subbasin .....	994
Determination of Physical Parameters and Boundary Conditions.....	996
Model Calibration for Simulation of the Lithium Tracer Profile.....	996
Model Calibration for Copper, Iron, and Zinc Simulations.....	998
Remediation Simulations .....	1002
Simulation of the Effect of Changed Conditions at the Mogul Mine .....	1005
Animas River, Eureka to Howardsville.....	1008
Determination of Physical Parameters and Model Calibration for Simulation of the Chloride Tracer Profile .....	1010
Model Calibration for Zinc Simulations.....	1010
Remediation Simulations .....	1012
Animas River, Howardsville to Silverton .....	1014
Determination of Physical Parameters and Model Calibration for Simulation of the Chloride Tracer Profile .....	1016
Model Calibration for Zinc Simulations.....	1016
Remediation Simulations .....	1016
Significance of Metal Removal Processes in Cement Creek and the Upper Animas River.....	1019
Comparison of Remediation Using OTIS and a Mass-Loading Model.....	1021
Summary and Conclusions.....	1022
References Cited.....	1023
Appendix. Calibration of the Solute-Transport Model OTIS.....	1025
Determination of Physical Parameters .....	1025
Model Calibration for Conservative Solutes .....	1025
Model Calibration for Reactive Solutes .....	1027
Physical Parameters for OTIS Models.....	1027

## Figures

1.	Map showing location of study area and study reaches, Animas River watershed study area, Colorado.....	981
2.	Graph showing variation in dissolved bromide concentration with time at transport sites T1, T2, and T3, upper Cement Creek tracer injection, September 1999.....	983
3.	Map showing detail of upper Cement Creek study reach .....	986
4–7.	Graphs showing:	
4.	Upper Cement Creek, September 1999: variation in bromide concentration in synoptic samples, variation in streamflow discharge calculated from bromide concentrations in synoptic samples, distances corresponding to model reaches in calibrated OTIS model .....	988
5.	Upper Cement Creek, September 1999: variation in OTIS lateral-inflow concentrations and observed inflow concentrations for dissolved copper, iron, and zinc with distance from injection site.....	990
6.	Upper Cement Creek, September 1999: OTIS results for conservative and reactive simulations for dissolved copper, iron, and zinc .....	991
7.	Upper Cement Creek, September 1999: OTIS results for five remediation scenarios for dissolved copper, iron, and zinc .....	993
8.	Map showing detail of lower Cement Creek study reach.....	995
9–15.	Graphs showing:	
9.	Lower Cement Creek, September 1996: variation in lithium concentration in synoptic samples, variation in streamflow discharge calculated from lithium concentrations in synoptic samples, distances corresponding to model reaches in calibrated OTIS model .....	998
10.	Lower Cement Creek, September 1996: variation in OTIS lateral-inflow concentrations and observed inflow concentrations for filtered copper, total iron, and filtered zinc with distance from injection site .....	999
11.	Lower Cement Creek, September 1996: OTIS results for conservative and reactive simulations for filtered copper, total iron, and filtered zinc .....	1001
12.	Lower Cement Creek, September 1996: OTIS remediation simulations for filtered copper, total iron, and filtered zinc .....	1004
13.	Lower Cement Creek, September 1996: OTIS results for simulation of 1999 conditions in Cement Creek and South Fork Cement Creek.....	1006
14.	Gauge at mouth of Cement Creek (CC48): record of observed streamflow, filtered (0.45 $\mu\text{m}$ ) copper, total iron, and filtered (0.45 $\mu\text{m}$ ) zinc concentrations and filtered (0.1 $\mu\text{m}$ ) copper, total iron, and filtered (0.1 $\mu\text{m}$ ) zinc concentrations simulated for 1999 conditions using calibrated OTIS model.....	1007
15.	Lower Cement Creek, residual concentrations of copper and zinc at Cement Creek gauge versus time for regression models constructed using environmental data collected between 1996 and 2001 .....	1008
16.	Map showing detail of upper Animas River, Eureka to Howardsville study reach .....	1009
17–20.	Graphs showing:	
17.	Animas River, Eureka to Howardsville, August 1998: variation in chloride concentration in synoptic samples, variation in streamflow discharge calculated from chloride concentrations in synoptic samples, distances corresponding to model reaches in calibrated OTIS model .....	1011

18.	Animas River, Eureka to Howardsville, August 1998: variation in OTIS lateral-inflow concentrations and observed inflow concentrations for dissolved zinc with distance along study reach .....	1012
19.	Animas River, Eureka to Howardsville, August 1998: OTIS results for conservative and reactive simulations for zinc.....	1013
20.	Animas River, Eureka to Howardsville, August 1998: OTIS results for two remediation scenarios .....	1014
21.	Map showing detail of upper Animas River, Howardsville to Silverton study reach.....	1015
22–25.	Graphs showing:	
22.	Animas River, Howardsville to Silverton, September 1997: variation in chloride concentration in synoptic samples, variation in streamflow discharge calculated from chloride concentrations in synoptic samples, distances corresponding to model reaches in calibrated OTIS model.....	1017
23.	Animas River, Howardsville to Silverton, September 1997: variation in OTIS lateral-inflow concentrations and observed inflow concentrations for dissolved zinc with distance along study reach .....	1018
24.	Animas River, Howardsville to Silverton, September 1997: OTIS results for conservative and reactive simulations for zinc.....	1019
25.	Animas River, Howardsville to Silverton, September 1997: OTIS results for two remediation scenarios .....	1020
26.	Flow chart indicating actions necessary to calibrate the solute transport model OTIS.....	1026

## Tables

1.	Summary of mass-loading studies used for OTIS simulations.....	982
2.	Upper Cement Creek, reach number, distance at end of reach, and description of reaches used in OTIS modeling of synoptic samples collected for upper Cement Creek (September 1999).....	987
3.	Upper Cement Creek, samples and methods used to estimate lateral-inflow concentrations ( $C_L$ ) for copper, iron, and zinc in calibrated OTIS model .....	989
4.	Upper Cement Creek, first-order removal coefficients ( $\lambda$ ) by metal and reach for calibrated OTIS model .....	992
5.	Simulated concentration at the downstream end of the upper Cement Creek mass-loading study reach resulting from various remediation scenarios .....	994
6.	Lower Cement Creek, reach number, distance at end of reach, and description of reaches used in OTIS modeling of synoptic samples collected for lower Cement Creek (September 1996).....	997
7.	Lower Cement Creek, samples and methods used to estimate lateral-inflow concentrations ( $C_L$ ) for copper, iron, and zinc in calibrated OTIS model .....	1000
8.	Lower Cement Creek, first-order removal coefficients ( $\lambda$ ) by metal and reach for calibrated OTIS model .....	1002
9.	Lower Cement Creek, simulated concentrations at the mouth of lower Cement Creek resulting from five remediation scenarios, and from changed conditions at the Mogul mine (scenario 6).....	1003

10. Animas River, Eureka to Howardsville, reach number, distance at end of reach, and description of reaches used in OTIS modeling of synoptic samples (August 1998) .....	1010
11. Animas River, Howardsville to Silverton, reach number, distance at end of reach, and description of reaches used in OTIS modeling of synoptic samples (September 1997) .....	1017
12. Damkohler number ( $D_n$ ) for upper Animas River OTIS solute-transport study reaches that have first-order removal coefficients .....	1021
13. Summary of maximum simulated reductions in zinc load for all four study areas using OTIS and using a simple mass-loading model .....	1022
14. Model reaches, reach lengths, and hydraulic parameters for upper Cement Creek OTIS simulations .....	1028
15. Model reaches, reach lengths, and hydraulic parameters for lower Cement Creek OTIS simulations .....	1028

## Conversion Factors, Terms, and Abbreviations

Multiply	By	To obtain
cubic foot (ft <sup>3</sup> )	0.02832	cubic meter
foot (ft)	0.3048	meter
foot per second (ft/s)	0.3048	meter per second
cubic foot per second (ft <sup>3</sup> /s)	0.0283	cubic meter per second
gallon (gal)	3.785	liter
mile (mi)	1.609	kilometer
square foot (ft <sup>2</sup> )	0.09290	square meter

Degrees Celsius (°C) may be converted to degrees Fahrenheit (°F) as follows:

$$^{\circ}\text{F} = 9/5(^{\circ}\text{C}) + 32$$

The following terms and abbreviations also are used in this report:

cubic feet per second (ft<sup>3</sup>/s)  
 cubic meters per second (m<sup>3</sup>/s)  
 cubic meters per second per meter (m<sup>3</sup>/s-m)  
 inverse second (s<sup>-1</sup>)  
 kilogram (kg)  
 kilogram per second (kg/s)  
 kilogram per day (kg/d)  
 liters per minute (L/min)  
 liters per second (L/s)  
 meters (m)  
 meters per second (m/s)  
 micrometer (μm)  
 milligrams per liter (mg/L)  
 natural logarithm (ln)  
 square meters per second (m<sup>2</sup>/s)



## **Chapter E24**

# **Using the OTIS Solute-Transport Model to Evaluate Remediation Scenarios in Cement Creek and the Upper Animas River**

By Katherine Walton-Day, Suzanne S. Paschke, Robert L. Runkel, and Briant A. Kimball

### **Abstract**

The OTIS (One-dimensional Transport with Inflow and Storage) solute-transport model was used to simulate ambient water-quality conditions and effects of hypothetical remediation scenarios on water quality for four subbasins of the Animas River watershed study area in southwestern Colorado. Samples collected during metal-loading studies conducted in upper and lower Cement Creek, and the Animas River from Eureka to Howardsville and from Howardsville to Silverton, provided data to calibrate the models and simulate ambient conditions. Hypothetical remediation targets in each subbasin included either the largest sources of loading, the largest sources of loading that occurred on Federal land, or sources of mining-related loading. Results of the simulations indicate that remediation is likely to effect the greatest water quality improvement in areas where loading is limited to a small number of distinct inflows, such as in upper Cement Creek. Simulations conducted by removing all copper and zinc loading from the Queen Anne and Grand Mogul mines, the Mogul mine, and North Fork Cement Creek indicated reduction of copper and zinc concentrations at the downstream end of the study reach by 90 and 82 percent. Remediation will have a smaller effect in streams where a significant proportion of the load is supplied from diffuse sources of seepage and ground-water inflow such as lower Cement Creek. Remediation scenarios in lower Cement Creek that reduced copper and zinc loading by as much as 75 percent from Prospect Gulch, Ohio Gulch, and the May Day mine area only reduced copper and zinc concentrations at the lower end of the study reach by 19 and 9 percent. Ambient conditions in Cement Creek (low pH and elevated metal concentrations) complicate any remediation scheme: even though simulated remediation in upper Cement Creek projected the greatest water quality improvement of all the remediation scenarios considered in the four subbasins, simulated post-remediation metal concentrations exceeded levels favorable for aquatic life, as represented by hardness-based toxicity standards. Remediation scenarios considered for the two Animas River subbasin study reaches simulated

post-remediation concentrations of zinc near levels considered favorable for aquatic life (0.18 mg/L). Ambient water quality in the Animas River had near-neutral pH values, and metal concentrations were much lower than those in Cement Creek. Although loading was not confined to distinct sources such as in upper Cement Creek, remediation simulations affected water-quality improvement sufficient to improve aquatic habitat in some portions of the stream because of the lower initial metal concentrations and higher pH. These results indicate that remediation will be most successful, in terms of improving aquatic habitat, if applied to areas where degradation is less severe. Severely impaired areas, and areas where significant proportions of the load are supplied from non-mining-affected acid drainage, may continue to negatively affect water quality even when remediation of other large sources is attempted.

Additional simulations conducted for lower Cement Creek indicated that the model successfully predicts trends in dissolved copper, total iron, and dissolved zinc concentrations that have resulted from changes in metal loading in upper Cement Creek.

### **Introduction**

Planning remedial actions in streams affected by acid mine drainage is a complex process. One must first understand the location and magnitude of sources of metal loading to the stream. Sources can then be ranked by the severity of their effect on stream-water quality. Generally, those sources having the greatest effect will be chosen for remediation. However, if a stream receives acid and metal loading from many diffuse sources, or sources that cannot be readily remediated (such as ground-water inflow to the stream), it may be difficult to significantly improve stream-water quality through remediation. In the context of multiple sources of water-quality degradation to a stream and limited resources available for remediation, tools are needed to understand the effects of various remedial actions. Solute-transport modeling is one such tool.

Multiple metal-loading studies that combined tracer dilution with synoptic sampling were conducted on the upper Animas River and its primary tributaries Cement Creek and Mineral Creek from 1996 through 2000 (Kimball and others, this volume, Chapter E9). The tracer-dilution method provides estimates of streamflow that were used to quantify the amount of water entering the stream through tributaries and groundwater inflow. Synoptic sampling of mainstem and inflow chemistry provided a spatially detailed snapshot of stream-water quality. When used together, these techniques provide a description of the watershed that includes both streamflow and water quality, which can be used to construct mass-loading profiles for the stream. These profiles can be used to identify and quantify the greatest sources of mass loading to a stream (Kimball and others, this volume). Sources having the greatest mass loads may then be the target of remedial actions. The results from mass-loading studies can also be used to calibrate OTIS (One-dimensional Transport with Inflow and Storage), a solute-transport model (Runkel, 1998). The calibrated model can be modified to simulate the results of various remediation scenarios, providing a guide for remediation decisions.

OTIS is used to describe the hydrologic processes controlling solute transport in streams. In particular, OTIS quantifies the effects of storage zones on solute transport. Storage zones in streambeds delay the transport of a constituent and contribute to dispersion. OTIS also can account for chemical reaction using first-order decay or removal. First-order decay means that the rate of decrease in concentration of a constituent follows first-order kinetics and is directly proportional to the concentration of the constituent. This approach for considering chemical reactions is an alternative to equilibrium-based approaches used in models such as WATEQ and MINTEQ (Allison and others, 1991; Ball and Nordstrom, 1991). OTIS has been used to quantify hydrologic processes in a mountain stream (Broshears and others, 1993), to quantify the combined effects of hydrologic and geochemical processes on manganese transport (Harvey and Fuller, 1998), and more recently, to examine the effects of remedial alternatives in streams affected by acid mine drainage (Paschke and others, 2005; Walton-Day and others, 1999). OTIS-P is a modified version of OTIS that couples OTIS with a nonlinear regression package to automate the parameter-estimation process (Runkel, 1998).

Using OTIS to understand the effects of remedial alternatives is a fairly straightforward process. The model is calibrated using data collected during synoptic sampling of the stream. Model calibration entails adjusting variables (parameters) in the model so that the model generally reproduces (simulates) the downstream profile of various chemical constituents observed during synoptic sampling (ambient conditions). The primary data used in the model include the concentration of constituents at the upstream end of the profile (known as the upstream boundary condition), the location and concentration of constituents that are flowing into the stream at various locations along the profile (known as lateral-inflow concentrations,

or  $C_L$ ); and the rate of inflow of water at various locations along the profile (known as the lateral inflow, or  $q_L$ ). Once the model is calibrated, it allows rapid simulation and comparison of the effects of multiple remedial alternatives for a stream. The effects of remediation are simulated by adjusting lateral-inflow concentrations ( $C_L$ ) to mimic the effects of the hypothetical remediation, and the resulting downstream profile of constituent concentration is compared to the profile constituent concentration from the calibrated model.

The use of OTIS to model ambient conditions and the effects of remediation has several advantages. First, once the model is calibrated, simulation and comparison of the effects of multiple remediation scenarios is quick and easy. Second, the model accounts for chemical reactions by using first-order removal coefficients. Mass-balance approaches, which are commonly used to examine the effects of removal of various sources of load to a stream, do not account for the instream reactivity of metals and may overestimate or underestimate the effects of remediation by not accounting for secondary changes that result from the removal of the source to the stream. Third, if temporal variations in streamflow and chemistry are known, the effects of remediation under differing hydrologic scenarios (variable flow) can readily be examined.

## Purpose and Scope

The purpose of this chapter is:

- To demonstrate the utility of a solute-transport modeling approach to describe ambient stream conditions and investigate the effects of hypothetical remediation scenarios on trace-metal concentrations in the streams.

Specifically, the objectives of this chapter are to:

- Apply the solute-transport model OTIS to results of four of the mass-loading studies conducted in Cement Creek and the Animas River (Kimball and others, this volume). Four stream reaches in the Animas River watershed study area were used for this demonstration: upper and lower Cement Creek, the Animas River from Eureka to Howardsville, and the Animas River from Howardsville to Silverton (fig. 1; table 1). These reaches demonstrate the range in chemical conditions in the Animas River watershed study area: from low pH and elevated metal concentrations throughout much of Cement Creek, to near-neutral pH values and lower concentrations of metals in the upper Animas River reaches.
- Construct solute-transport models that simulate the ambient hydrologic and geochemical characteristics of each stream reach (also referred to as “calibrated models”)

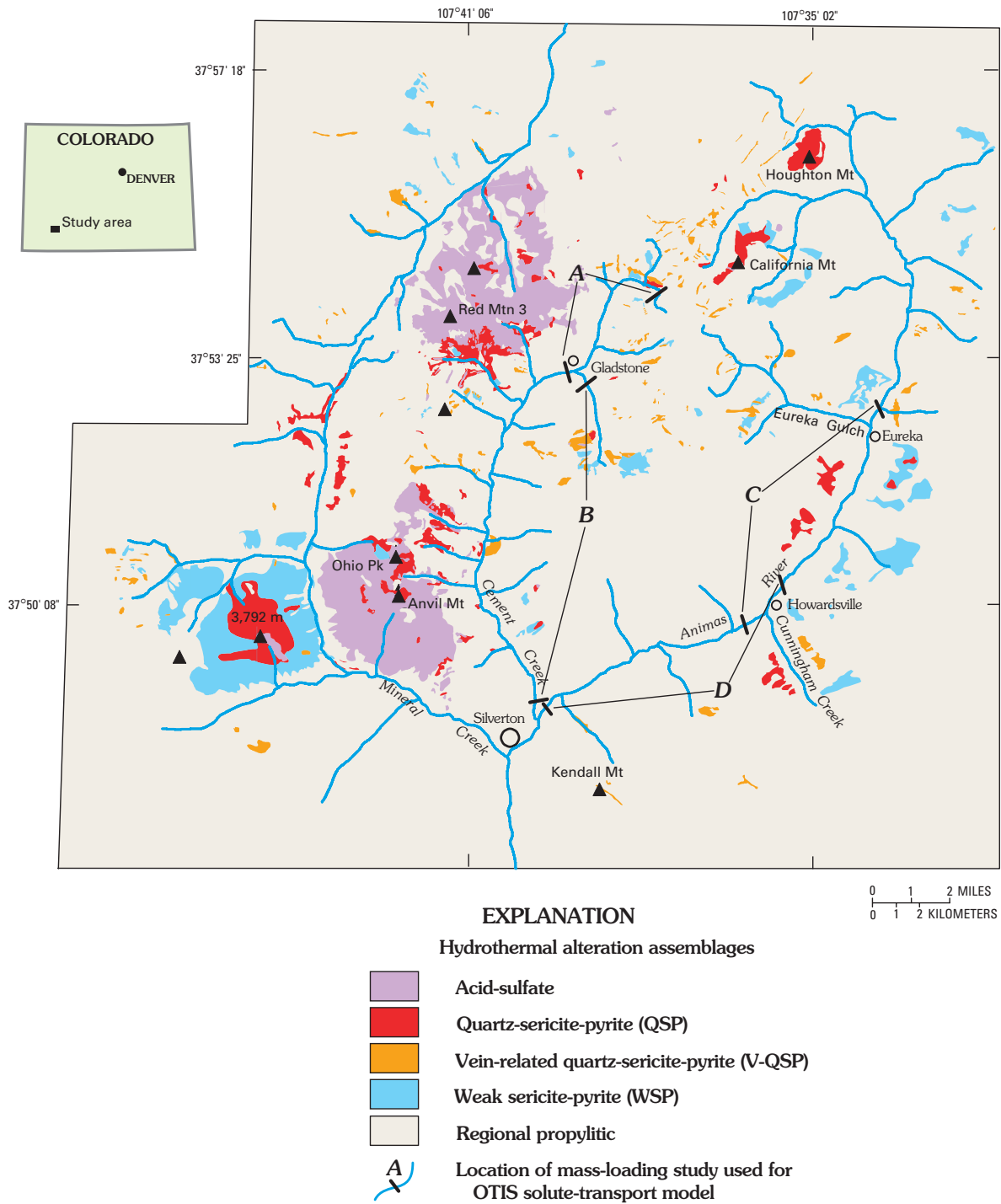


**Figure 1.** Location of Animas River watershed study area and four study reaches used in solute-transport modeling. Reach A, upper Cement Creek; reach B, lower Cement Creek; reach C, upper Animas River, from Eureka to Howardsville; reach D, upper Animas River, from Howardsville to Silverton. Map shows alteration assemblages mapped by Bove and others (this volume, Chapter E3).

- Evaluate the consistency of the models with ambient stream conditions by comparing inflow concentrations and first-order removal used in the model with environmental data and observations
- Evaluate the possible effects of remediation scenarios by decreasing or eliminating the loads of different sources of metal to the streams within the models. Although the models do not address all possible effects of remediation on stream chemistry, the model results indicate possible changes to instream concentrations resulting from the simulated remediation.

## Methods

Data collected during mass-loading studies were used to construct the solute-transport models for each stream reach. A brief overview of mass-loading studies and tracer-injection methods is followed by an explanation of the solute-transport model OTIS, and the steps employed to construct, calibrate, and investigate the effects of remediation using the model.

### Mass-Loading Studies

Application of mass-loading studies to identify sources of trace-metal loading in areas affected by inactive mining-related features has been demonstrated by Bencala and McKnight (1987), Kimball and others (1994), and Kimball (1997). The approach includes using tracer injections to quantify streamflow by tracer dilution (Kilpatrick and Cobb, 1985) and synoptic sampling to provide spatial profiles of pH and constituent concentrations. The tracer-dilution method entails continuous injection of a tracer that is geochemically nonreactive into a stream at a constant rate and concentration. Given sufficient time, all portions of the stream including side pools and the hyporheic zone become saturated with tracer, and instream concentrations will plateau (Kimball, 1997). Decreases in plateau concentration with stream length indicate dilution of tracer by additional water entering the channel from surface- and ground-water inflows. Consideration of this dilution allows the calculation of streamflow at each

**Table 1.** Summary of mass-loading studies used for OTIS simulations.

[LiBr, lithium bromide; LiCl, lithium chloride; NaCl, sodium chloride]

Location of tracer injection	Date of mass-loading study	Length of study reach	Tracer used
Upper Cement Creek	September 20, 1999	4,133 m	LiBr
Lower Cement Creek	September 20, 1996	10,548 m	LiCl
Animas River, Eureka to Howardsville.	August 14, 1998	7,250 m	NaCl
Animas River, Howardsville to Silverton.	September 14, 1997	7,858 m	NaCl

stream site. Streamflow and concentration can be combined to construct load profiles (Kimball and others, this volume). Analysis and interpretation of load profiles helps to rank the sources that have the greatest effects on stream chemistry and also helps to identify targets for remedial activities.

The four mass-loading studies used for the modeling exercise were conducted over a 3-year period (table 1). During this time, filtration methods varied as more efficient equipment was incorporated into the sample-processing scheme. Consequently, the earliest mass loading study (lower Cement Creek) used 0.1  $\mu\text{m}$  filtration. Subsequent studies used ultrafiltration (10,000 Dalton molecular weight nominal pore size). Thus, the filtered samples for lower Cement Creek represent a larger filter size than those for the other three mass-loading studies presented here, and could contain substantial amounts of colloidal material relative to ultrafiltered samples. To distinguish this difference in filtration techniques, concentrations in figures and text from the lower Cement Creek samples are referred to as "filtered," whereas concentrations in figures and text from the other three studies are referred to as "dissolved."

### Solute-Transport Modeling with OTIS

The data generated from mass-loading studies can also be used to construct solute-transport models that reproduce, or simulate, the ambient hydrologic and geochemical characteristics of the stream. These models can then be used to examine changes in instream concentrations that might result from remediation.

Like most solute-transport models, OTIS is based on the advection dispersion equation that describes downstream movement of solute mass. Additional terms are included to simulate lateral inflow and first-order removal, leading to the following governing equation (Runkel, 1998):

$$\frac{Q}{A} \frac{\partial C}{\partial x} = \frac{1}{A} \frac{\partial}{\partial x} \left( AD \frac{\partial C}{\partial x} \right) + \frac{q_L}{A} (C_L - C) - \lambda C \quad (1)$$

where

- $C$  is solute concentration in the main channel (mg/L),
- $C_L$  is the lateral inflow solute concentration (mg/L),
- $x$  is distance along the stream reach (meters),
- $t$  is time (seconds),
- $Q$  is the volumetric flow rate ( $\text{m}^3/\text{s}$ ),
- $D$  is the longitudinal dispersion coefficient ( $\text{m}^2/\text{s}$ ),
- $A$  is the main channel cross-sectional area ( $\text{m}^2$ ),
- $q_L$  is the lateral inflow or flow added to the stream along each reach which is usually in units of volume per time (in this case, the inflow is distributed along the length of a stream reach, so the appropriate units are cubic meters per second per meter,  $\text{m}^3/\text{s}\cdot\text{m}$ ),

and

$\lambda$  is the main channel first-order removal coefficient (this term is a rate constant, and is reported in units of reciprocal time, in this case, inverse seconds,  $s^{-1}$ ).

Four steps were used in the solute-transport modeling process:

1. Determination of physical parameters
2. Model calibration for conservative solutes
3. Model calibration for reactive solutes
4. Simulation of remediation scenarios.

All four steps were used for the simulations on lower Cement Creek and both reaches of the Animas River. For the upper Cement Creek data set, however, physical parameters determined for lower Cement Creek were used. This shortcut is permissible because in steady-state conditions (when constituent

concentration and streamflow are constant with time), simulations are mostly insensitive to variations in dispersion ( $D$ ) and cross-sectional area ( $A$ ) (Runkel and Kimball, 2002). However, the steps are included for the reader interested in time-variable transport.

### Determination of Physical Parameters

Physical parameters (dispersion ( $D$ ), and stream cross-sectional area ( $A$ )) were determined using data collected at transport sites. Transport sites are where periodic samples were collected and analyzed for tracer concentration. Profiles of tracer concentration through time (fig. 2) are influenced by the hydrologic characteristics of a stream reach. Sites located directly downstream from the tracer injection demonstrate an abrupt concentration increase and decrease caused by the beginning and end of the tracer injection (site T1, fig. 2). Data collected from sites moving downstream (sites T2 and

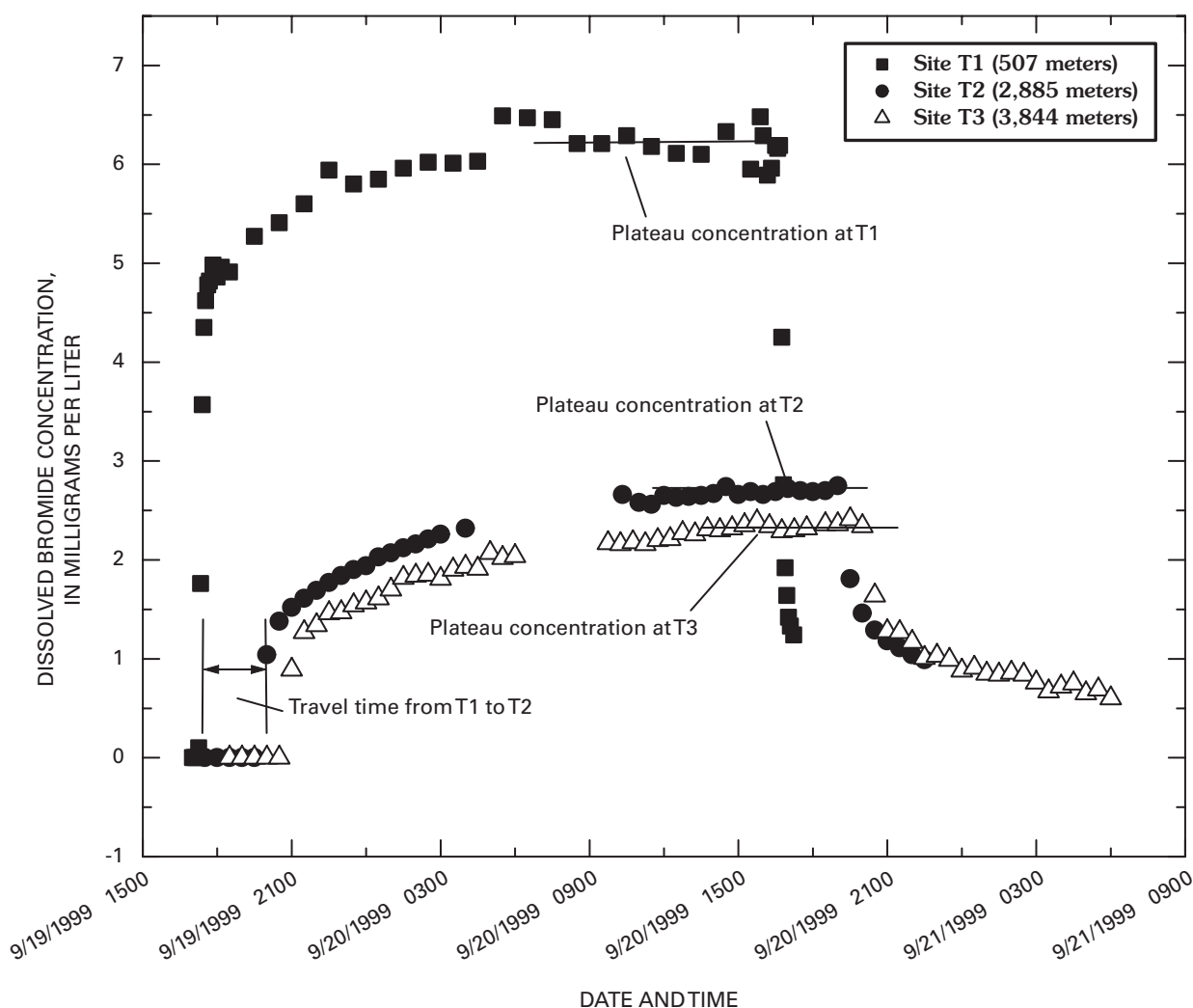


**Figure 2.** Variation in dissolved-bromide concentration with time at transport sites T1, T2, and T3, upper Cement Creek tracer injection, September 1999. The difference in travel time for the tracer between sites T1 and T2 is used to calculate stream cross-sectional area. Plateau concentrations are used to calculate streamflow.

T3, fig. 2) from the injection site exhibit several features that are affected by the physical transport of the tracer from the injection site to the transport site. First, the arrival of the tracer at downstream sites occurs later than at T1 because of the greater transport distance. Second, the plateau concentrations of tracer will be lower at downstream sites as the tracer is diluted by surface- and ground-water inflow. Finally, the arrival and departure of the tracer pulse will be less distinct indicating the effects of storage and dispersion as distance from the injection increases. The shapes of these curves were used to fit the hydrologic (or physical) parameters representing dispersion ( $D$ ), and stream cross-sectional area ( $A$ ) using the solute-transport models OTIS and OTIS-P (Runkel, 1998). The appendix provides details of the steps to accomplish this process. Once the physical parameters were determined, the next process was to calibrate the model in steady-state (where streamflow and constituent concentration were constant at each site through time) for each constituent of interest using data from the synoptic sampling. The calibration procedure varied depending on whether the constituent was conservative or reactive. A conservative constituent is one that is not removed from the water column by chemical reactions, so that its mass is conserved during downstream transport. There may be additions to mass from inflows, but there are no losses of mass from the water column. A reactive constituent is removed from the water column by geochemical reactions so that constituent mass in the water column may decrease during downstream transport.

### Model Calibration for Conservative Solutes

The first step in calibration for conservative solutes was to use the tracer data to estimate streamflow for each stream site where synoptic samples were collected (Appendix and Kimball and others, this volume). Each modeled reach was then divided into subreaches (known as model reaches) chosen to bracket the major surface-water and ground-water inflows to the stream, including mine drainage from adits or tributaries. Lateral inflow ( $q_L$ ) was then estimated for each model reach (Appendix) using the tracer estimates of streamflow.

The next step was estimation of lateral-inflow concentrations ( $C_L$ ) for each model reach. The lateral-inflow concentration used in each model reach depended on whether the model reach contained any inflows that were sampled during the synoptic sampling event, and whether there was any increase in streamflow along the reach. For model reaches that contained no inflow, both lateral inflow ( $q_L$ ) and lateral-inflow concentration ( $C_L$ ) were zero. In model reaches that contained no sampled inflow, but where flow and constituent load increased along the reach, lateral-inflow concentration was approximated using the concentration from an inflow sample in an adjacent reach, or by using the effective inflow concentration ( $C_I^E$ ) calculated from:

$$C_I^E = \frac{C_C Q_C - C_B Q_B}{(Q_C - Q_B)} \quad (2)$$

where

$C_C$  is concentration of the constituent of interest at the downstream site,

$Q_C$  is streamflow at the downstream site,

$C_B$  is concentration of the constituent of interest at the upstream site,

and

$Q_B$  is streamflow at the upstream site.

In model reaches that contained one sampled inflow, the chemistry of that inflow was used as a first-estimate of lateral-inflow concentration. For model reaches that contained more than one inflow, lateral-inflow concentration was derived from a flow-weighted average concentration of the inflow samples, or the concentration of the most representative inflow sample was used.

After comparing concentration profiles produced by the model to profiles of data from the synoptic sampling, values of lateral-inflow concentration ( $C_L$ ) were adjusted using an iterative process (Appendix) until the model results generally matched the data.

### Model Calibration for Reactive Solutes

Calibration of the model for reactive solutes requires all of the previous steps noted for conservative solutes. The distinction between conservative and reactive solutes becomes important during calibration of lateral-inflow concentrations. For a conservative solute, when appropriate values were chosen for the inflows, the simulation matched the data. For a reactive solute, when appropriate values were chosen for the inflows, the simulation overestimated the data. It seems somewhat counterintuitive to use lateral-inflow concentrations during the calibration process that caused the simulations to overestimate the data. However, elevated lateral-inflow concentrations ( $C_L$ ) were used to match large, incremental increases in stream concentration in some model reaches for some constituents. Downstream from these model reaches, all possible choices for lateral-inflow concentrations ( $C_L$ ) (including  $C_L = 0$ ) sometimes resulted in simulations that overestimated the observed data. Therefore, removal of the constituent (using first-order removal coefficients) was needed for the simulations to match the observed data.

First-order removal coefficients ( $\lambda$ ) were used to offset the large concentration increases in certain model reaches and were estimated using OTIS-P (Appendix) (Runkel, 1998). Simulations resulting from initial estimates of first-order removal coefficients ( $\lambda$ ) were compared to the data. Generally, good agreement was quickly obtained; however, agreement sometimes required multiple modeling efforts. In this study, first-order removal coefficients ( $\lambda$ ) for iron were estimated first. Then first-order removal coefficients ( $\lambda$ ) for solutes that might sorb to or coprecipitate with iron, such as copper or zinc, were estimated so that the resulting model simulated their removal in reaches having favorable geochemical conditions (that is, coincident removal of iron).

## Simulation of Remediation

The calibrated model contained appropriate lateral inflow ( $q_L$ ), lateral-inflow concentrations ( $C_L$ ), and first-order removal coefficients ( $\lambda$ ) to generally reproduce, or simulate, the data collected during synoptic sampling. Simulation of remediation entailed changing lateral-inflow concentrations ( $C_L$ ) to mimic potential remediation scenarios. For instance, if one model reach had a tributary inflow where remediation could occur, then post-remediation lateral-inflow concentrations were estimated. The resulting lateral-inflow concentrations replaced the calibrated lateral-inflow concentrations in the model. The revised model estimated new instream concentrations for the constituent downstream from the point of remediation. For a conservative solute, the result was the same as might be obtained using a mass-loading model. For a reactive (nonconservative) solute, the result incorporated any first-order removal that occurred downstream from the point of remediation. Thus, the resulting improvement in water quality was more than what would be predicted from a mass-loading model. An advantage of the OTIS modeling approach was that once a model was calibrated, rapid simulation of multiple remediation scenarios for multiple elements was possible. A disadvantage of the approach was that the first-order removal coefficients oversimplify the interaction between constituents. Remediation of an inflow would likely increase the pH conditions of the inflow that could, in turn, cause instream pH to increase. Greater instream pH would result in greater removal of reactive constituents than predicted by the first-order removal coefficients in the calibrated model. To model such pH-dependent processes would require use of a model that incorporates chemical equilibrium such as OTEQ (Runkel and Kimball, 2002). However, herein, such an approach was not utilized because preliminary modeling with OTEQ in Cement Creek indicated that remediation simulations were not likely to significantly change instream pH; numerous non-mining-affected inflows supply low-pH water to the stream and offset the pH benefits of simulated remediation. Similarly, in the two modeled reaches in the upper Animas River basin, pH values were near neutral and would increase slightly with simulated remediation, but probably not enough to make a significant difference to instream pH. Finally, underestimating the effects of remediation was an advantage because it was desirable to produce a conservative estimate of the effects of remediation.

## OTIS Solute-Transport Modeling

Four subbasins (upper and lower Cement Creek, and the Animas River, Eureka to Howardsville and Howardsville to Silverton) were separately modeled using the OTIS solute-transport model. Results of mass-loading analyses (Kimball and others, this volume) identified locations of surface- and ground-water sources of acid and metal to the rivers, and the extent of attenuation occurring for certain constituents. These results were used to help divide each of the four synoptic

sample study basins into model reaches, and to guide choices about appropriate lateral-inflow concentrations ( $C_L$ ) and first-order removal coefficients ( $\lambda$ ) for each modeled reach and stream. This section presents a description of each of the study reaches along with a brief summary of the chemical and loading conditions for each, and then presents the results of calibration and remediation simulations.

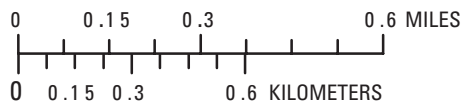
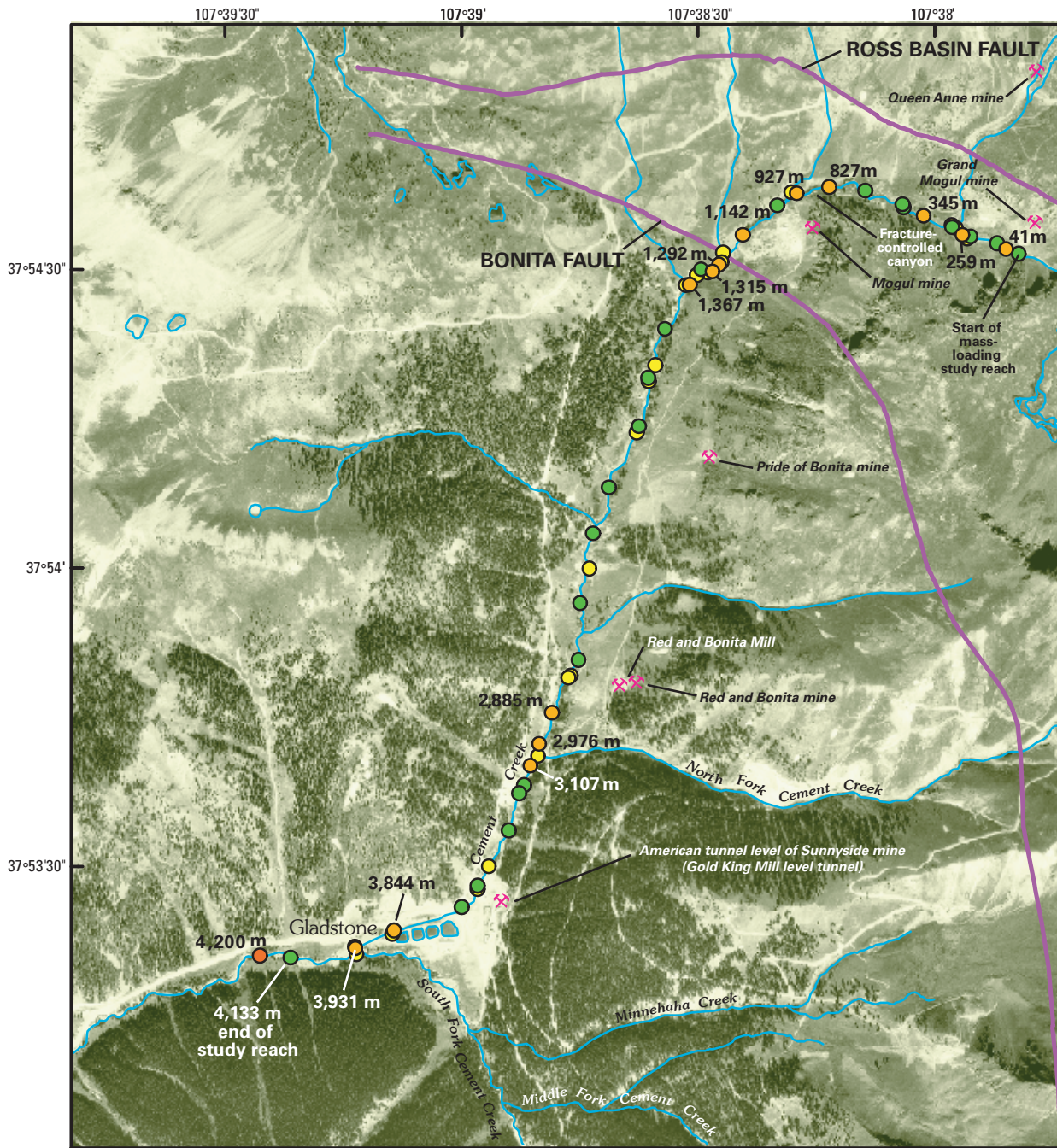
## Upper Cement Creek Subbasin

The September 1999 upper Cement Creek study reach covered 4,133 m of stream starting downstream from Ross Basin and continuing to just downstream from the confluence with South Fork Cement Creek near Gladstone (figs. 1 and 3). This stream reach included inflows from the Queen Anne and Grand Mogul mines at 271 and 298 m and the Mogul mine at 1,318 and 1,348 m, as well as several others. North Fork Cement Creek, which included drainage from several historical mines, joins Cement Creek at 3,076 m (table 2). Treated effluent from the American tunnel (site # 96)<sup>1</sup> enters the stream at 3,853 m. This effluent contains mine drainage that is collected from underground workings associated with the Sunnyside mine, and is treated and released to Cement Creek under a National Pollutant Discharge Elimination System (NPDES) permit. This source will be referred to as "Sunnyside mine effluent." South Fork Cement Creek enters Cement Creek at 4,001 m. Numerous additional historical mines and prospects exist in the watershed (see Church, Mast, and others, this volume, Chapter E5). Stream elevation ranges from approximately 3,595 m at the injection site to 3,170 m at the downstream end of the study reach. Average stream gradient is approximately 12 percent (Blair and others, 2002).

A continuous injection of lithium bromide solution occurred from September 19 through September 20, 1999 (Kimball and others, this volume). Synoptic sampling occurred during the injection from approximately 0900 to 1500 hours on September 20, 1999. A total of 36 stream sites and 23 inflow sites were sampled. A Parshall flume located at the Sunnyside mine effluent provided an independent measure of that inflow.

The water quality in upper Cement Creek changed from the injection site to the end of the study reach. At the upstream end of the study reach, pH was 6.8; sulfate and zinc concentrations were 70 and 0.5 mg/L, respectively. At the downstream end of the study reach, pH was 4.0 and sulfate and zinc concentrations were 400 and 4.0 mg/L. Along the study reach, pH values were as low as 3.3, and sulfate and zinc concentrations were as high as 600 and 12 mg/L, respectively. The results of the loading analysis in the upper Cement Creek subbasin indicated that, during the 1999 sampling, there were four primary

<sup>1</sup>Mine, mill, and mill-tailings deposit names in this chapter are identified by their AML\_MINE\_ID number in the Animas River watershed database. See Church, Mast, and others, this volume, Chapter E5, especially table 1, which contains names in numerical order as well as latitude and longitude of each feature.



**EXPLANATION**

- ✕ Mines, mills, and mine tunnels
- Hydrography
- OTIS model downstream boundary
- Sampled inflow sites
- Sampled stream sites
- 3,844 m Sampled and labeled stream sites and end of OTIS model reach
- Fault

**Table 2.** Upper Cement Creek, reach number, distance at end of reach, and description of reaches used in OTIS modeling of synoptic samples collected for upper Cement Creek (September 1999).

[Distance is downstream from arbitrary stream datum. Reach numbers correspond to those in figures 4–6; m, meter]

Model reach	Distance (m)	Brief description of reach and significant inflows
1	41	Cement Creek downstream from tracer-injection site.
2	259	Cement Creek downstream from tracer-injection site, upstream from Queen Anne and Grand Mogul mines.
3	345	Cement Creek downstream from Queen Anne and Grand Mogul mines.
4	827	Cement Creek upstream from fracture-controlled canyon.
5	927	Cement Creek downstream from fracture-controlled canyon.
6	1,142	Cement Creek where canyon ends and stream flows in more open valley.
7	1,292	Cement Creek between canyon and start of Mogul mine inflows.
8	1,315	Cement Creek upstream from Mogul mine inflows.
9	1,367	Cement Creek downstream from Mogul mine inflows.
10	2,885	Cement Creek downstream from area with the most ferricrete and iron-bog inflows.
11	2,976	Cement Creek upstream from North Fork Cement Creek.
12	3,107	Cement Creek downstream from North Fork Cement Creek.
13	3,844	Cement Creek upstream from Sunnyside mine tunnel inflow.
14	3,931	Cement Creek downstream from Sunnyside mine tunnel inflow and upstream from South Fork Cement Creek.
15	4,200	Cement Creek downstream from South Fork Cement Creek.

sources of loading to the stream: the Mogul mine, North Fork Cement Creek, and South Fork Cement Creek accounted for from 63 to 97 percent of the copper, iron, and zinc loads (Kimball and others, this volume), whereas the Sunnyside mine effluent and South Fork Cement Creek accounted for 87 and 76 percent of the calcium and sulfate loads. Combined, the Grand Mogul and Queen Anne mines accounted for less than 5 percent of the calcium, copper, iron, sulfate, and zinc loads.

### Determination of Physical Parameters and Boundary Conditions

The upper Cement Creek study reach was divided into 15 model reaches for the steady-state simulations (table 2; fig. 4). The model reaches bracketed locations of all major and some of the minor sources of load to the stream (Kimball and others, this volume). The model included 4,200 m of the stream with the last model reach containing the last synoptic sampling site at 4,133 m. The modeled reach was slightly

longer than the synoptic sampling reach (fig. 3) to account for the fact that in the model, the concentration gradient at the downstream boundary condition is zero (Runkel, 1998).

Required model parameters include the dispersion coefficient ( $D$ ), the cross-sectional area of the stream ( $A$ ), an upstream-boundary condition ( $U_b$ ) for each solute of interest, and the lateral inflow ( $q_L$ ) and concentration ( $C_L$ ) for each model reach. In addition, some model reaches used first-order removal coefficients ( $\lambda$ ). The appendix contains discussion of the values of  $D$  and  $A$ . Determination and values of  $U_b$ ,  $q_L$ ,  $C_L$ , and  $\lambda$  are presented herein.

OTIS simulations used streamflow estimates from the bromide tracer data and ultrafiltered concentrations of copper, iron, and zinc. The upstream boundary condition ( $U_b$ ) for simulating the bromide profile was 27.2 mg/L, the concentration at the 41 m site during the synoptic sampling. The upstream boundary condition was 0.016 mg/L for copper, 0.005 mg/L for iron, and 0.490 mg/L for zinc. These values represent the ultrafiltered concentrations of the metals at the site 41 m downstream from the injection site.

**Figure 3 (facing page).** Location of stream reach for upper Cement Creek mass-loading study (September 1999) and OTIS solute-transport model. Stream- and inflow-sample data provided in Sole and others (this volume, Chapter G). Mining features shown (and inventory numbers, from Church, Mast, and others this volume, Chapter E5) include American tunnel level of Sunnyside mine (# 96); Grand Mogul mine (# 35); Mogul mine (# 31); Pride of Bonita mine (# 101); Red and Bonita mine (# 99) and Red and Bonita Mill (# 97); and Queen Anne mine (# 34). Mining features shown limited to those discussed in the text. See Church, Mast, and others (this volume) for a complete inventory. Location of Bonita fault from Yager and Bove (this volume, Chapter E1, pl. 1). Base from Digital Orthophoto Quads, Transverse Mercator, -105.00 central meridian, 1927 datum.

### Model Calibration for Simulation of the Bromide Tracer Profile

Several problems complicated the calculation of streamflow from the tracer data. Some portions of stream water and tracer were probably lost to ground water in the far upstream portion of the study reach. Streamflow along the study reach was therefore calculated by calibrating the bromide concentrations to streamflow measurements made using a velocity meter and extrapolating the bromide mass-flux upstream (Kimball and others, this volume). The resulting simulated bromide profile matched the data downstream from 260 m (fig. 4). The simulation underestimated the data in model reach 2.

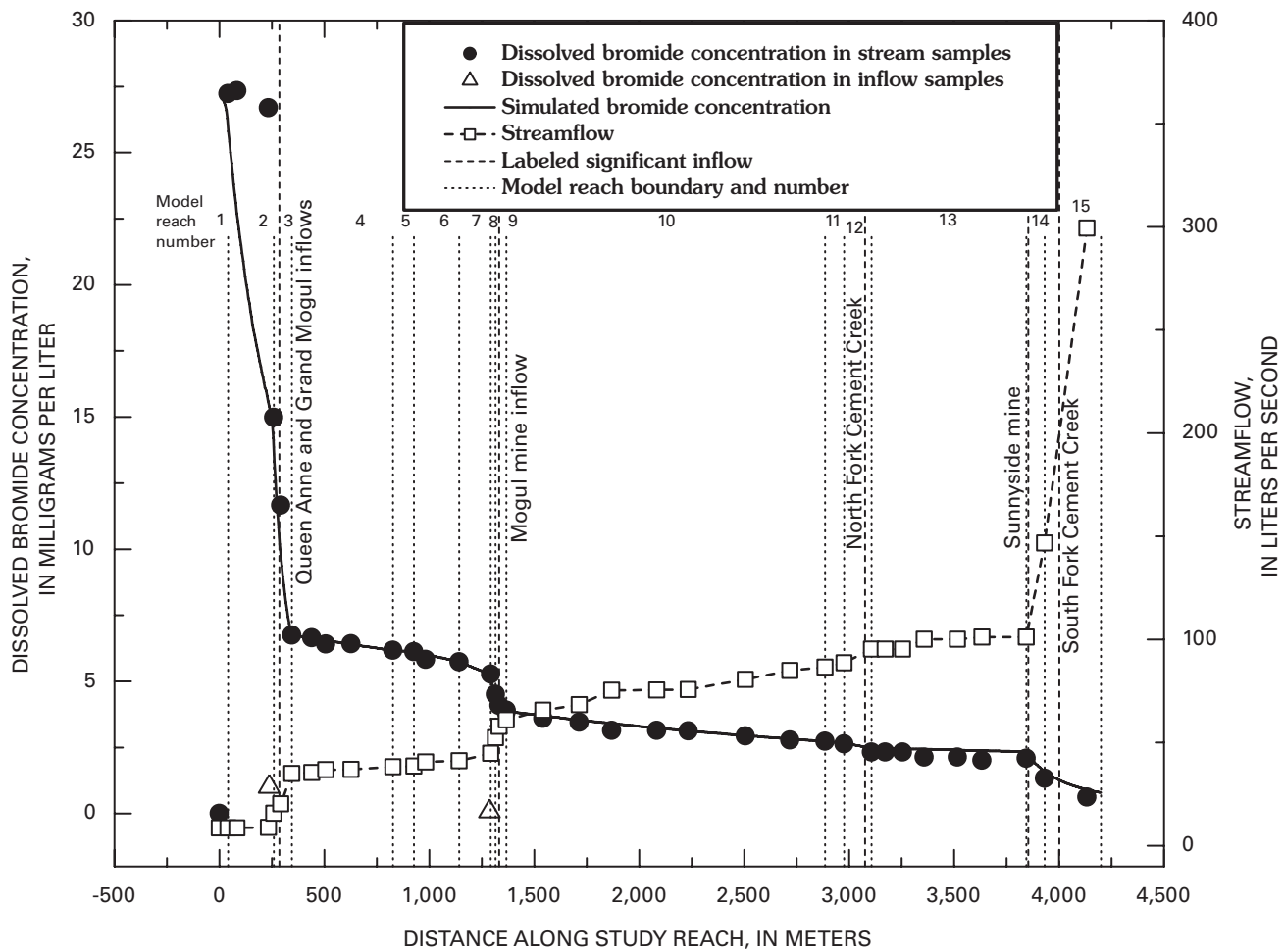


**Figure 4.** Variation in dissolved bromide concentration, streamflow, and simulated bromide concentration with distance, showing location of OTIS model reaches and significant features, upper Cement Creek mass-loading study (September 1999) and OTIS solute-transport model.

This pattern occurred because very little flow (approximately 0.1 L/s) was coming into the stream reach except for a visible surface inflow at 237 m. In the simulations, the inflow volume was distributed evenly along the entire model reach from 41 to 259 m. The simulation and data matched well at the upstream and downstream ends of model reach 2 (41 to 259 m) indicating that the lateral-inflow ( $q_L$ ) value was appropriate for that reach. Downstream, the match between the simulation and the data indicated that the streamflow and  $q_L$  values were appropriate. The discrepancy in reach 2 was inconsequential as there were no inflows of interest in that reach. Streamflow at the upper end of the study reach was 9 L/s. Streamflow downstream from the confluence with South Fork Cement Creek at the end of the study reach (4,200 m) was 299 L/s. Six distinct inflow areas (the Queen Anne mine, the Grand Mogul mine, the Mogul mine, North Fork Cement Creek, the Sunnyside mine effluent at the American tunnel (site # 96), and South Fork Cement Creek) accounted for 79 percent of the increased streamflow along the study reach. The remaining 21 percent of the streamflow originated in smaller tributaries, seeps, springs, and diffuse subsurface inflow that discharged to the stream.

### Model Calibration for Copper, Iron, and Zinc Simulations

Simulations for upper Cement Creek utilized a variety of estimation techniques for lateral-inflow concentration ( $C_L$ ) values (table 3; fig. 5). In model reaches 1 and 4,  $C_L$  for copper, iron, and zinc was zero. In model reach 11,  $C_L$  for zinc was zero.  $C_L$  values for model reaches 3 and 7 were flow-weighted average values calculated from two inflows. Model reaches 2, 5, 6, and 12 through 15 used representative inflow concentrations for  $C_L$  values from tributaries that were located within each reach. Model reaches 8 through 11 used effective inflow concentrations (equation 2) for  $C_L$  values, except for iron in model reach 10, where a flow-weighted average value was used, and zinc in model reach 11, where  $C_L$  was zero. The use of effective inflow for these four model reaches is justified because for most elements listed, prior analyses of mass loading showed the reaches to be locations of diffuse, subsurface inflow (Kimball and others, this volume). Iron is the exception. Because iron load decreased in the course of model reach 10, an effective inflow concentration could not be calculated.

**Table 3.** Upper Cement Creek, samples and methods used to estimate lateral-inflow concentrations ( $C_L$ ) for copper, iron, and zinc in calibrated OTIS model.

[Synoptic samples collected September 1999. Numeric values represent distances (in meters, m) of inflow samples used in estimation technique (inflow samples are in project database, Sole and others, this volume). Alpha characters indicate method used to estimate lateral inflow: NI, no lateral-inflow concentration in that reach; R, representative inflow concentration used for lateral-inflow concentration; F, flow-weighted average value used for lateral-inflow concentration; E, effective inflow concentration used for lateral-inflow concentration. Lateral-inflow concentration values shown in figure 5]

Model reach	Distance (m)	Dissolved copper	Dissolved iron	Dissolved zinc
1	41	NI	NI	NI
2	259	R, 237	R, 237	R, 237
3	345	F, 271, 298	F, 271, 298	F, 271, 298
4	827	NI	NI	NI
5	927	R, 880	R, 880	R, 880
6	1,142	R, 933	R, 933	R, 933
7	1,292	F, 1,237, 1,287	F, 1,237, 1,287	F, 1,237, 1,287
8	1,315	E	E	E
9	1,367	E	E	E
10	2,885	E	F, 1,411, 1,679, 1,719, 1,884, 2,407, 2,761, 2,763	E
11	2,976	E	E	NI
12	3,107	R, 3,076	R, 3,076	R, 3,076
13	3,844	R, 3,518	R, 3,518	R, 3,518
14	3,931	R, 3,853	R, 3,853	R, 3,853
15	4,200	R, 4,001	R, 4,001	R, 4,001

Therefore, a flow-weighted average concentration of the seven inflows was used for  $C_L$ . This flow-weighted average value is large relative to iron concentrations measured in inflows in model reach 10 (fig. 5B). In addition, in model reach 10, the relative value of  $C_L$  for iron compared to the distribution of sampled inflow concentrations is similar to the relative values of  $C_L$  for copper and zinc compared to sampled inflow concentrations (fig. 5 A–C). This similarity adds confidence to the value of  $C_L$  used for iron in model reach 10.

The wide variation in lateral-inflow concentration ( $C_L$ ) values is consistent with and similar to the wide variation in concentrations of the sampled inflow values for each element along the study reach (fig. 5). In some cases the effective inflow values chosen for  $C_L$  are similar to or within the range of inflow values in a model reach (for example, model reaches 9 and 10; fig. 5).

First-order removal coefficients ( $\lambda$ ) were used to improve the fit between the data and the simulations for some model reaches. Conservative simulations of copper, iron, and zinc (fig. 6) indicated that simulations slightly overestimated the ambient data. Simulations with OTIS-P were used to estimate first-order removal coefficients for some of the model reaches. Simulations including first-order removal coefficients indicated a better fit to the data (fig. 6). Large first-order removal coefficients (ranging from  $1.0 \times 10^{-4}$  to  $1.0 \times 10^{-1} \text{ s}^{-1}$ ) were used in reaches 1 through 3 for copper, iron, and zinc, and for iron in model reaches 14 and 15 (table 4). Smaller first-order removal coefficients (approximately  $1.0 \times 10^{-4} \text{ s}^{-1}$  or less) were used in model reaches 10 through 12 for iron. The use of large first-order removal coefficients in the upstream model reaches is

consistent with the high pH values (5.7 to 6.8) of the stream and indicates possible precipitation of amorphous iron minerals and coprecipitation or sorption of copper and zinc with the iron minerals. Simulated removal of iron from the water column in model reach 10 is consistent with the results of the loading analysis that indicated removal of iron in the stream reach from 1,367 to 2,885 m (Kimball and others, this volume). Simulated removal of iron in model reach 12 is consistent with the large iron load supplied by North Fork Cement Creek, which accounted for approximately 50 percent of the total iron load reported by the end of the study reach (Kimball and others, this volume). Iron removal in model reach 11 could be caused by excess iron loads to the stream similar to model reach 10, or by contributions of iron in the subsurface upstream from the North Fork Cement Creek tributary. The large amount of iron removal required in model reaches 14 and 15 is consistent with the addition of high-pH water (7.9) from the Sunnyside mine effluent in model reach 14, and with the addition of pH 5.5, relatively iron rich water in model reach 15 from South Fork Cement Creek. Overall, except for the model reaches described, first-order removal coefficients were not required to achieve a fit between the simulations and the data. The relatively small size and limited distribution of removal coefficients indicate that, except in a few model reaches, reactive processes are operating only to a minimal extent in the study reach. This result is consistent with low pH values that occurred in the stream throughout most of the upper Cement Creek study reach. At these low pH values (3–4), iron removal can occur, but sorption of metals to precipitating iron would be minimal.

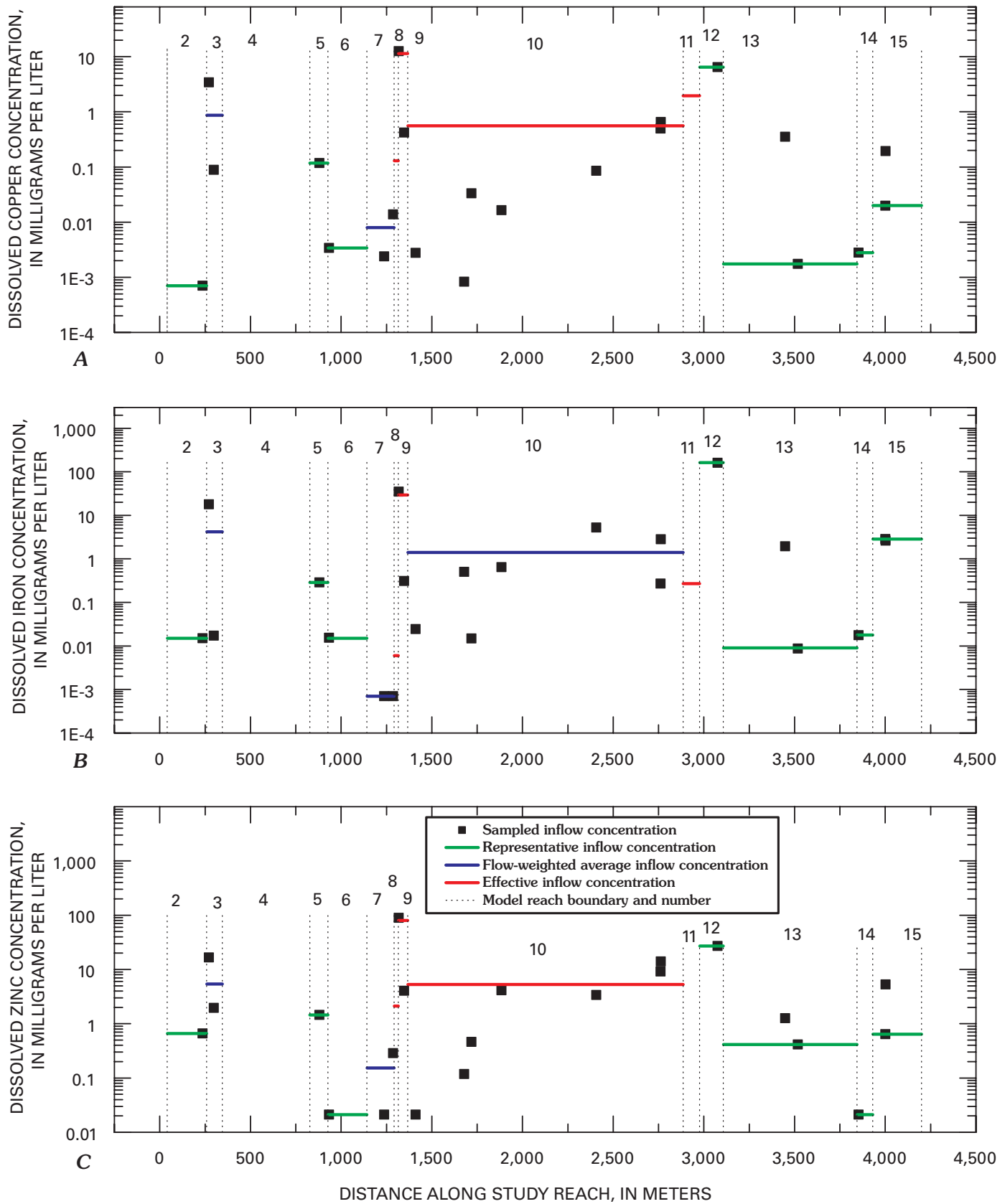


**Figure 5.** Variation in calibrated lateral-inflow concentrations and observed inflow concentrations (September 1999) with distance for A, dissolved copper; B, dissolved iron; C, dissolved zinc showing OTIS model reaches, upper Cement Creek OTIS model.

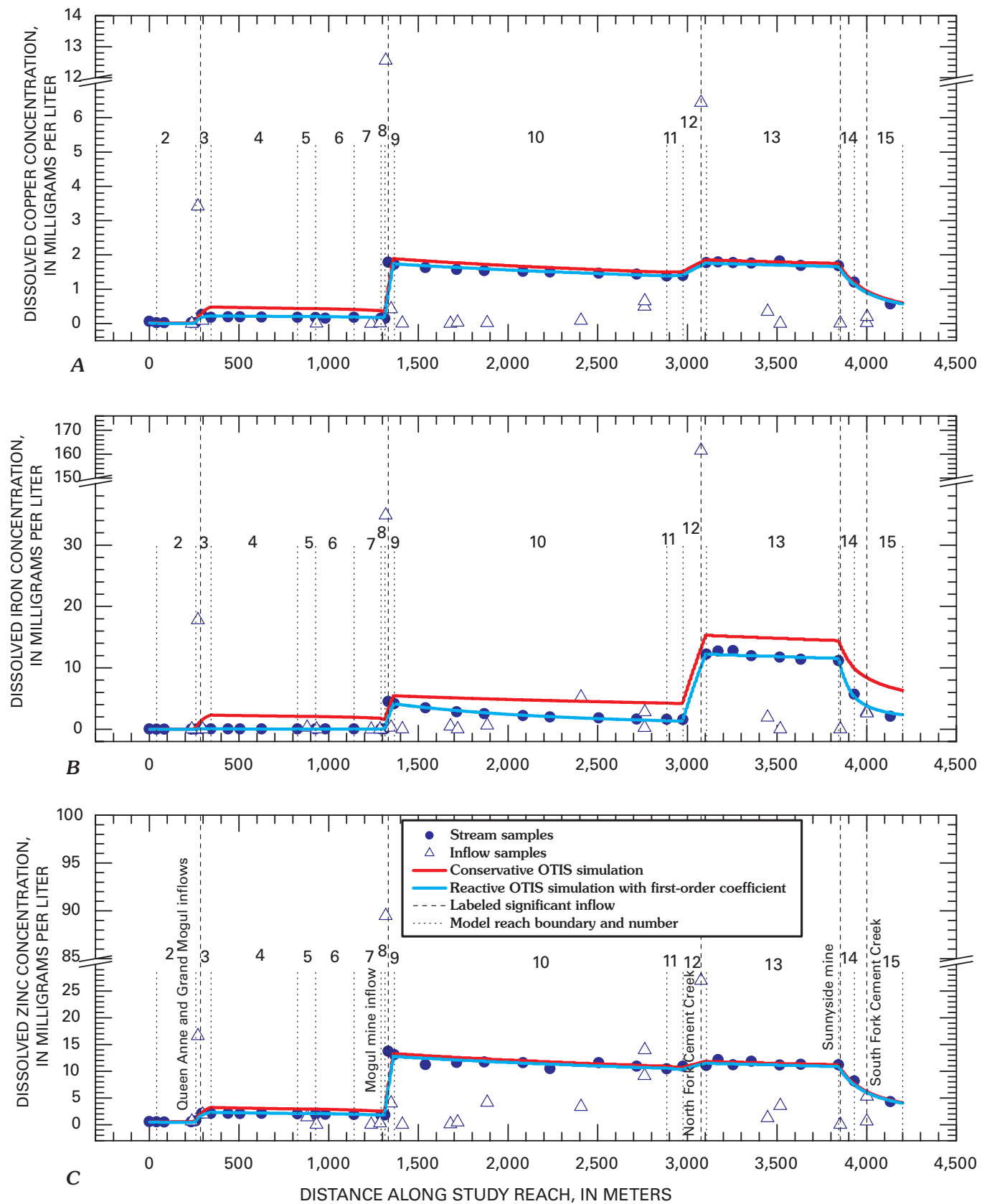


**Figure 6.** Variation in concentrations of A, dissolved copper; B, dissolved iron; C, dissolved zinc with distance in stream and inflow samples and in OTIS conservative and calibrated reactive simulations, showing model reach and number and location of significant features, upper Cement Creek, September 1999. Reactive OTIS simulation included first-order removal coefficients ( $\lambda$ ).

**Table 4.** Upper Cement Creek, first-order removal coefficients ( $\lambda$ ) by metal and reach for calibrated OTIS model.[All values in second<sup>-1</sup>]

Model reach	Distance (m)	Dissolved copper	Dissolved iron	Dissolved zinc
1	41	$3.0 \times 10^{-3}$	$1.04 \times 10^{-1}$	$1.19 \times 10^{-4}$
2	259	$3.0 \times 10^{-3}$	$1.04 \times 10^{-1}$	$1.19 \times 10^{-4}$
3	345	$3.0 \times 10^{-3}$	$1.04 \times 10^{-1}$	$9.98 \times 10^{-4}$
4	827	0.00	0.00	0.00
5	927	0.00	0.00	0.00
6	1,142	0.00	0.00	0.00
7	1,292	0.00	0.00	0.00
8	1,315	0.00	0.00	0.00
9	1,367	0.00	0.00	0.00
10	2,885	0.00	$1.07 \times 10^{-4}$	0.00
11	2,976	0.00	$9.19 \times 10^{-5}$	0.00
12	3,107	0.00	$9.19 \times 10^{-5}$	0.00
13	3,844	0.00	0.00	0.00
14	3,931	0.00	$1.26 \times 10^{-3}$	0.00
15	4,200	0.00	$1.26 \times 10^{-3}$	0.00

## Remediation Simulations

Remediation scenarios tested using the calibrated model included eliminating metal loading individually from the Queen Anne and Grand Mogul mines, from the two inflows to the stream from the Mogul mine, from North Fork Cement Creek, and then from all of these inflows together (fig. 7; table 5). For demonstration purposes, this approach assumed that total remediation of the inflows could be accomplished and that concentrations of copper, iron, and zinc from these sources would be negligible following remediation. However, given the extensive hydrothermal alteration mapped in this area (fig. 1; Bove and others, this volume, Chapter E3), total elimination of the metals from these sources is not realistic. For remediation of the Queen Anne and Grand Mogul mines, lateral-inflow concentrations ( $C_L$ ) of copper, iron, and zinc in model reach 3 were set to zero. For remediation of contributions from the Mogul mine, lateral-inflow concentrations in model reaches 8 and 9 were set to zero. Model reach 8 was included in the Mogul mine remediation because analysis of the loading results (Kimball and others, this volume) indicated that some subsurface flow from the Mogul mine was probably entering the stream in this reach, which is directly upstream from the reach containing the primary inflow from the Mogul mine. For remediation of North Fork Cement Creek, lateral-inflow concentrations ( $C_L$ ) of copper, iron, and zinc in model reaches 11 and 12 were set to zero. Reach 12 contains North Fork Cement Creek. Similar to the Mogul mine, there was possibly some subsurface flow from North Fork Cement Creek that entered Cement Creek upstream from the tributary. We assumed that this flow was contributed to the subsurface from surface flow in North Fork Cement Creek during transport across the alluvial cone of North Fork Cement Creek, and represented surface water that was only in the subsurface for a short time and distance before entering Cement Creek. Therefore, we

assumed that remediation of surface flow upstream in North Fork Cement Creek also would clean up this subsurface flow. The final remediation simulation combined the results of the three previous simulations. Percent changes in load resulting from the simulated remediations were calculated relative to the simulated concentration value in the calibrated model at the last stream sampling site, 4,133 m.

The remediation simulations indicate that the largest changes in copper and zinc concentrations would result from remediation of the Mogul mine inflows to the stream, whereas the largest changes in iron concentration would result from elimination of iron from North Fork Cement Creek (table 5). These results are consistent with the results of the loading analysis that indicated that the Mogul mine was the largest source of copper and zinc loading to the stream, whereas North Fork Cement Creek was the largest source of iron (Kimball and others, this volume). Simulation results indicate that remediation of all the sources together could result in a 90 percent reduction in copper concentration, a 62 percent reduction in iron concentration, and an 82 percent reduction in zinc concentration at the last synoptic sampling site (4,133 m) at the downstream end of the study reach near Gladstone. Realistically, remediation of these sources would probably not accomplish 100 percent metal reduction as was simulated here. Particularly in North Fork Cement Creek, hydrothermally altered rocks that generate acid water are present (fig. 1 and Bove and others, this volume) and would likely continue to generate acid water after remediation of mining-related sources in the basin. Thus, the reductions presented here are the maximum possible from elimination of the mining-related sources identified in the basin.

The simulated concentration profiles for the aggregate remediation scenario indicate that even though the major sources of metal loading are removed, there are other sources of metal loading to the stream that cause elevated concentrations at the downstream end of the study reach (fig. 7). There is a distinct increase in iron concentration near the downstream end of the study reach that is caused by the confluence with South Fork Cement Creek (4,001 m). There is a gradual increase in copper, iron, and zinc concentrations in the stream between the Mogul mine and North Fork Cement Creek. This increase is probably caused by diffuse subsurface flow along that zone. During the synoptic sampling event and other field activities, we observed some small, distinct inflows along that reach that were probably related to mine waste and drainage originating from historical mining and milling activity at the Pride of Bonita and Red and Bonita mines (# 101 and # 99). However, these inflows were generally not traceable back to the mines as distinct surface flow, but rather emerged as springs near the stream. In addition, this reach of stream contains abundant ferricrete deposits (Yager and Bove, this volume, Chapter E1 and pl. 2). These ferricrete deposits indicate previous and possibly current discharge of iron from metal-rich ground water in the stream reach (Wirt and others, this volume, Chapter E17; Verplanck and others, this volume, Chapter E15) over the last 10,000 years. Therefore, the simulated elevated concentrations of iron and zinc that

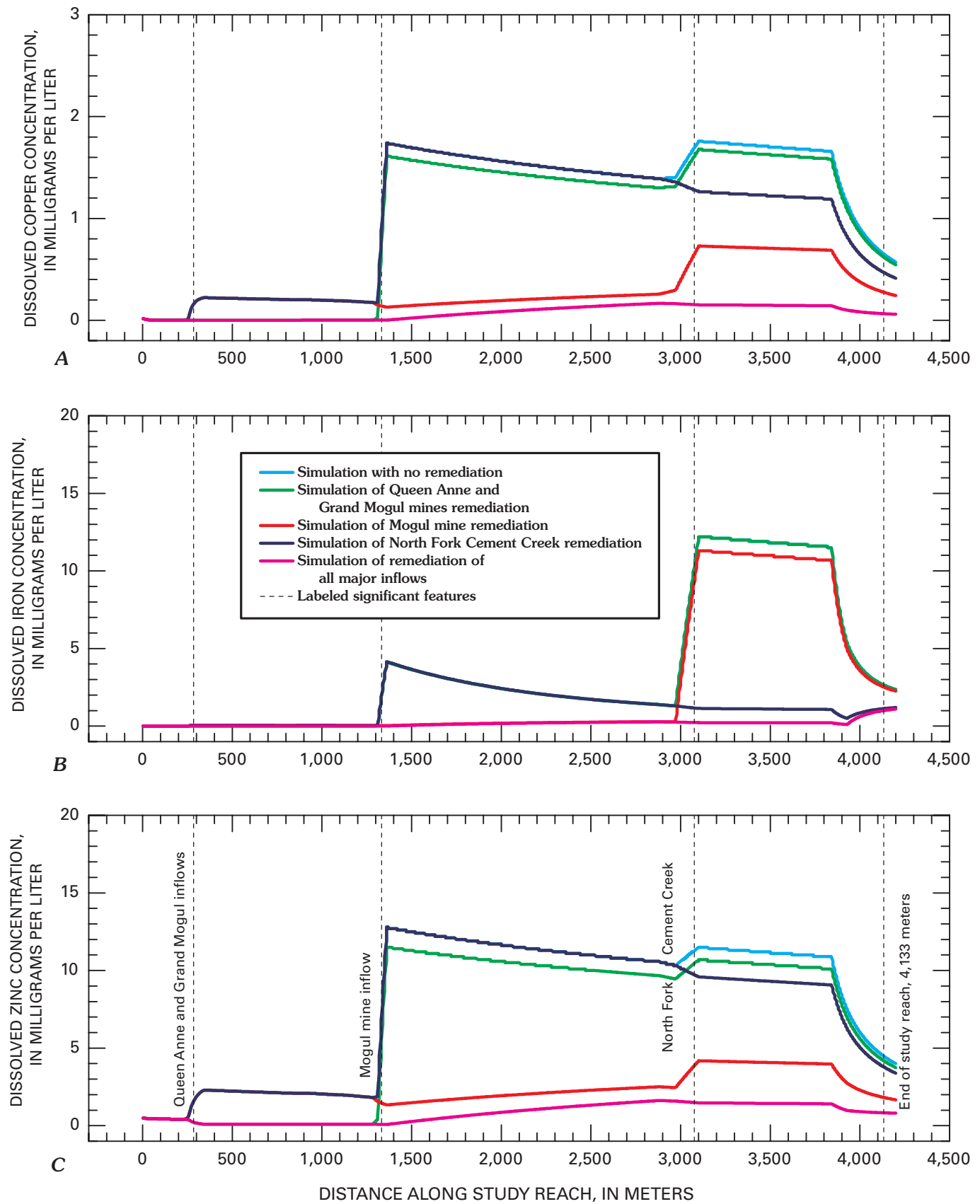


**Figure 7.** Variation in concentrations of A, dissolved copper; B, dissolved iron; C, dissolved zinc with distance in OTIS simulations of remediation scenarios, showing location of some significant features, upper Cement Creek. Details of remediation scenarios are in table 5.

**Table 5.** Simulated concentration at the downstream end of the upper Cement Creek mass-loading study reach resulting from various remediation scenarios.

[Dissolved copper, iron, and zinc concentration values in milligrams per liter; m, meter]

Remediation		Copper	Iron	Zinc
Simulated concentration at end of study reach (4,133 m) in calibrated model.		0.650	2.65	4.48
Total remediation of Queen Anne and Grand Mogul mine sources.	Simulated concentration at end of study reach (4,133 m).	0.621	2.65	4.19
	Percent reduction	4.5	0	6.5
Total remediation of Mogul mine sources	Simulated concentration at end of study reach (4,133 m).	0.275	2.52	1.82
	Percent reduction	58	5	59
Total remediation of North Fork Cement Creek sources.	Simulated concentration at end of study reach (4,133 m).	0.469	1.13	3.79
	Percent reduction	28	57	15
Simulation of remediation of all major inflows.	Simulated concentration at end of study reach (4,133 m).	0.064	1.0	0.830
	Percent reduction	90	62	82

remain following remediation probably result from groundwater discharge to the stream and would most likely remain following remediation of the distinct mining sources simulated in the model. In addition, note that the concentration of zinc was 0.49 mg/L at the upstream end of the study reach indicating that sources for that metal lie upstream from the study reach. Dissolved zinc concentrations greater than 2 mg/L were reported in one spring upstream from the study reach (Mast and others, 2000), and vein-related quartz, sericite, and pyrite alteration that can cause elevated metal concentrations in water crossing through it was mapped in the drainage basin upstream from the study reach (fig. 1; Bove and others, this volume; Mast and others, this volume, Chapter E7). In addition, Bove and others (this volume) hypothesized that high background-metal concentrations noted in water samples in the area were from interaction of the water with mineralized, unmined veins. Although the aggregate remediation scenario achieved metal reduction of as much as 90 percent for copper, elevated metal concentrations remained at the downstream end of the study reach from discharge of metal-rich ground water to the stream along the study reach, and from inflow of metals upstream from the study reach.

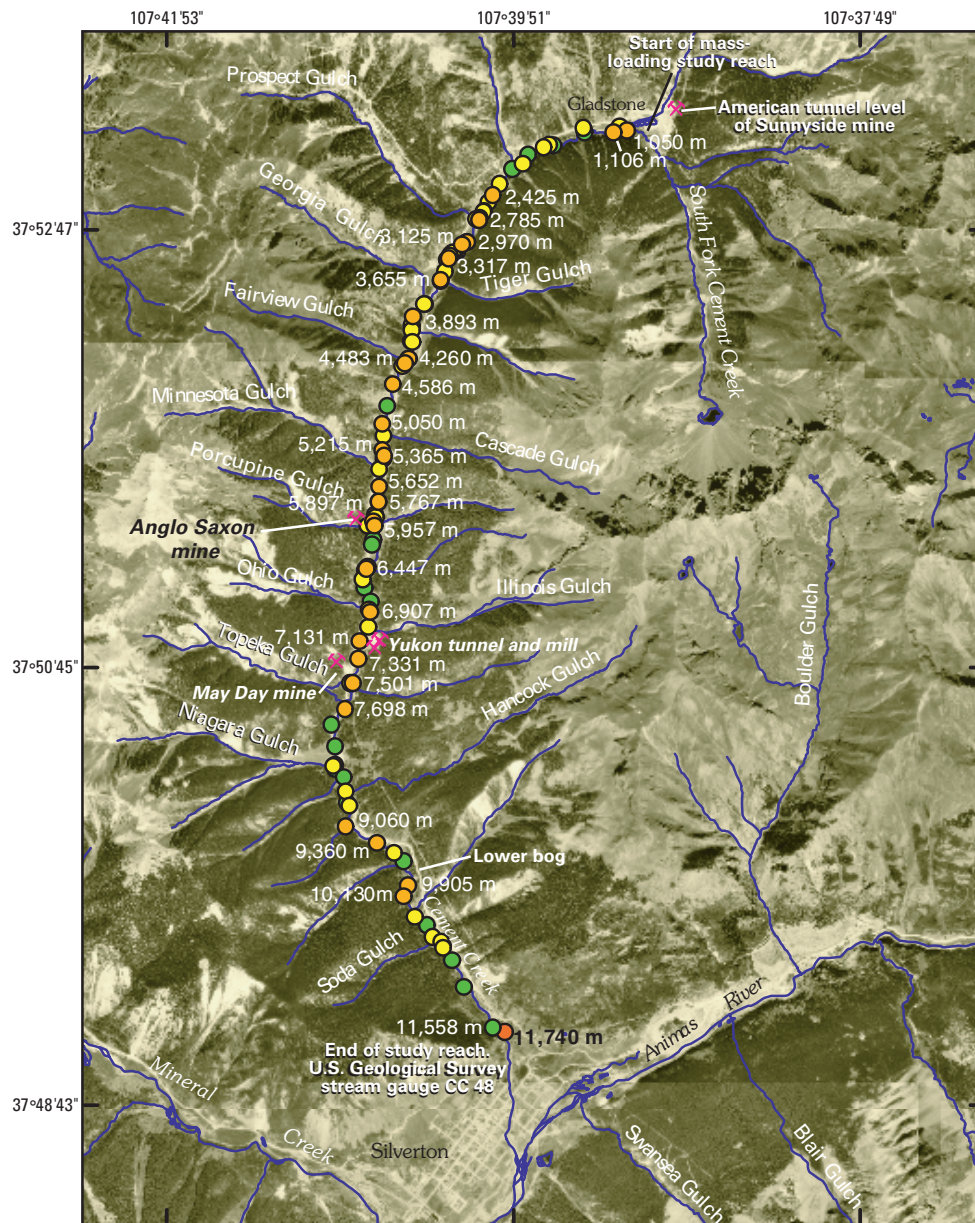
### Lower Cement Creek Subbasin

The study reach for lower Cement Creek covered approximately 10,500 m of stream starting on South Fork Cement Creek, just upstream from the confluence with Cement Creek, and continued to the U.S. Geological Survey stream-flow gauging station (CC48) near the mouth of Cement Creek in Silverton at 11,558 m (figs. 1 and 8). The arbitrary start for measuring distance along the stream was located upstream from North Fork Cement Creek. The study reach included inflows from Cement Creek (1,080 m), Prospect Gulch (2,795 m), Tiger Gulch (3,670 m), Georgia Gulch (3,793 m), Fairview

Gulch (4,493 m), Cascade Gulch (5,100 m), Minnesota Gulch (5,490 m), the Anglo-Saxon mine (# 183; 5,817 m), Porcupine Gulch (5,907 m), Ohio Gulch (6,781 m), Illinois Gulch (7,006 m), Topeka Gulch (7,548 m), Niagara Gulch (8,422 m), and Hancock Gulch (8,735 m). Numerous inactive mines and prospects exist in the subbasin (Church, Mast, and others, this volume). Iron bogs and springs and alluvial ferricrete deposits occur throughout the watershed but are particularly plentiful in the stream reach that contains the inflow from Prospect Gulch from 2,500 to 3,300 m (Stanton, Yager, and others, this volume, Chapter E14; Wirt and others, this volume; Verplanck and others, this volume; Yager and Bove, this volume, pl. 2). Stream elevation ranges from 3,185 m at the injection site on South Fork Cement Creek to 2,860 m at the downstream end of the stream reach. Stream gradient ranges from 1 to 5.3 percent (Blair and others, 2002) and averages about 3 percent.

During the 1996 mass-loading study, all of the flow in Cement Creek was collected just downstream from the confluence of North Fork Cement Creek and diverted into the treatment system at the Sunnyside mine. Part of the treated mine drainage and stream water was returned to the Cement Creek through a conduit located just upstream from the confluence with South Fork Cement Creek (1,080 m). The chemical composition of water discharged from the conduit reflected the net result of treatment of the Sunnyside mine effluent and upper Cement Creek.

From September 19 through 21, 1996, a continuous injection of lithium chloride solution took place on South Fork Cement Creek approximately 40 m upstream from the confluence with Cement Creek (1,080 m). Synoptic sampling was done on September 20, 1996. The sampling divided the 10,518-m study reach into 54 segments. The segments bracketed major and minor tributary inflows and areas of likely subsurface inflow. Stream-sampling sites were located sufficiently downstream from inflows to capture both visible tributary inflow and any additional subsurface inflow that



**EXPLANATION**

- Mines, mills, and mine tunnels
- Hydrography
- OTIS model downstream boundary
- Sampled inflow sites
- Sampled stream sites
- Sampled and labeled stream sites and end of OTIS model reach

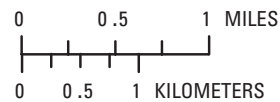


**Figure 8.** Location of stream reach of lower Cement Creek mass-loading study (September 1996) and OTIS solute-transport model. Stream- and inflow-sample data provided in Sole and others (this volume). Mining features shown (and inventory numbers, from Church, Mast, and others, this volume) include American tunnel level of Sunnyside mine (# 96); Anglo Saxon mine (# 183); May Day mine (# 181); and Yukon Mill (# 184) and tunnel (# 186). Mining features shown are limited to those discussed in the text. See Church, Mast, and others (this volume) for a complete inventory. Base from Digital Orthophoto Quads, Transverse Mercator, -105.00 central meridian, 1927 datum.

might have been associated with the surface flow. In addition to the 54 stream samples, 44 inflow sites were sampled to characterize watershed contributions to the stream.

Water quality in lower Cement Creek deteriorated somewhat from the site of the injection to the end of the study reach as evidenced by lower pH and greater loads of metals. In 1996, all of the flow from upper Cement Creek was being diverted into the treatment system for the Sunnyside mine effluent. Consequently, Cement Creek upstream from the South Fork Cement Creek confluence had a near-neutral pH (7.5). South Fork Cement Creek was acidic (pH was 3.7). Below the confluence, at 1,106 m, Cement Creek had a pH of 6.5 that decreased to 3.7 at the U.S. Geological Survey's streamflow gauging station at 11,558 m. Similarly, total (unfiltered) copper, iron, and zinc concentrations in the mainstem of Cement Creek upstream from South Fork Cement Creek were approximately 0.03, 0.5, and 0.8 mg/L and were 0.04, 3.7, and 0.9 mg/L in South Fork Cement Creek. These streams mixed to yield water downstream from the confluence (at 1,106 m) having 0.04, 2.7, and 0.9 mg/L copper, iron, and zinc. At the end of the study reach (11,558 m), total concentrations of copper, iron, and zinc were 0.04, 7.8, and 0.8 mg/L. As the flow had increased approximately 8-fold from the upstream end of the study reach to the downstream end, the downstream concentrations, though similar to the upstream concentrations, represent much larger metal loads.

The results of the lower Cement Creek basin-loading analysis (Kimball and others, this volume; Kimball and others, 2002) indicated that during the 1996 sampling, more than 50 percent of the load of copper, iron, and zinc was from diffuse subsurface flow to the stream. Distinct areas where significant loading occurred for one, two, or all three of the metals include areas upstream from the study reach in the mainstem of Cement Creek and South Fork Cement Creek; the Prospect Gulch and upper iron bog area; the Minnesota Gulch area; Ohio Gulch; the Yukon tunnel (# 186) at the mouth of Illinois Gulch; and the lower bog (fig. 8).

## Determination of Physical Parameters and Boundary Conditions

Lower Cement Creek (from Gladstone to Silverton) was divided into 30 model reaches (table 6). Model parameters required for these simulations include the dispersion coefficient ( $D$ ), the cross-sectional area of the stream ( $A$ ), an upstream-boundary condition ( $U_b$ ), and the lateral inflow rate ( $q_L$ ) and concentration ( $C_L$ ) for each reach. A uniform dispersion coefficient of 1.0 m was used for all reaches. The coefficient  $A$  was estimated using OTIS-P (Appendix). Determination and values of  $U_b$ ,  $q_L$ ,  $C_L$ , and  $\lambda$  are presented in this section.

The 30 model reaches were chosen to bracket inflows shown to be significant during the loading analysis (Kimball and others, this volume). Simulations were constructed for the lithium tracer, and for filtered (0.1  $\mu\text{m}$ ) concentrations of copper and zinc, and unfiltered (total) concentrations of iron. A large proportion of iron in lower Cement Creek is colloidal,

and the ratio of total iron to colloidal iron shifts as the pH changes in the creek. When pH decreases enough that colloids dissolve, the dissolved iron load increases. Conversely, when pH increases enough that iron colloids precipitate, the dissolved iron load decreases. If dissolved iron concentration is used in the model, these decreases and increases in dissolved iron load can be mistaken as sinks and sources of iron in the stream, rather than as shifts in iron speciation. The use of total iron concentration in the model avoids this misinterpretation of the data. But then, the loss of total iron from the stream is due to settling, or precipitation and settling of iron mineral phases, not simply chemical precipitation of iron phases. (Note, in upper Cement Creek, colloidal iron concentrations were low, so dissolved iron concentrations were used in the OTIS solute-transport model—see Kimball and others, this volume, fig. 9). The upstream boundary of the model was at 990 m, on South Fork Cement Creek, just upstream from the confluence with Cement Creek and approximately coinciding with the location of the start of the tracer injection (fig. 8). Cement Creek upstream from South Fork Cement Creek was treated as a tributary that was sampled at 1,050 m distance along the study reach. In presentation of the results, samples collected from this site on Cement Creek were shown as the most upstream inflow. South Fork Cement Creek upstream from the confluence was treated as the mainstem for plots of the data and modeling results. The most upstream sampling point on South Fork Cement Creek was located upstream from the confluence, but downstream from the tracer injection at 1,041 m. In the model, the confluence between South Fork Cement Creek and Cement Creek occurred in model reach 2 (table 6) and the streams were assumed mixed by the end of that model reach (1,106 m). The upstream boundary conditions were as follows: lithium 2.96 mg/L, filtered copper 0.04 mg/L, total iron 3.75 mg/L, and filtered zinc 0.87 mg/L. These concentrations were measured in the stream at site 1,041 m, the first sampling site downstream from the injection.

## Model Calibration for Simulation of the Lithium Tracer Profile

The simulated steady-state lithium profile is consistent with the data (fig. 9) and indicates that calculated streamflow was consistent with the dilution of lithium observed at the synoptic-sampling sites. Flow at the upstream end of the study reach was 91 L/s. Flow at the downstream end of the study reach was 703 L/s. Lithium concentrations were 3.0 mg/L at the beginning of the study reach and were diluted by inflows to 0.39 mg/L at the end of the study reach. Visible and sampled surface-water inflow and ground-water seepage accounted for 74 percent of the inflow. The principal inflows to the study reach were the main fork of Cement Creek at 1,050 m that contributed 91 L/s to streamflow;

- Prospect Gulch, 2,795 m, 9.7 L/s;
- Georgia Gulch, 3,793 m, 16.3 L/s;
- Minnesota Gulch, 5,512 m, 14.3 L/s;
- Porcupine Gulch, 5,907 m, 22.7 L/s;

**Table 6.** Lower Cement Creek, reach number, distance at end of reach, and description of reaches used in OTIS modeling of synoptic samples collected for lower Cement Creek (September 1996).

[Distance is downstream from arbitrary stream datum; m, meter. Reach numbers correspond to those in figures 9–11]

Model reach	Distance (m)	Brief description of reach and significant inflows
1	1,050	South Fork Cement Creek upstream from confluence with Cement Creek.
2	1,106	Cement Creek downstream from confluence with South Fork Cement Creek.
3	2,245	Cement Creek downstream from Dry Gulch inflow. Some iron bog inflow on right bank.
4	2,785	Cement Creek upstream from Prospect Gulch, some iron bog inflow on right bank.
5	2,970	Cement Creek downstream from Prospect Gulch inflow (2,795 m).
6	3,125	No sampled inflows in this reach.
7	3,317	Cement Creek downstream from numerous iron bog inflows on both banks.
8	3,655	Cement Creek upstream from Tiger Gulch.
9	3,893	Cement Creek downstream from Tiger (3,670 m) and Georgia (3,793 m) Gulches.
10	4,260	Cement Creek at 4,260 m.
11	4,483	Cement Creek upstream from Fairview Gulch.
12	4,586	Cement Creek downstream from Fairview Gulch (4,493 m).
13	5,050	Cement Creek upstream from Cascade Gulch.
14	5,215	Cement Creek downstream from Cascade Gulch (5,100 m).
15	5,365	Cement Creek upstream from Minnesota Gulch.
16	5,652	Cement Creek downstream from Minnesota Gulch (5,490 and 5,512 m).
17	5,767	Cement Creek upstream from Anglo-Saxon mine.
18	5,897	Cement Creek downstream from Anglo-Saxon mine inflows (5,817 and 5,857 m).
19	5,957	Cement Creek downstream from Porcupine Gulch (5,907 m).
20	6,447	Cement Creek upstream from Ohio Gulch.
21	6,907	Cement Creek downstream from Ohio Gulch (6,781 m).
22	7,131	Cement Creek downstream from Illinois Gulch (7,006 m).
23	7,331	Cement Creek downstream from the Yukon tunnel (no visible surface inflow).
24	7,501	Cement Creek downstream from the May Day mine and dump (no visible surface inflow).
25	7,698	Cement Creek downstream from Topeka Gulch (7,548 m).
26	9,060	Cement Creek downstream from Niagara (8,422 m) and Hancock (8,735 m) Gulches.
27	9,360	Cement Creek upstream from lower iron bog.
28	9,905	Cement Creek downstream from lower iron bog inflow (9,543 m).
29	10,130	Cement Creek downstream from unnamed mine (no surface inflow).
30	11,740	Cement Creek downstream from the gauging station (11,558 m).

Ohio Gulch, 6,781 m, 9.7 L/s;  
 Illinois Gulch, 7,006 m, 52.3 L/s;  
 Topeka Gulch, 7,548 m, 12.9 L/s;  
 Niagara Gulch, 8,422 m, 13.5 L/s; and  
 Hancock Gulch, 8,735 m, 14.1 L/s.

Tiger Gulch (3,670 m) and Cascade Gulch contributed less than 5 L/s each. Dry Gulch and Fairview Gulch contained no surface inflow during the synoptic sampling. Two adits discharged flow directly into Cement Creek: an unnamed adit at 4,493 m contributed 15.2 L/s, and the Anglo Saxon mine (# 183) at 5,817 and 5,857 m contributed a total of 14 L/s. Twenty-six percent of the flow represented unsampled ground-water inflow that was dispersed along the length of the study reach (Kimball and others, 2002; Kimball and others, this volume). Some of this unsampled inflow was spatially associated with alluvial ferricrete deposits, sedge bogs, and springs in the stream reach from 9,360 to 9,905 m (Yager and Bove, this volume, pl. 2). These ferricrete deposits and iron-rich springs

were similar to those prevalent along the Prospect Gulch reach. The springs in this area are referred to as the lower bog and are indicative of ground-water inflow. Slickensides were also observed on rock outcrops along this reach, indicating that faulting has occurred in the area; the faults may be conduits for ground-water flow into the stream. Minor adjustments were made to streamflow in the model reach from 9,060 to 9,360 m relative to the streamflow presented in Kimball and others (this volume) and Sole and others (this volume, Chapter G, project database). In Kimball and others (this volume), no increase occurred in streamflow for this reach. However, iron data showed significant concentration increases in the model reach that could not be simulated without the inclusion of some increase in flow along the model reach. For the simulations, flow at 9,060 m was 636 L/s; flow at 9,360 m was 648 L/s versus 636 L/s at both sites in Kimball and others (this volume). At all other locations, streamflow was the same as that used by Kimball and others (this volume).

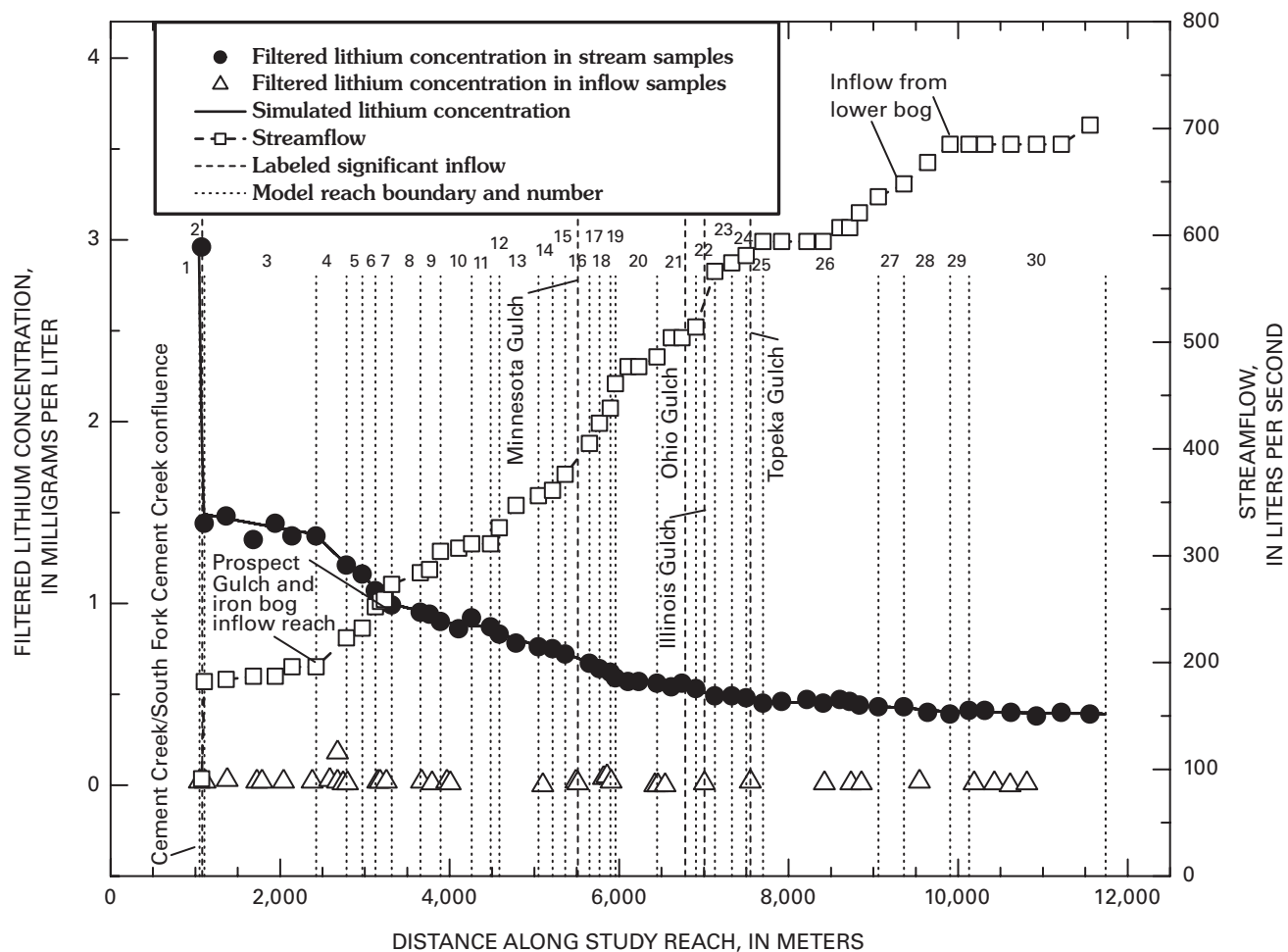


**Figure 9.** Variation in lithium concentration, streamflow, and simulated lithium concentration with distance, showing location of OTIS model reaches and significant features, lower Cement Creek mass-loading study (September 1996) and OTIS solute-transport model.

## Model Calibration for Copper, Iron, and Zinc Simulations

Simulations for lower Cement Creek used a variety of estimation techniques for lateral-inflow concentrations ( $C_L$ ). In general, the techniques were not nearly as consistent across lower Cement Creek model reaches or between metals as for upper Cement Creek. Effective or representative inflow concentrations were used most often in the copper, iron, and zinc simulations (fig. 10; table 7). Only two model reaches used flow-weighted average concentrations: model reach 16 for copper, and model reach 26 for iron. Thirteen model reaches showed no inflow concentration for copper; 7 model reaches showed no inflow concentration for iron; and 5 model reaches showed no inflow concentration for zinc (table 7). In these reaches streamflow increased, but no increase in metal load occurred in the reach. For copper, one reach (model reach 17) used the  $C_L$  value from the adjacent upstream reach; and one reach (model reach 26) used a  $C_L$  value that was greater than the value from the representative inflow in the reach, but less than the calculated effective inflow. For iron, one reach (model

reach 8) used a  $C_L$  value that was the average of the value used in the adjacent upstream and downstream reaches, and two reaches (model reaches 17 and 27) used  $C_L$  values from the adjacent downstream model reaches. For zinc, two reaches (model reaches 6 and 17) used  $C_L$  values from the adjacent downstream reaches; a value greater than the representative inflow but less than the calculated effective inflow was used in model reach 20, and in model reaches 27 and 28,  $C_L$  values were greater than calculated effective inflow. For all metals, the highest  $C_L$  value is greater than the highest concentration of the observed inflows (fig. 13). In particular, in the reaches including Ohio Gulch (model reach 21), the Yukon tunnel (# 186; model reach 23), and the tailings at May Day mine (# 181; model reach 24), some of the  $C_L$  values for copper and zinc were greater than any sampled inflow values. Additional sampling within the May Day mine (# 181) identified water samples having extremely elevated concentrations of copper and zinc (almost as high as 70 mg/L copper and approximately 200 mg/L zinc—Wright, Kimball, and Runkel, this volume, Chapter E23). In addition, a low-pH, metal-rich seep along the west bank of Cement Creek in the vicinity of the May Day

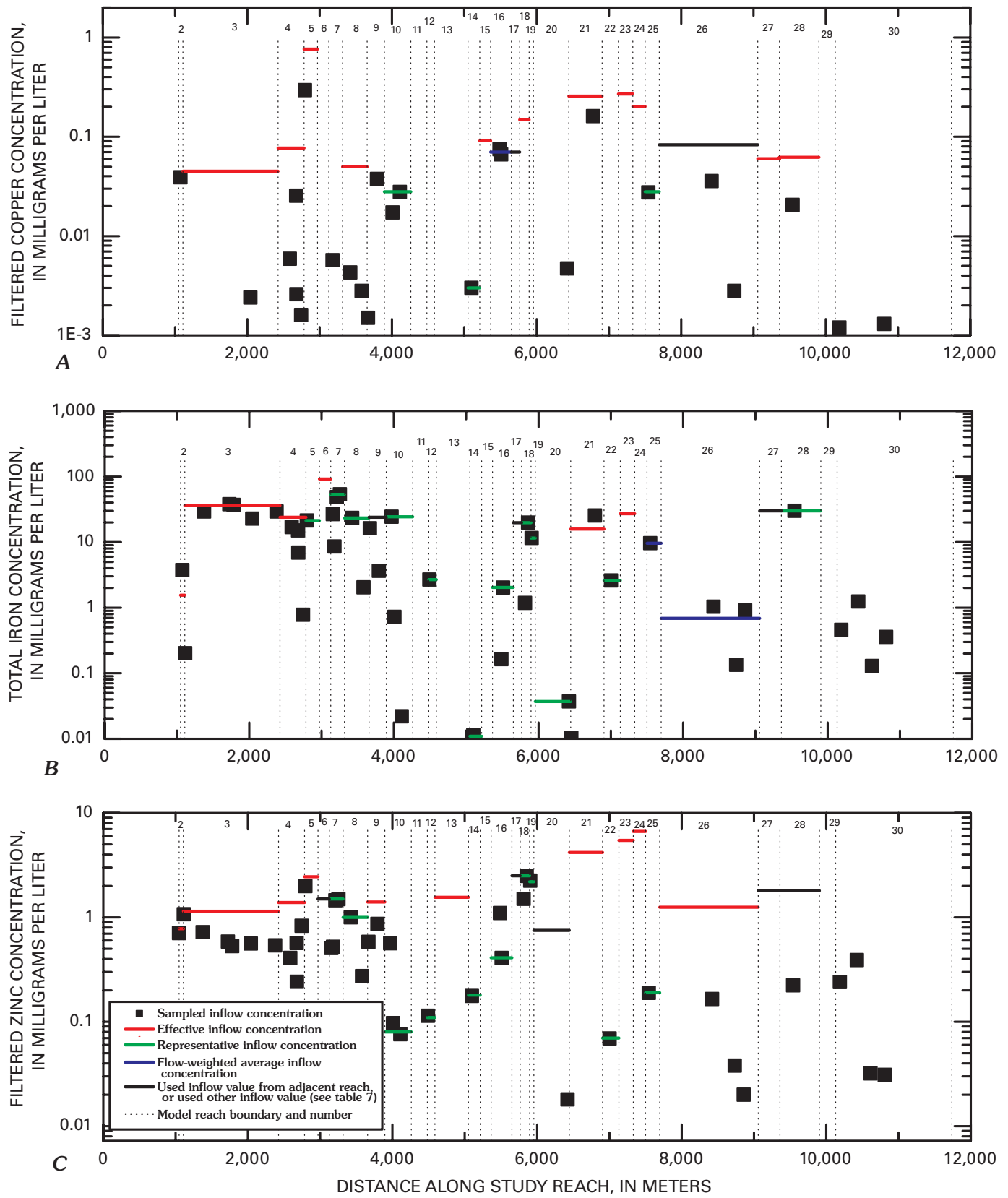


**Figure 10.** Variation in calibrated lateral-inflow concentrations and observed inflow concentrations (September 1996) with distance for A, filtered copper; B, total iron; C, filtered zinc showing OTIS model reaches, lower Cement Creek OTIS model.

**Table 7.** Lower Cement Creek, samples and methods used to estimate lateral-inflow concentrations ( $C_L$ ) for copper, iron, and zinc in calibrated OTIS model.

[Synoptic samples collected September 1996. Numeric values represent distances (in meters, m) of inflow samples used in estimation technique (inflow samples are in project database, Sole and others, this volume). **Bold** indicates the end of an adjacent model reach whose value was used for lateral-inflow concentration. Alpha characters indicate method used to estimate lateral inflow: NI, no lateral-inflow concentration; R, representative inflow concentration used for lateral-inflow concentration; F, flow-weighted average value used for lateral-inflow concentration; E, effective inflow concentration used for lateral-inflow concentration. Lateral-inflow concentration values shown in figure 10]

Model reach	Distance (m)	Dissolved copper	Total iron	Dissolved zinc
1	1,050	NI	NI	NI
2	1,106	NI	E	E
3	2,425	E	E	E
4	2,785	E	E	E
5	2,970	E	R, 2,795	E
6	3,125	NI	E	<b>3,317</b>
7	3,317	NI	R, 3,255	R, 3,255
8	3,655	E	R, 3,425	R, 3,425
9	3,893	NI	<b>3,655, 4,260<sup>a</sup></b>	E
10	4,260	R, 4,110	R, 3,968	R, 4,110
11	4,483	NI	NI	NI
12	4,586	NI	R, 4,493	R, 4,493
13	5,050	NI	NI	E
14	5,215	R, 5,100	R, 5,100	R, 5,100
15	5,365	E	NI	NI
16	5,652	F 5,490, 5,512	R, 5,512	R, 5,512
17	5,767	<b>5,652</b>	<b>5,897</b>	<b>5,897</b>
18	5,897	E	R, 5,857	R, 5,857
19	5,957	NI	R, 5,907	R, 5,907
20	6,447	NI	R, 6,422	0.75 mg/L <sup>b</sup>
21	6,907	E	E	E
22	7,131	NI	R, 7,006	R, 7,006
23	7,331	E, 0.270	E	E
24	7,501	E, 0.202	NI	E
25	7,698	R, 7,548	R, 7,548	R, 7,548
26	9,060	0.083 (<E, >R)	F, 8,422, 8,735, 8,860	E
27	9,360	E, 0.060	<b>9,905</b>	1.8 mg/L (>E)
28	9,905	E	R, 9,543	1.8 mg/L (>E)
29	10,130	NI	NI	NI
30	11,740	NI	NI	NI

<sup>a</sup>In model reach 9, the lateral-inflow concentration for total iron was the average value used in the adjacent upstream and downstream model reaches.

<sup>b</sup>The lateral-inflow concentration value for dissolved zinc in model reach 20 was less than the effective inflow concentration and greater than the representative inflow concentration.

tailings pile contained copper concentrations of approximately 0.3 mg/L and zinc concentrations of approximately 5 mg/L (Wright, Kimball, and Runkel, this volume). Geophysical surveys showed a high conductivity zone in the area that indicated near-surface ground-water flow paths as a source of water containing high dissolved solids (Smith and others, this volume, Chapter E4); they were probably the source for this seep. The seep was not sampled during the 1996 mass-loading study, but the concentrations cited previously are similar to those used for  $C_L$  in that reach. Therefore, it was not unrealistic to use elevated values in the Ohio Gulch to Topeka Gulch reach of the stream that includes the May Day mine and tailings.

Steady-state, conservative simulations of iron, copper, and zinc (fig. 11) overestimated the ambient concentrations. Therefore, simulations with OTIS-P were conducted to estimate first-order removal coefficients ( $\lambda$ ) for some of the model reaches (table 8). Simulations including first-order removal coefficients fit the data well (fig. 14). First-order removal coefficients (greater than  $1.0 \times 10^{-5} \text{s}^{-1}$ ) were used in model reaches 7, 18, 19, 22, 24, and 30 for all three metals. First-order removal coefficients were used for two of the metals in model reaches 3, 8, 9, 10, and 12 (table 8). First-order removal coefficients were used for iron only in model reaches 11 and 15. Stream pH decreased from a high of 6.45 downstream from the confluence with South Fork Cement Creek (1,106 m), to 5.25 upstream

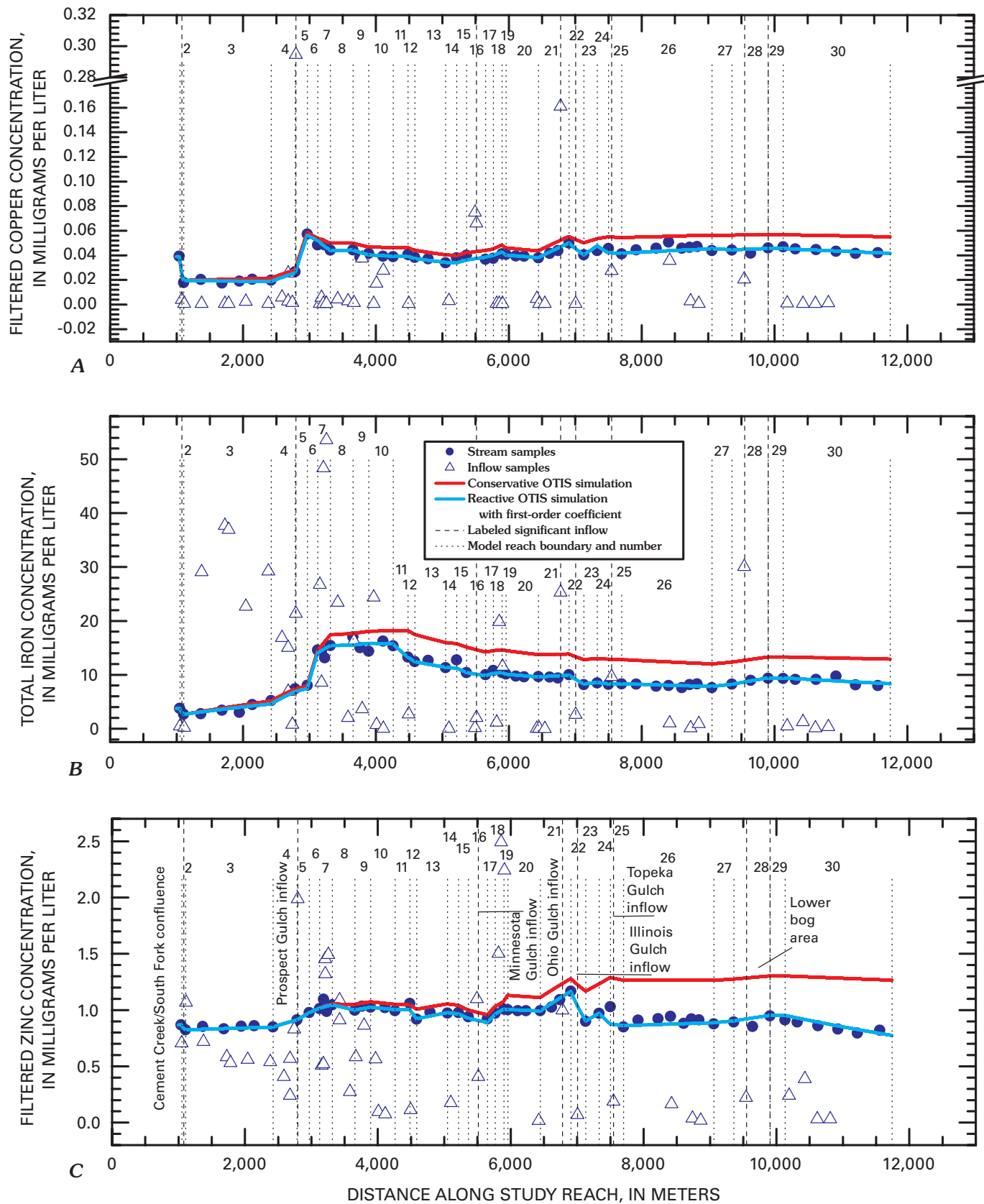


**Figure 11.** Variation in *A*, filtered copper; *B*, total iron; *C*, filtered zinc concentrations with distance in stream and inflow samples (September 1996) and in OTIS conservative and calibrated reactive simulations, showing model reach and number and location of significant features, lower Cement Creek. Reactive OTIS simulation included first-order removal coefficients ( $\lambda$ ).

**Table 8.** Lower Cement Creek, first-order removal coefficients ( $\lambda$ ) by metal and reach for calibrated OTIS model.[All values in second<sup>-1</sup>]

Model reach	Distance (m)	Dissolved copper	Total iron	Dissolved zinc
1	1,050	0.00	0.00	0.00
2	1,106	0.00	0.00	0.00
3	2,245	$3.40 \times 10^{-5}$	$3.72 \times 10^{-5}$	0.00
4	2,785	0.00	0.00	0.00
5	2,970	0.00	0.00	0.00
6	3,125	0.00	0.00	0.00
7	3,317	$1.90 \times 10^{-4}$	$2.47 \times 10^{-4}$	$1.45 \times 10^{-5}$
8	3,655	0.00	$2.02 \times 10^{-5}$	$5.96 \times 10^{-5}$
9	3,893	$4.06 \times 10^{-5}$	$2.02 \times 10^{-5}$	0.00
10	4,260	$2.06 \times 10^{-5}$	$2.02 \times 10^{-5}$	0.00
11	4,483	0.00	$2.87 \times 10^{-4}$	0.00
12	4,586	0.00	$9.90 \times 10^{-5}$	$1.61 \times 10^{-4}$
13	5,050	0.00	0.00	0.00
14	5,215	0.00	0.00	0.00
15	5,365	0.00	$9.82 \times 10^{-5}$	0.00
16	5,652	0.00	0.00	0.00
17	5,767	0.00	0.00	0.00
18	5,897	$5.84 \times 10^{-5}$	$5.66 \times 10^{-5}$	$1.30 \times 10^{-5}$
19	5,957	$5.84 \times 10^{-5}$	$2.51 \times 10^{-5}$	$4.50 \times 10^{-4}$
20	6,447	0.00	0.00	0.00
21	6,907	0.00	0.00	0.00
22	7,131	$2.70 \times 10^{-4}$	$2.54 \times 10^{-4}$	$3.8 \times 10^{-4}$
23	7,331	0.00	0.00	0.00
24	7,501	$3.70 \times 10^{-4}$	$6.62 \times 10^{-5}$	$5.50 \times 10^{-4}$
25	7,698	0.00	0.00	0.00
26	9,060	0.00	0.00	0.00
27	9,360	0.00	0.00	0.00
28	9,905	0.00	0.00	0.00
29	10,130	0.00	0.00	0.00
30	11,740	$2.00 \times 10^{-5}$	$3.14 \times 10^{-5}$	$6.0 \times 10^{-5}$

from Prospect Gulch (2,785 m), and to 4.23 downstream from Prospect Gulch (3,125 m); pH remained at less than 4.5 for the downstream extent of the study reach. First-order removal coefficients generally were located in model reaches downstream from inflows that had elevated concentrations of metals or downstream from inflows that had high pH. Examples of model reaches having a first-order removal coefficient and located downstream from inflows having elevated metal concentrations are model reach 3 downstream from the upper iron bog inflows; model reaches 7 through 10, which included areas downstream from Prospect Gulch (2,795 m), iron bog inflows, Tiger Gulch (3,670 m), and Georgia Gulch (3,793 m); model reach 18 downstream from the Anglo-Saxon mine inflow (# 183); model reach 19 downstream from Porcupine Gulch; and model reach 24 downstream from the May Day mine (# 181). Examples of model reaches having first-order removal coefficients and located downstream from high-pH inflows are model reach 12 downstream from an adit inflow (pH = 7.25);

model reach 22 downstream from Illinois Gulch (pH = 7.6); and model reach 30, where all inflows along the reach had pH values greater than 6.90. Metal removal downstream from areas that receive metal loading probably occurred because stream water was supersaturated with respect to iron oxyhydroxide phases such as schwertmannite or ferrihydrite, which precipitate out of solution. Cement Creek is colored orange from precipitating iron minerals for much of the study reach, and schwertmannite has been identified in streambed-sediment samples (Desborough and others, 2000). Coprecipitation or sorption of the copper and zinc with the iron phase accounts for the accompanying removal of these metals. Removal of metals downstream from high-pH inflows probably occurs in the mixing zones of the high-pH tributary and the creek. In this case, solubility of iron phases such as schwertmannite or ferrihydrite is probably exceeded because of the elevated pH in the mixing zone, rather than because of an increase in metal concentrations. In each case, the net effect is similar; amorphous iron minerals precipitate and contain sorbed or coprecipitated copper and zinc. The relatively small size (less than  $10^{-3}$  s<sup>-1</sup>) and limited distribution of removal coefficients, however, indicate that reactive processes are operating only to a minimal extent for the metals considered in the study reach.

Removal coefficients in model reaches 3 (1,106 to 2,245 m) and 15 (5,215 to 5,365 m) are more difficult to explain as neither reach fits the two scenarios just described. However, model reach 3 was an area of the stream that experienced elevated metal loading and where pH also was elevated. So, precipitation of iron minerals is possible. Model reach 15 is 265 m downstream from the confluence with Cascade Gulch (5,100 m), which had a pH of 7.13. Removal in reach 15 may be due to the effects of the high-pH inflow or to some iron loading that occurred associated with the Minnesota Gulch area inflows described in Kimball and others (2002).

## Remediation Simulations

Five remediation scenarios were simulated using the calibrated OTIS model for lower Cement Creek (table 9)<sup>2</sup>. The maximum remediation that could be assigned to mining was chosen for each target location. Whereas the large contributions attributed to mining in some of the scenarios may be debatable, even though most are derived from published sources, these large numbers were used to illustrate the maximum effect that might occur from cleanup of mining-associated effects on water quality.

The first scenario simulated remediation of inflows to Prospect Gulch associated with historical mining activity on Federal land. These inflows were quantified in a metal-loading study conducted during low-flow conditions in September 1999 (Wirt and others, 2001). The study concluded that inflows

<sup>2</sup>Table 9 describes the five remediation scenarios and scenario 6, which is a simulation of instream effects of the changed conditions at the Mogul mine—which is covered in the following section.

**Table 9.** Lower Cement Creek, simulated concentrations at the mouth of lower Cement Creek resulting from five remediation scenarios, and from changed conditions at the Mogul mine (scenario 6).

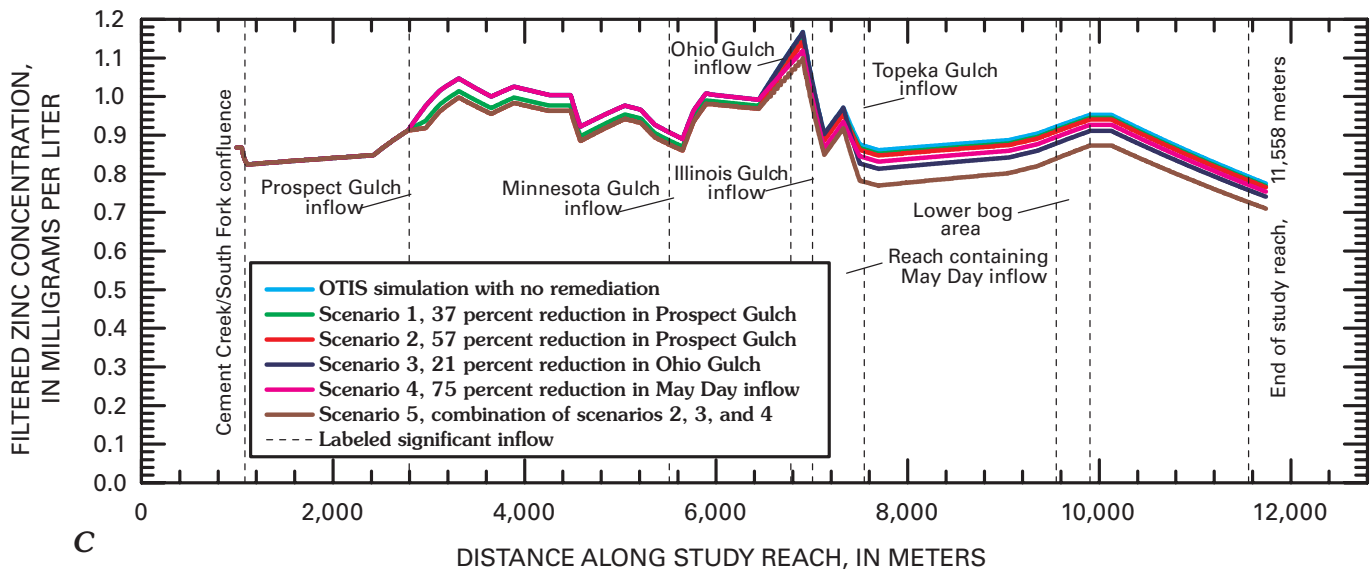
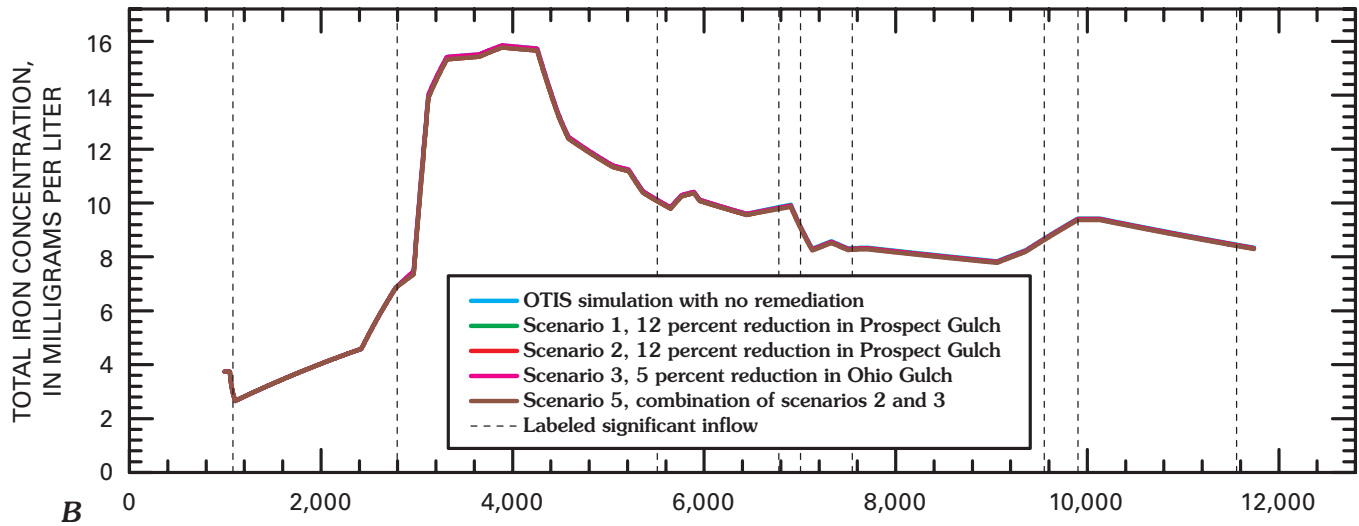
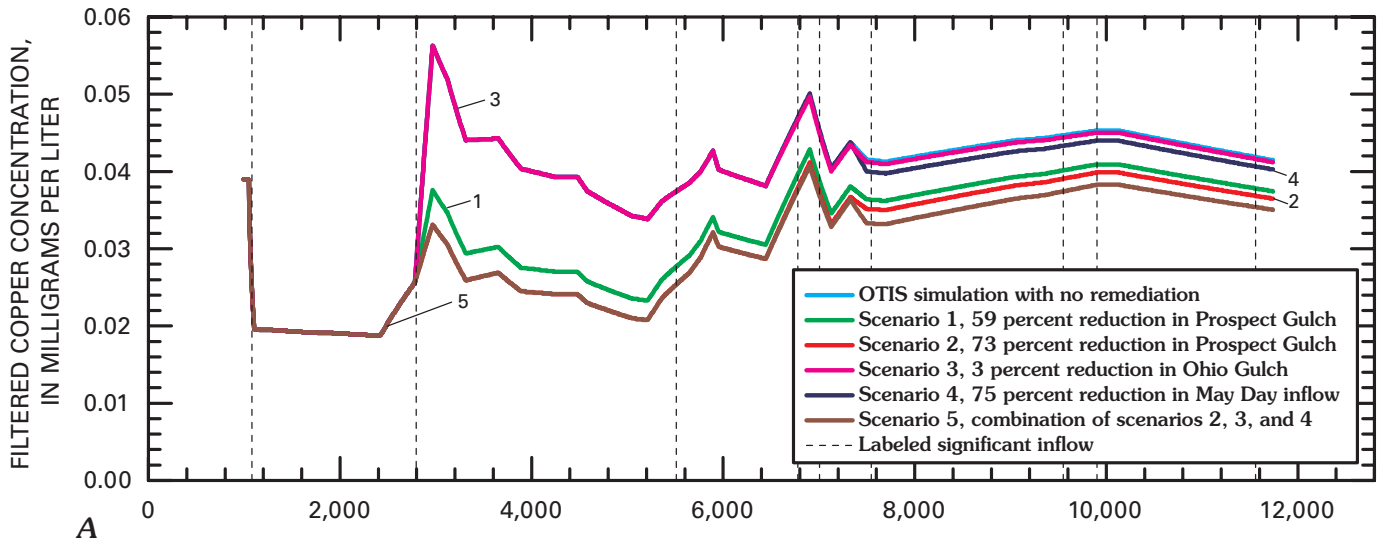
[Concentration values in milligrams per liter. NA, not applicable]

Remediation		Filtered copper	Total iron	Filtered zinc
Simulated concentration at end of study reach (11,558 m) in calibrated model.		0.042	8.45	0.793
Scenario 1: Prospect Gulch: 59 percent reduction in copper, 12 percent reduction in iron, 37 percent reduction in zinc.	Simulated concentration at end of study reach (11,558 m).	0.038	8.44	0.786
	Percent reduction	10	0.1	0.9
Scenario 2: Prospect Gulch: 73 percent reduction in copper, 12 percent reduction in iron, 57 percent reduction in zinc.	Simulated concentration at end of study reach (11,558 m).	0.037	8.44	0.783
	Percent reduction	12	0.1	1.3
Scenario 3: Ohio Gulch: 3 percent reduction in copper, 5 percent reduction in iron, 21 percent reduction in zinc.	Simulated concentration at end of study reach (11,558 m).	0.042	8.43	0.772
	Percent reduction	0	0.2	2.6
Scenario 4: May Day mine: 75 percent reduction in copper, 75 percent reduction in zinc.	Simulated concentration at end of study reach (11,558 m).	0.041	NA	0.758
	Percent reduction	2.4	NA	4.4
Scenario 5: Combined result of scenarios 2, 3, and 4.	Simulated concentration at end of study reach (11,558 m).	0.035	8.41	0.727
	Percent reduction	17	0.5	8.3
Scenario 6: Simulating changes in the mainstem of Cement Creek due to changes at the Mogul mine. Upper boundary conditions of the OTIS model were copper, 1.22 mg/L; iron, 5.7 mg/L; zinc, 7.27 mg/L.	Simulated concentration at end of study reach (11,558 m).	0.180	8.83	1.46
	Percent increase	329	5	84

associated with inactive mines located on Federal land caused 59 percent of the copper loading, 12 percent of the iron loading, and 37 percent of the zinc loading observed at the mouth of Prospect Gulch. Remediation scenario 1 reduced loads in Prospect Gulch by these amounts. The second remediation scenario reduced all mining-related inflows (those on both private and Federal land) in Prospect Gulch to negligible concentrations. Wirt and others (2001) indicated that mining-related contribution from private and Federal land caused 73 percent of the copper load, 12 percent of the iron load, and 57 percent of the zinc load observed at the mouth of Prospect Gulch. Remediation scenario 2 reduced loads in Prospect Gulch by these amounts. Scenario 3 reduced mining-related inflows from three mines in Ohio Gulch. Detailed mass-loading studies were not conducted in Ohio Gulch. However, the three largest mining contributors were sampled and caused approximately 3, 5, and 21 percent of the copper, iron, and zinc loading observed at the mouth of the gulch (W.G. Wright, written commun., 2002). Scenario 4 considered the reach of the stream affected by the May Day mine (# 181) and tailings. Detailed mass-loading and geochemical studies along that reach indicated that, at most,

75 percent of the load to the stream was related to mining activity at the May Day site (Wright, Kimball, and Runkel, this volume). Accordingly, remediation scenario 4 reduced copper and zinc concentrations in the model reach containing the May Day mine by 75 percent each. The calibrated lateral-inflow concentration ( $C_L$ ) value for iron was 0.00 in that model reach, so the simulation of a reduced iron concentration was not possible. Remediation scenario 5 combined remediation scenarios 2, 3, and 4.

The results of the remediation scenarios (fig. 12; table 9) indicated that the combined remediation (remediation scenario 5) reduced copper, iron, and zinc concentrations by approximately 17 percent, 0.5 percent, and 8.3 percent at the mouth of Cement Creek. Remediation scenario 2 (the larger of the Prospect Gulch remediations) had the greatest effect on copper concentrations and reduced them by 12 percent at the mouth of Cement Creek. The May Day remediation had the largest effect on zinc concentrations and reduced zinc concentrations at the mouth of Cement Creek by 4.4 percent. Iron concentrations were not reduced by any of the remediation scenarios. Although the maximum possible reductions



for mining sources were chosen for the areas targeted in the simulations, the resulting metal reductions were relatively small. These modest reductions resulted because metal sources to lower Cement Creek were spread over much of the length of the study reach, both in tributaries that were not considered in the remediation scenarios (such as Minnesota Gulch and related inputs in the area near 5,500 m) and in diffuse ground-water inflows (such as in the iron bog area in the vicinity of Prospect Gulch, and the lower iron bog area). These results differ from those for upper Cement Creek, where the metal sources were largely confined to four major inflows, and where remediation simulations showed larger effects on metal concentrations.

### Simulation of the Effect of Changed Conditions at the Mogul Mine

In early September 1996, a bulkhead was placed in the American tunnel (# 96, Finger and others, this volume, Chapter F). Results of synoptic studies performed in Cement Creek indicated that the chemistry and flow from the Mogul mine changed between the lower Cement Creek metal-loading study in 1996 and the upper Cement Creek metal-loading study in 1999 (Kimball and others, this volume; Bove and others, this volume). The result of this change was that metal concentrations in upper Cement Creek downstream from the Mogul mine were greater in 1999 than in 1996 (Kimball and others, this volume). The calibrated OTIS model for lower Cement Creek was used to simulate the potential effects of this changed chemistry on metal concentrations at the mouth of Cement Creek.

Two changes were made in the upstream-most reaches of the calibrated model to simulate the changed conditions in upper Cement Creek in 1999. First, the calibrated model used metal concentrations and streamflow measured in 1996 at the mainstem Cement Creek upstream from South Fork Cement Creek for lateral-inflow concentrations ( $C_L$ ) and lateral inflow ( $q_L$ ) in model reach 2. To simulate concentration changes resulting from change upstream at the Mogul mine, the  $C_L$  and  $q_L$  values for this reach were adjusted to match the values measured in 1999 during the upper Cement Creek mass-loading study. Second, the 1999 upper Cement Creek data set also provided concentration and flow information for South Fork Cement Creek just upstream from the confluence. The boundary conditions (streamflow and concentrations of filtered copper, total iron, and filtered zinc) of the 1996 model were changed to represent the 1999 conditions at this point.

**Figure 12 (facing page).** Variation in *A*, filtered copper; *B*, total iron; *C*, filtered zinc concentrations with distance in OTIS simulations of remediation scenarios, showing location of significant features, lower Cement Creek. Details of remediation scenarios, table 9. In view *A*, OTIS simulation with no remediation is upper line and is overprinted by remediation scenarios 3 and (or) 4 until just upstream from Topeka Gulch inflow. Simulations all overprint each other in view *B*.

The simulation was then performed with no other changes to observe the effect at the mouth of Cement Creek. This simulation is referred to as “Scenario 6” in table 9.

Agreement is good between the streamflow predicted by the model in 1999 and the streamflow measured at the gauge on September 20, 1999. In the simulation, streamflow at the bottom of the study reach (11,558 m) was 820 L/s compared to 703 L/s for the calibrated 1996 model. This increase was due to the increased flow used at the boundary condition (91 L/s in 1996, 147 L/s in 1999) and the inflow reach (model reach 2) for the mainstem of Cement Creek (91 L/s 1996; 152 L/s 1999). The simulated streamflow value was only 3 percent greater than the average daily streamflow on September 20, 1999 (793 L/s; Crowfoot and others, 1997), the day that the model attempted to recreate. The good agreement between flow values in the model and the environmental data increases confidence in the modeling results.

The results of the simulation of Scenario 6 indicate that at the gauge at Cement Creek, filtered copper and zinc concentrations increased 329 percent and 84 percent. Total iron concentration increased 5 percent (table 9; fig. 13).

It is possible to compare the simulated increases in filtered copper and zinc concentrations to data collected at the mouth of Cement Creek to assess whether the simulation approximated environmental conditions observed at the mouth of Cement Creek. In the course of several sampling programs, samples were routinely collected at the mouth of Cement Creek from 1996 to 2001 (Leib and others, 2003). The results for filtered copper, total iron, and filtered zinc concentrations (using 0.45- $\mu$ m filtration) seem to show a shift to higher copper and zinc concentrations sometime between July 1999 and August 1999 (fig. 14). Dates where flow conditions approximate those observed on September 20, 1996 and 1999 (approximately 20 to 30 ft<sup>3</sup>/s, or 566 to 850 L/s) are indicated on the graph (fig. 14). On the six dates indicated, copper and zinc concentrations are greater on the three later dates than on the earlier dates. The shift to higher copper and zinc concentrations beginning around July 1999 is more apparent with a rigorous analysis of the relations between filtered copper and zinc concentrations and streamflow.

Linear regression models were constructed between filtered copper and zinc and streamflow using the data presented in figure 14. For each model, copper and zinc concentrations were log-transformed. The streamflow data were transformed using a hyperbolic transformation:

$$Q_{trans} = 1/(1+(beta * Q)) \tag{3}$$

where

$Q_{trans}$  is the transformed streamflow value,  
 $Q$  is the streamflow data,

and

$beta$  is a parameter that can vary from  $10^{-3} * Q_m^{-1}$  to  $10^2 * Q_m^{-1}$  (where  $Q_m$  is the mean value of the measured streamflow) to obtain the most linear representation of the data (Crawford and others, 1983).

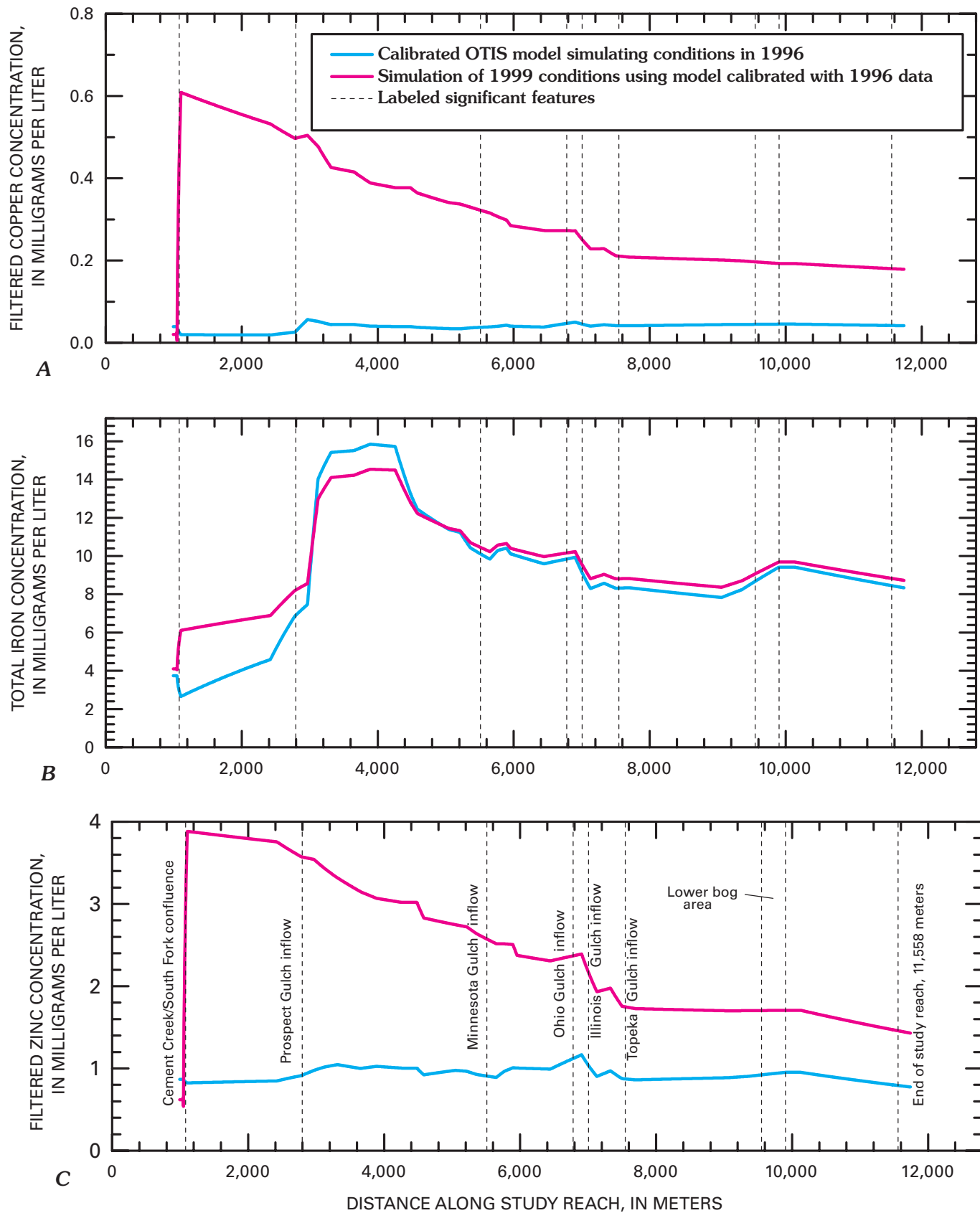


**Figure 13.** Variation in A, filtered copper; B, total iron; C, filtered zinc with distance in calibrated OTIS simulations and OTIS simulations of 1999 conditions in Cement Creek and South Fork Cement Creek, lower Cement Creek.

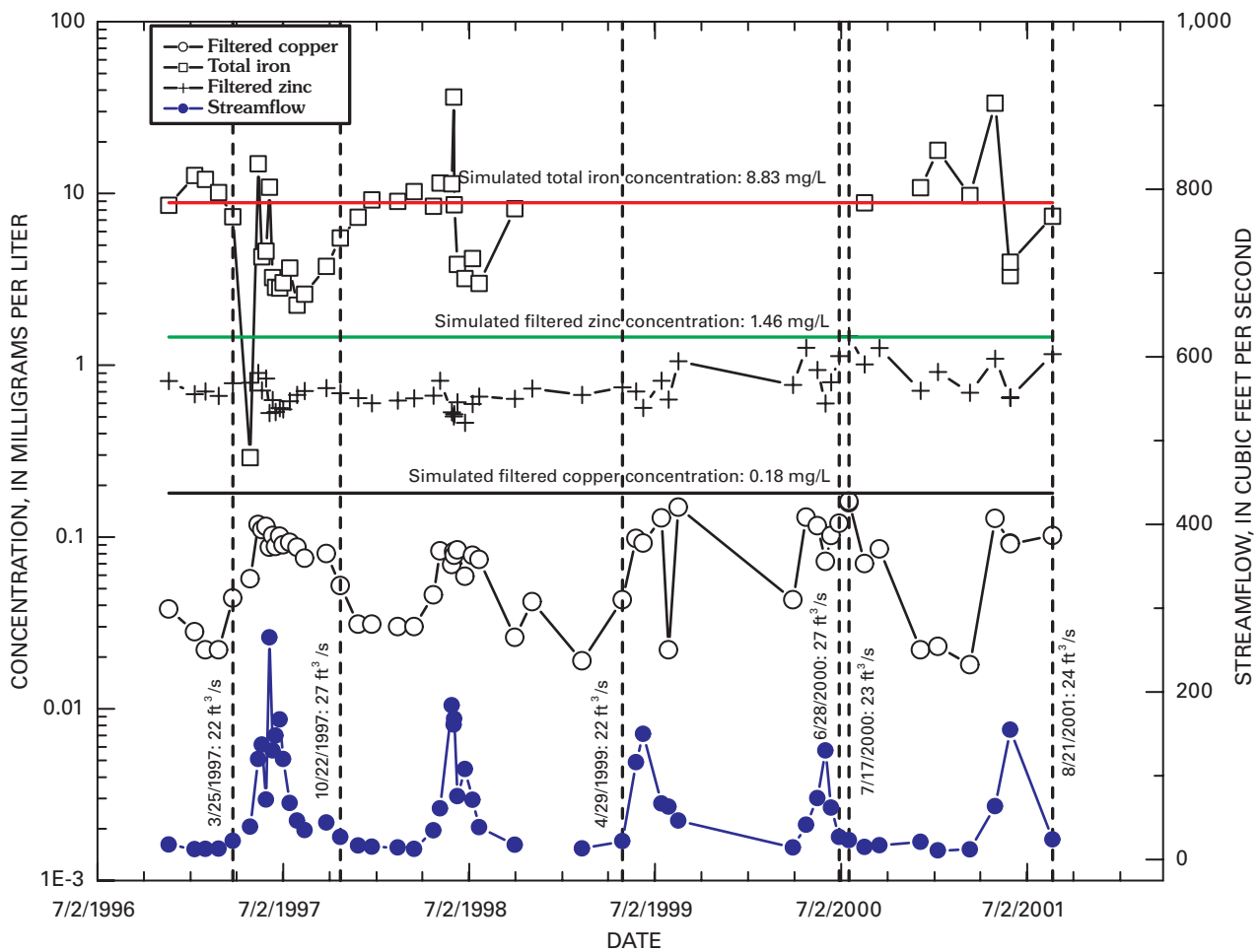


**Figure 14.** Variation in observed streamflow, filtered (0.45- $\mu\text{m}$  filtration) copper, total iron, and filtered (0.45- $\mu\text{m}$  filtration) zinc concentrations with time at the gauge (CC48) at the mouth of Cement Creek. Filtered (0.1  $\mu\text{m}$ ) copper, total iron, and filtered (0.1  $\mu\text{m}$ ) zinc concentrations simulated for 1999 conditions using calibrated OTIS model are horizontal lines. Vertical lines indicate environmental streamflow conditions (20 to 30  $\text{ft}^3/\text{s}$ ; data from Crowfoot and others, 1998, 1999, 2000, 2001, and 2002) similar to those modeled using OTIS. Environmental chemistry data at CC48 from various sources described in Leib and others (2003).

For copper,  $\beta = 1.0/67 \text{ ft}^3/\text{s}$  and for zinc  $\beta = 10^{-3}/67 \text{ ft}^3/\text{s}$ . (The regressions were conducted on the raw data obtained from Leib and others (2003), where streamflow data were presented in  $\text{ft}^3/\text{s}$ .)

The regression model for copper was  $\log(\text{Cu}) = -0.11(Q_{\text{trans}}) - 0.95$  with  $r^2$  (the coefficient of determination) = 0.53 ( $p$ -value,  $p < 0.0001$ ). For zinc, the regression model was  $\log(\text{Zn}) = 6.7(Q_{\text{trans}}) - 6.7$  with  $r^2 = 0.24$  ( $p < 0.0001$ ). These regression models are not particularly strong, partly because factors other than streamflow affect instream metal concentrations, and possibly because of changing conditions in the basin. Plots of the residuals of the regression models indicate a greater scatter for zinc residuals than for copper residuals, which reflects the smaller  $r^2$  value for zinc (fig. 15). In addition, plots of the residuals of the regression models also show when changes may have occurred. The distinct scattering in the residuals for copper and zinc shows a positive bias beginning in late July to early August 1999. The timing of the beginning of this high bias is consistent with the 1999

mass-loading study in upper Cement Creek (September 1999) and indicates that since August 1999, concentrations of copper and zinc generally were greater at the stream gauge at the mouth of Cement Creek than they were before August 1999.

Although the data indicated that higher concentrations of copper and zinc have occurred at the mouth of Cement Creek since summer 1999, simulations of these values using the 1996 calibrated OTIS model with minor adjustments to streamflow, inflow, and boundary conditions, as previously described, overestimated the observed environmental conditions at the gauge. This overestimation may have occurred for several reasons. First, although the simulation attempted to adjust for higher streamflow and concentration at the start of the modeled reach using the 1999 data, inflow throughout the rest of the model remained at 1996 levels. Increased inflow from tributaries and ground water containing lower concentrations of copper and zinc than the mainstem of Cement Creek upstream from South Fork Cement Creek would help dilute simulated concentrations. In addition, the overestimation of environmental

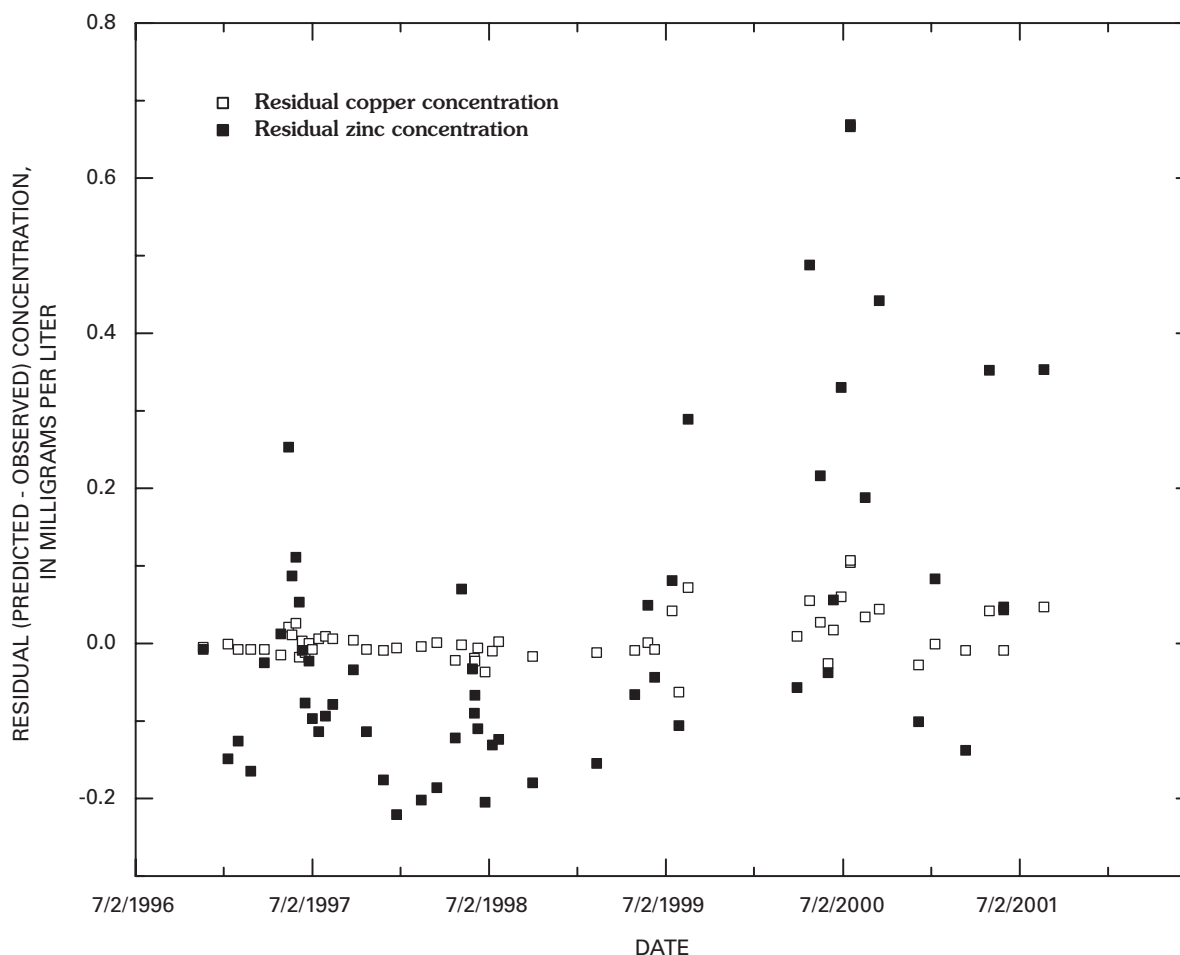


**Figure 15.** Lower Cement Creek, variation in residual concentrations of filtered copper and zinc at the Cement Creek gauge (11,558 m) with time for regression models constructed using environmental data collected between 1996 and 2001 (Leib and others, 2003) and presented in figure 14.

conditions by the model may indicate that chemical reactions that would remove copper and zinc from solution, such as coprecipitation and sorption, were underestimated in the calibrated model. In spite of these shortcomings, however, it is noteworthy that, at low flow, the model simulated increases in copper and zinc concentrations as opposed to little change for iron, and that the environmental data generally recorded these trends. The ability of the calibrated model to estimate these trends increases confidence in the model results.

### Animas River, Eureka to Howardsville

The Eureka to Howardsville mass-loading study was conducted on a 7,250 m reach of the upper Animas River extending from near the historical mining town of Eureka to downstream from Howardsville (figs. 1, 16). The study reach included inflows from Eureka Gulch (347 m), the Forest Queen mine (# 195 at 2,090 m), Minnie Gulch (2,465 m), Maggie Gulch (3,450 m), Cunningham Creek (6,558 m), and Hematite Gulch (6,633 m). Unique features of this stream reach included two intensely braided reaches (from 786 to 2,030 m, and from

3,150 to 3,435 m), the Kittimack mine (# 201), Kittimack Mill (# 194), and tailings (# 192) near 3,165 m, and the mill and tailings at Howardsville (# 233, 234) with inflow to the stream occurring at 6,438 m.

A continuous injection of sodium chloride was pumped into the river from August 12 through August 14, 1998. On August 14, 1998, synoptic samples were collected from 35 stream sites and 18 inflow sites. Chloride concentrations were used to calculate streamflow (Kimball and others, this volume; Paschke and others, 2005). Dissolved zinc (using ultrafiltration, 10,000 Dalton molecular weight nominal pore size) was the only metal modeled using OTIS, due to the low concentrations of other metals (Paschke and others, 2005).

Water-quality conditions at the time of the mass-loading study indicated better water quality in this reach of the Animas River than in Cement Creek. Values of pH were near neutral throughout the study reach and showed no clear downstream trend. Zinc concentrations ranged from 0.55 mg/L near the upstream end of the study reach to 0.28 mg/L near the downstream end of the study reach. The greater pH in the Animas River was likely due to lesser amounts of acid-altered rock in

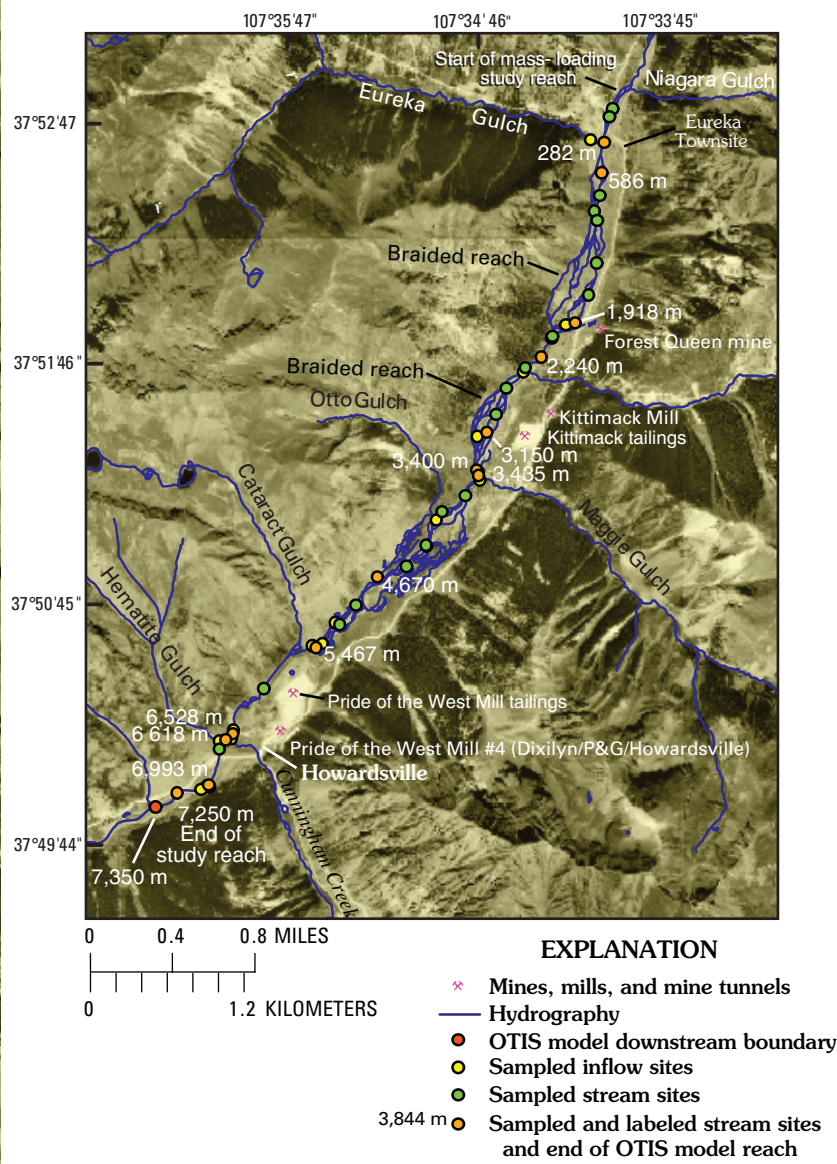


**Figure 16.** Location of stream reach of the Animas River, Eureka to Howardsville mass-loading study (August 1998) and OTIS solute-transport model. Stream- and inflow-sample data provided in Sole and others (this volume). Mining features shown (and inventory numbers, from Church, Mast, and others, this volume) include Forest Queen mine (# 195); Kittimack mine (# 201), Kittimack Mill (# 194), and tailings (# 192); and the Pride of the West Mill #4 (# 233) and tailings (# 234) at Howardsville. Mining features shown are limited to those discussed in the text. See Church, Mast, and others (this volume) for a complete inventory. Base from Digital Orthophoto Quads, Transverse Mercator, -105.00 central meridian, 1927 datum.

the upper Animas River drainage as compared to the Cement Creek drainage, and a higher proportion of propylitically altered rock that helped buffer the effects of acidic mine drainage and acidic alteration (fig. 1; Bove and others, this volume). The near-neutral pH in the stream limited the solubility of acid-soluble metals such as aluminum, copper, and iron, and helped account for their lower concentrations in this stream compared to Cement Creek.

Although zinc concentrations decreased through the study reach, zinc loads increased from 10 kg/d at the upstream end of the study to 60 kg/d downstream. The greatest sources of zinc load to the study reach were unsampled inflows to the river downstream from the braided reach near the Forest Queen mine at 1,940 m (13 percent of the zinc load); inflows near the Kittimack tailings (at 3,165 and 3,405 m) that contributed 12 percent of the zinc load; and

the inflow near Howardsville (6,438 m) that contributed 19 percent of the zinc load. Undifferentiated upstream sources represented 14 percent of the zinc load, and the inflow from Eureka Gulch (347 m) contributed 6 percent of the load (Paschke and others, 2005).

### Determination of Physical Parameters and Model Calibration for Simulation of the Chloride Tracer Profile

The Eureka to Howardsville study reach (fig. 16) was divided into 14 model reaches (table 10) based on streamflow calculations (fig. 17) and mass-loading graphs (Kimball and others, this volume; Paschke and others, 2005). Model parameters required for the OTIS simulations include the dispersion coefficient ( $D$ ), the cross-sectional area of the stream ( $A$ ), an upstream-boundary condition ( $U_b$ ), and the lateral-inflow rate ( $q_L$ ) and concentration ( $C_L$ ) for each reach. In addition, some model reaches used first-order removal coefficients ( $\lambda$ ). The parameter  $A$  was determined using OTIS-P simulations of the transport-site data (Paschke and others, 2005). A uniform dispersion coefficient of 1.0 m was used for all model reaches. For each model reach, lateral inflow ( $q_L$ ) was computed based on the streamflow profile. The upstream boundary conditions for the model were 13.3 mg/L chloride and 0.468 mg/L zinc. Calibration and estimation of  $C_L$  and  $\lambda$  values are discussed following.

Simulation of the chloride profile represented the data well (fig. 17) and indicated that boundary conditions and lateral-inflow values ( $q_L$ ) used in the model were consistent with the dilution of chloride observed at the synoptic sampling sites. Streamflow at the upstream end of the study reach (0 m) was 260 L/s. Streamflow at the downstream end of the study reach (7,250 m) was 2,320 L/s. Chloride

concentrations were 14.2 mg/L at the top of the study reach and were diluted by inflows to 1.8 mg/L at the downstream end of the study reach.

Stream segments containing sampled surface-water inflow or seeps accounted for 70 percent of the inflow. The principal surface-water inflows to the study reach were Cunningham Creek (6,558 m), which contributed 445 L/s or 22 percent of the flow increase; Eureka Gulch (347 m), which contributed 161 L/s or 8 percent of the flow increase; Minnie Gulch (2,465 m), which contributed 90 L/s or 4 percent of the flow increase; and Maggie Gulch (3,450 m), which contributed 80 L/s or 4 percent of the flow increase. Ground-water inflow along the braided reach (from 786 to 2,030 m) contributed 11 percent of the flow increase (230 L/s). Additional ground-water inflow (72 L/s or approximately 3 percent of the inflow) occurred along the stream reach ending at 4,670 m that contained abundant willow vegetation and beaver ponds.

### Model Calibration for Zinc Simulations

Using lateral-inflow concentrations ( $C_L$ ) representative of measured inflow concentrations (fig. 18), the conservative simulation had greater instream zinc concentrations than measured instream concentrations downstream from Eureka Gulch (fig. 19). Consistent with the mass-loading graphs (Kimball and others, this volume), this simulation result indicates removal of dissolved zinc from the stream. The loss of dissolved zinc probably results from zinc adsorption onto iron oxyhydroxides or streambed sediment (Church and others, 1997) and was represented as a first-order process using OTIS. First-order removal coefficients ( $\lambda$ ) ranging from  $2.5 \times 10^{-5}$  to  $1.0 \times 10^{-4} \text{ s}^{-1}$  were assigned to model reaches 3 (586 to 1,918 m), 5 (2,240 to 3,150 m), 8 (3,435 to 4,670 m), and 13 (6,993 to 7,250 m) to represent the decrease of sampled

**Table 10.** Animas River, Eureka to Howardsville, reach number, distance at end of reach, and description of reaches used in OTIS modeling of synoptic samples (August 1998).

[Distance in meters (m) downstream from arbitrary stream datum. Reach numbers correspond to those in figures 17–20]

Model reach	Distance (m)	Brief description of reach and significant inflows
1	282	Animas River downstream from tracer-injection site.
2	586	Animas River downstream from Eureka Gulch.
3	1,918	Animas River downstream from most of braided reach.
4	2,240	Animas River downstream from Forest Queen mine (# 195).
5	3,150	Animas River upstream from Kittimack tailings (# 192).
6	3,400	Animas River downstream from Kittimack tailings.
7	3,435	Animas River downstream from flow increase at 3,405 m.
8	4,670	Animas River downstream from flow increase associated with willows and beaver ponds.
9	5,467	Animas River upstream from Howardsville.
10	6,528	Animas River downstream from Howardsville and upstream from Cunningham Creek.
11	6,618	Animas River downstream from Cunningham Creek.
12	6,993	Animas River at 6,993 m.
13	7,250	Animas River at end of study reach.
14	7,350	Animas River at downstream OTIS boundary.

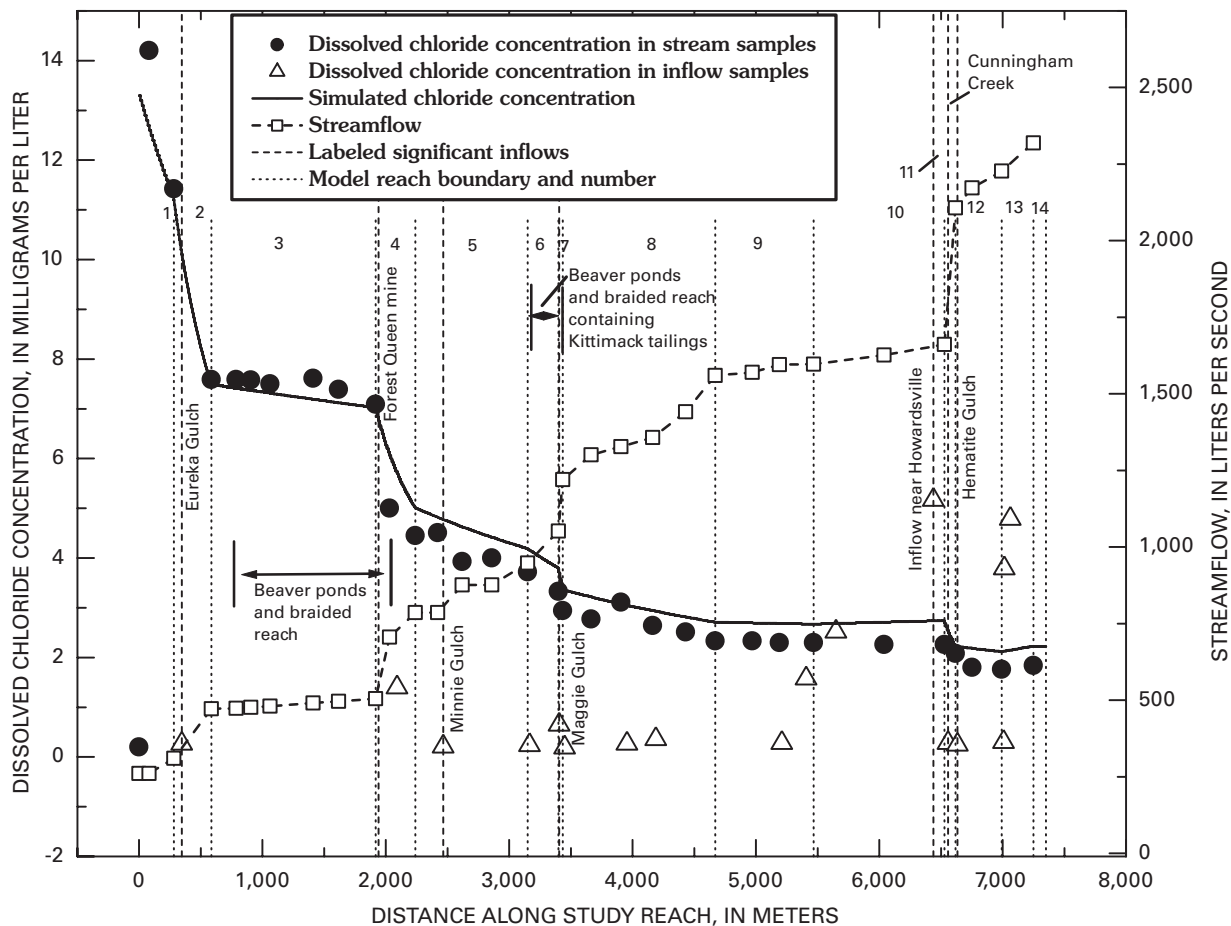


**Figure 17.** Variation in chloride concentration, streamflow, and simulated chloride concentration with distance, showing location of OTIS model reaches and significant features, Animas River, Eureka to Howardsville mass-loading study (August 1998) and OTIS solute-transport model.

instream zinc load through these model reaches noted in the results of the loading analysis (Paschke and others, 2005). The OTIS result for instream zinc concentrations using representative lateral-inflow concentrations ( $C_L$ ) and first-order removal (fig. 19) provided a reasonable match to the measured instream zinc concentrations and represented the calibrated model used for simulation of remediation scenarios. Similar to results in the Cement Creek basins, the limited distribution and the small magnitude of first-order removal coefficients indicate that reactive processes were operating only to a minimal extent in the study reach.

The instream zinc concentrations were generally greater than the model simulations in model reach 3 indicating that some zinc sources may exist in the model reach that were not represented in the model. This model reach contained one of the intensely braided reaches (fig. 17). Stream samples were collected along an individual, continuous channel throughout the reach, but because of the multiple channels, how representative each sample was of processes occurring along each stream segment was not known. Therefore, a conservative approach was chosen wherein the model was designed to lump the processes in the braided reach into one model reach in order not to emphasize small, possibly anomalous processes

occurring within the reach. The difference between the conservative and reactive simulations at the end of the model reach (fig. 19) indicates that some zinc inflow to the model reach was removed using first-order removal coefficients. Therefore, the model generally represents what was occurring within the model reach.

Removal of zinc onto streambed sediment in reaches 3, 5, 8, and 13 is geochemically consistent with other features of those reaches. Reach 3 contained the braided reach where ground water entered the stream. Because of multiple surface channels in this reach, and very coarse streambed sediment (gravel to cobble-sized), good interaction likely occurred between surface water and ground water that would increase sediment/water contact times and promote sorption. In addition, the fluctuation between high and low zinc concentrations in instream samples in this reach indicates that zinc was entering and being removed within the reach. Reach 5 was downstream from the Forest Queen mine (# 195). A reasonable interpretation is that mixing between mine drainage from the Forest Queen and the cleaner water of the Animas River caused formation and settling of some colloidal material. Reach 8 contained inflow from Maggie Gulch and from ground water. Mixing between the stream water and tributary surface

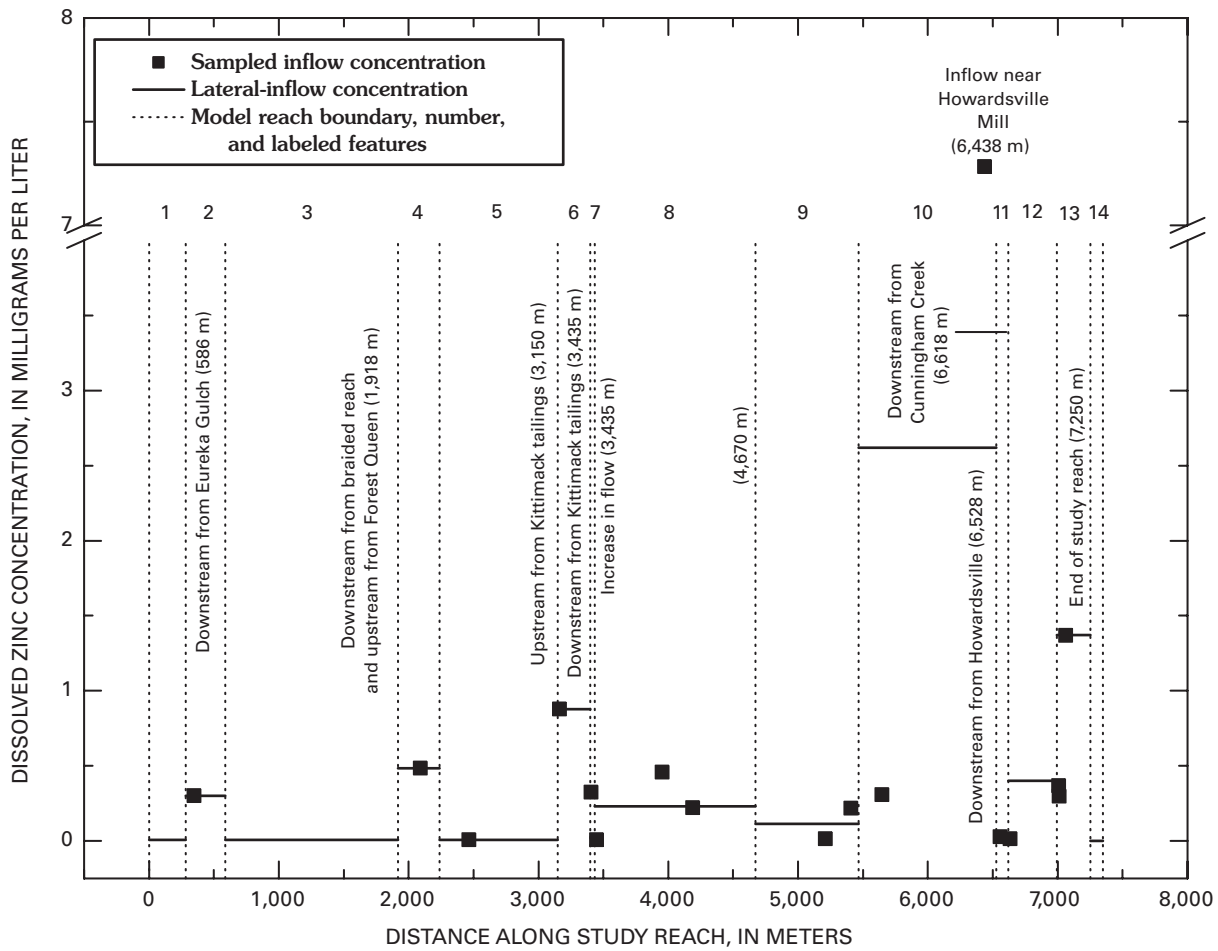


**Figure 18.** Variation in dissolved zinc calibrated lateral-inflow concentrations and observed inflow concentrations (August 1998) with distance and OTIS model reach, Animas River, Eureka to Howardsville OTIS model.

and ground water probably promoted formation of colloidal material that settled to the streambed. Reach 13 contained inflows that were enriched in zinc (fig. 18) and iron (Paschke and others, 2005). Mixing of this water with the Animas River likely promoted formation and settling of iron-rich colloidal material.

Though the modeling results indicated that reactive processes were minimal in Cement Creek and in the Animas River reach from Eureka to Howardsville, the reasons for minimal reactivity differ between the streams. In Cement Creek, reaction was minimal because the pH was too low to promote sorption of copper and zinc to precipitating iron phases that were present in the water column. In the Animas River, precipitation of iron minerals in the water column was not a major process, probably because of limited sources of dissolved iron to the river. Consequently, most surfaces (colloidal iron and aluminum minerals) available for zinc sorption were on the streambed. Interaction between zinc in the water column and streambed material was probably limited due to relatively fast flow conditions that limited the amount of sorption that occurred. Although this interaction was minimal in that the first-order removal coefficients were relatively small,

the reaction was sufficient to lower instream zinc concentrations (fig. 19) and metals accumulated in streambed sediment during the spring and summer: during low flow, colloidal streambed sediment that has accumulated since spring runoff can have zinc concentrations exceeding 1,500 ppm (Church and others, 1997). From the perspective of a solute-transport model that examines instantaneous processes, reaction was minimal. But, over time, this minimal reaction is sufficient to account for elevated concentrations of metals in streambed sediment. This interpretation is consistent with the conclusions of Church and others (1997), who reported that one of the major differences between Cement Creek and the Animas River upstream from Cement Creek was that in Cement Creek, metals were concentrated in the water column, whereas in the Animas River, metal concentrations were greater in colloids stored in the streambed sediment.

### Remediation Simulations

Two remediation scenarios were evaluated for the Eureka to Howardsville study reach. The first remediation scenario evaluated the effects of remediating unsampled inflow near

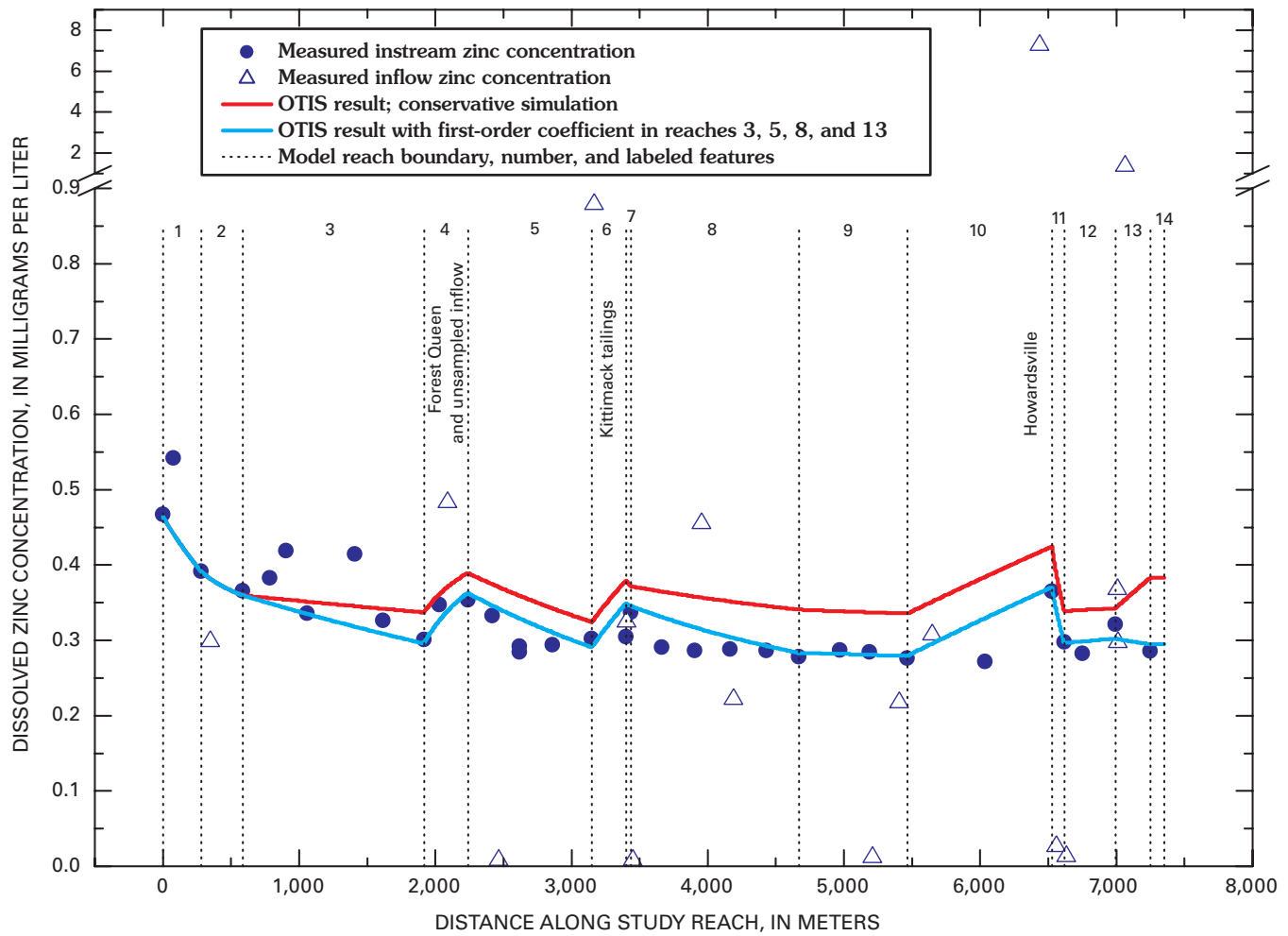


**Figure 19.** Variation in dissolved zinc concentrations with distance in stream and inflow samples (August 1998) and in OTIS conservative and calibrated reactive simulations, showing model reach and number and location of significant features, Animas River, Eureka to Howardsville.

1,940 m and the Forest Queen mine (model reach 4), and removing contributions from the Kittimack tailings (model reach 6). The second remediation scenario simulated the effects of remediating unsampled inflow near 1,940 m and the Forest Queen mine (model reach 4), the Kittimack tailings (model reach 6), and the various mills, both historical and active, near Howardsville (model reach 10).

To simulate remediation of stream reaches, the lateral-inflow concentrations ( $C_l$ ) were reduced from the measured inflow concentrations to concentrations representative of inflow after remediation. Because these post-remediation concentrations are uncertain, the remedial simulations for the Eureka to Howardsville study reach assumed a 75 percent reduction in zinc lateral-inflow concentrations ( $C_l$ ) for remediated model reaches.

Simulation results for the first remediation scenario indicated that downstream from the Kittimack tailings and upstream from Howardsville, instream zinc concentrations would approach and sometimes be less than 0.18 mg/L if zinc inflow concentrations were reduced by 75 percent in model

reaches 4 and 6 (fig. 20). An instream zinc concentration of 0.18 mg/L is the upper limit of acute toxicity for some sensitive aquatic species (Besser and Brumbaugh, this volume, Chapter E18).

Simulation results for the second remediation scenario (fig. 20) indicated that downstream from the Kittimack tailings and downstream from Howardsville, instream zinc concentrations would approach and sometimes be less than 0.18 mg/L if zinc inflow concentrations were reduced by 75 percent in the inflows to model reaches 4, 6, and 10. Paschke and others (2005) indicated that simulated instream zinc concentrations were greater than the State of Colorado hardness-based chronic and acute toxicity standards. Zinc sources that cause zinc concentrations to remain elevated in spite of the simulated remediations include sources upstream from the study reach, slight zinc loading along model reaches 8 and 9, the remaining 25 percent of the zinc loads at the Forest Queen, Kittimack, and Howardsville locations, and some loading that occurs in model reach 13.

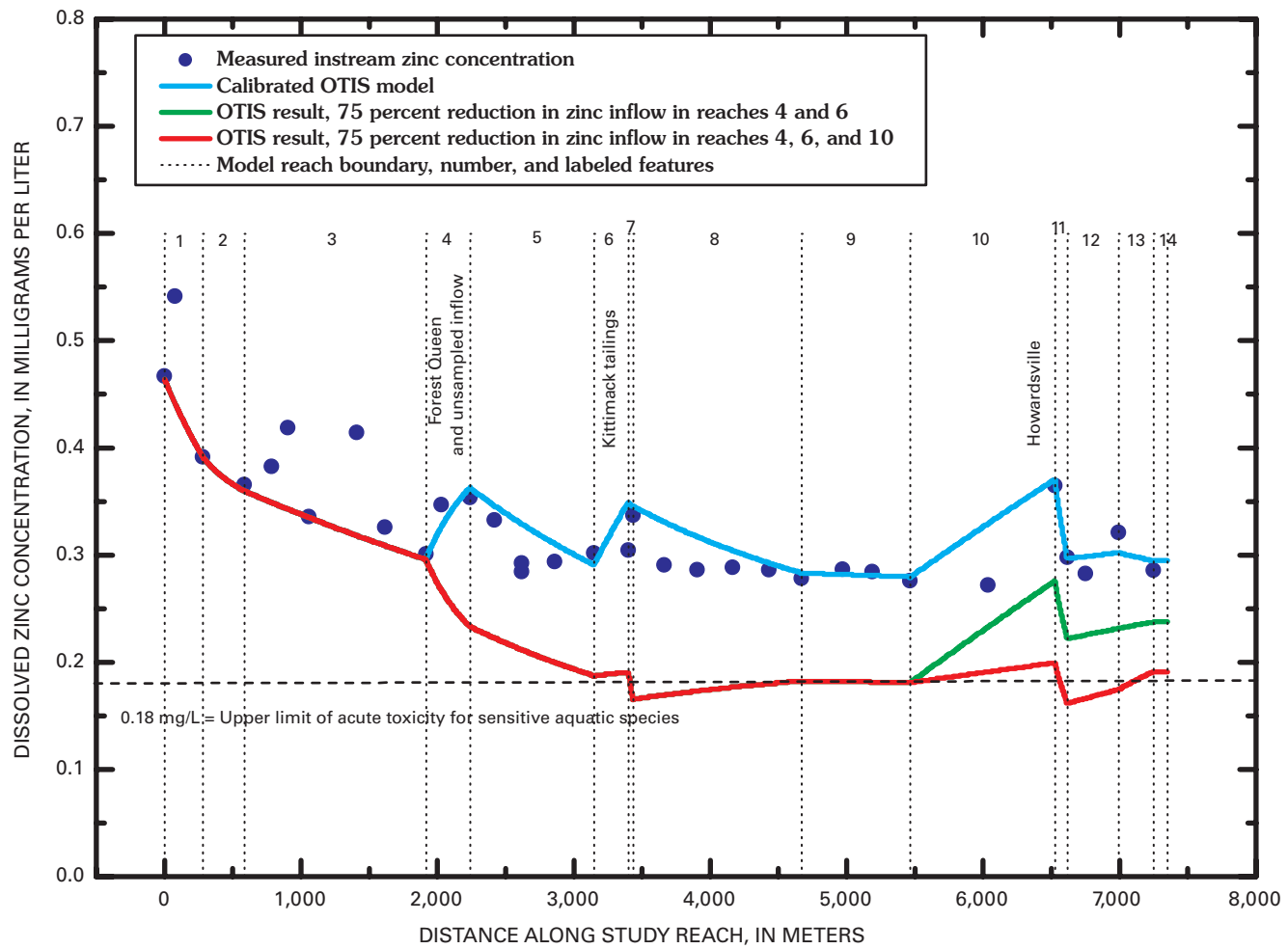


**Figure 20.** Variation in dissolved zinc concentrations with distance in calibrated OTIS model and in simulations of two remediation scenarios, showing location of some significant features, Animas River, Eureka to Howardsville.

### Animas River, Howardsville to Silverton

The Howardsville to Silverton mass-loading study was conducted on a 7,858 m reach of the upper Animas River starting near the historical mining town of Howardsville and extending to just upstream from Silverton at USGS gauging station number 09358000, now operated by the State of Colorado, gauging station A68 (figs. 1, 21).

The sampled reach included inflows from Cunningham Creek (1,075 m); Hematite Gulch (1,150 m); Arrastra Creek (4,186 m); Boulder Gulch (4,951 m), and Blair Gulch (5,221 m). Other notable locations on the stream reach include the town and mill at Howardsville (site # 233; 965 m), the Mayflower Mill (# 221) and reclaimed tailings ponds (sites # 507–510) from 4,500 to about 6,500 m, and the Lackawanna Mill (# 287; 7,103 m).

A continuous injection of sodium chloride was conducted on the river from September 13 through September 15, 1997. On September 14, 1997, synoptic samples were collected at 38 stream sites and 34 inflow sites. Chloride concentrations were used to calculate streamflow (Kimball and others, this volume; Paschke and others, 2005). Dissolved zinc (using

ultrafiltration, 10,000 Dalton molecular weight nominal pore size) was the only metal modeled using OTIS due to near-neutral instream pH and low concentrations of other metals (Paschke and others, 2005).

Water quality in this reach of the Animas River was better than in Cement Creek. Values of pH were near neutral throughout the stream reach and showed no clear downstream trend. In contrast to the Eureka to Howardsville study reach, dissolved zinc concentrations generally increased through the study reach, ranging from approximately 0.3 mg/L at the upstream end of the study reach to approximately 0.45 mg/L at the downstream end of the study reach. Zinc load increased from 10 to 80 kg/d through the study reach. Zinc load at the downstream end of the Eureka to Howardsville study reach was approximately 37 kg/d during the 1997 study in contrast to 60 kg/d during the 1998 study. Lower flow in 1997 compared to 1998 caused this difference.

The greatest sources of zinc load to the Animas River in the study reach were downstream from Howardsville (inflow at 965 m; downstream stream site at 1,059 m) which accounted for 9 percent of the load, and downstream from the tailings repositories near the Mayflower Mill (no sampled

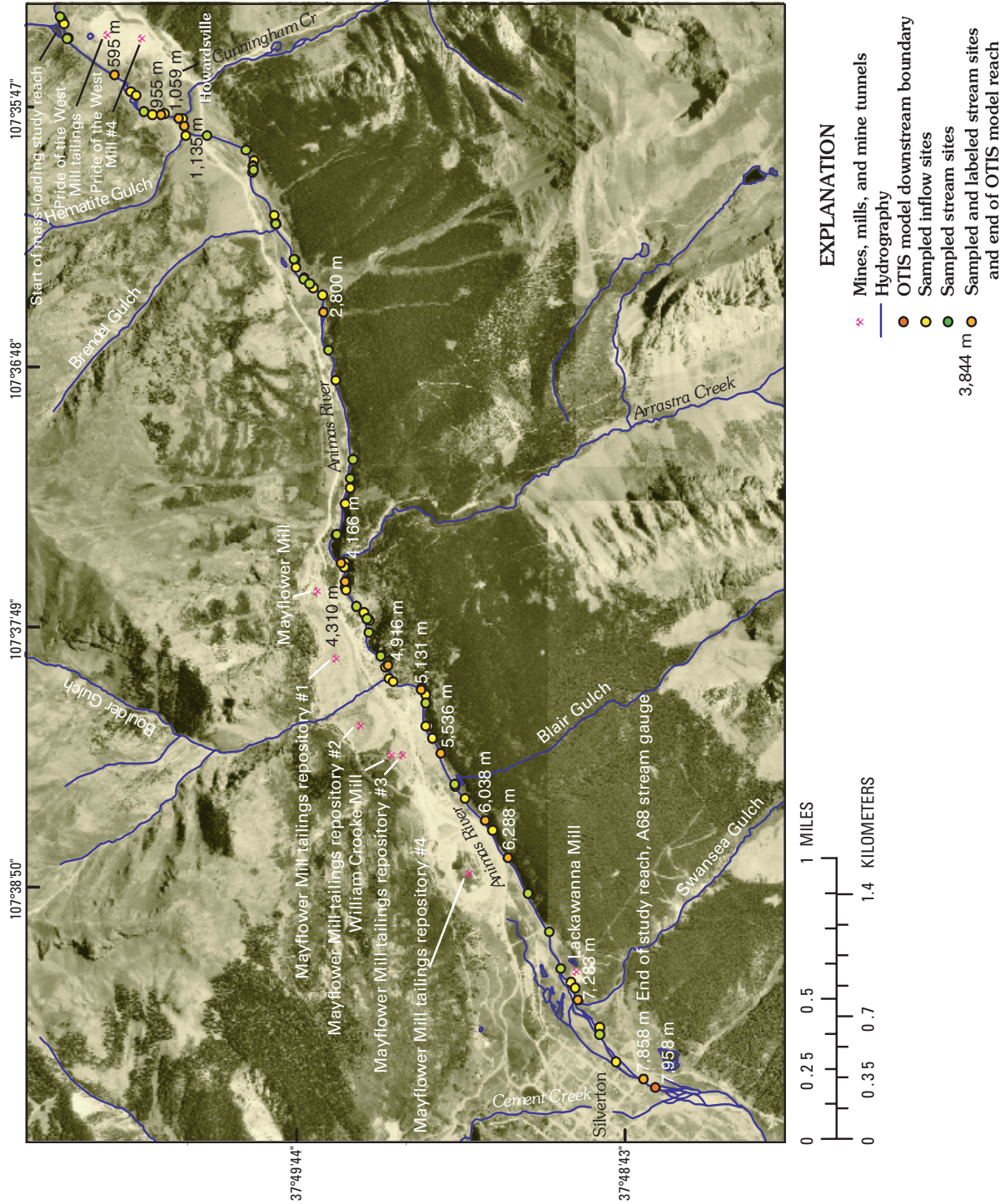


**Figure 21.** Location of stream reach of the Animas River, Howardsville to Silverton mass-loading study (September 1997) and OTIS solute-transport model. Stream- and inflow-sample data provided in Sole and others (this volume). Mining features shown (and inventory numbers, from Church, Mast, and others, this volume) include Pride of the West Mill #4 (# 233) and tailings (# 234) at Howardsville; Mayflower Mill (# 221); Mayflower Mill tailings repositories #1 (# 507), #2 (# 508), #3 (# 509), and #4 (# 510); William Crooke Mill (# 215); and Lackawanna Mill (# 287). Mining features shown are limited to those discussed in the text. See Church, Mast, and others (this volume) for a complete inventory. Base from Digital Orthophoto Quads, Transverse Mercator, -105.00 central meridian, 1927 datum.

inflows in the reach, downstream site at 6,288 m, fig. 21), which represented 15 percent of the load. Additional sources of load are presented in Paschke and others (2005) and Kimball and others (this volume).

### Determination of Physical Parameters and Model Calibration for Simulation of the Chloride Tracer Profile

The Howardsville to Silverton study reach (fig. 21) was divided into 15 model reaches (table 11; fig. 22) based on streamflow calculations and mass-loading graphs (Kimball and others, this volume; Paschke and others, 2005). Model parameters required for the OTIS simulations include the dispersion coefficient ( $D$ ), the cross-sectional area of the stream ( $A$ ), an upstream-boundary condition ( $U_p$ ), and the lateral-inflow rate ( $q_L$ ) and concentration ( $C_L$ ) for each reach. In addition, some model reaches used first-order removal coefficients ( $\lambda$ ). The parameter  $A$  was determined using OTIS-P simulations of the transport-site data (Paschke and others, 2005). A uniform dispersion coefficient of 1.0 m was used for all model reaches. For each model reach, lateral inflow ( $q_L$ ) was computed based on the streamflow profile. The upstream boundary conditions for the model were 2.19 mg/L chloride and 0.281 mg/L zinc. Model calibration and estimation of  $C_L$  and  $\lambda$  values are discussed following.

Simulation of the chloride profile represented the data well (fig. 22) and indicates that boundary conditions and lateral-inflow values ( $q_L$ ) used in the model are consistent with the dilution of chloride observed at the synoptic sampling sites. Chloride concentrations were 2.2 mg/L at the top of the study reach and were diluted by inflows to 1.1 mg/L at the downstream end of the study reach. Elevated chloride values in some inflows (fig. 22) resulted from precipitation runoff that flowed into the stream during the synoptic sampling and that contained magnesium chloride used to reduce road dust. The elevated chloride concentration in inflow samples complicated the calculation of streamflow values. However, streamflow values computed from the synoptic sampling results compare well with streamflow measured independently at the six transport sites (Paschke and others, 2005).

Streamflow at the injection site was 1,107 L/s and increased by 1,157 L/s over the course of the study reach to 2,264 L/s at the downstream end of the study reach (fig. 22). Stream segments containing sampled surface-water inflow or seeps accounted for 93 percent of the inflow along the reach. The principal sampled inflows along the study reach were Cunningham Creek (1,075 m), which contributed 386 L/s or 33 percent of the flow increase; Arrastra Creek (4,186 m) and a pipe discharging water diverted from Arrastra Creek<sup>3</sup> and

located just downstream from Arrastra Creek (4,190 m), which each contributed 110 L/s or 10 percent of the flow increase; Boulder Gulch (4,951 m), which contributed 78 L/s or 7 percent of the flow increase; and Hematite Gulch (1,150 m), which contributed 57 L/s or 5 percent of the flow. Small surface inflows and ground-water seeps caused the remaining streamflow increase along the study reach.

### Model Calibration for Zinc Simulations

Methods used to compute lateral-inflow concentrations ( $C_L$ ) varied with model reach. Upstream from Arrastra Creek, lateral-inflow concentrations were assigned to each model reach based on inflow concentrations measured during synoptic sampling (fig. 23). Downstream from Arrastra Creek, lateral-inflow concentrations were adjusted to obtain a reasonable match between simulated and measured instream zinc concentrations. Paschke and others (2005) provided details supporting the choices of lateral-inflow concentrations and first-order removal coefficients.

The conservative simulation overestimated instream conditions (fig. 24), and indicated loss of zinc in some model reaches. Mass-loading results (Paschke and others, 2005) indicated loss of zinc in model reaches 11 (5,536 to 6,038 m) and 13 (6,288 to 7,283 m). Consequently, first-order removal coefficients were applied in those model reaches (reach 11,  $4.0 \times 10^{-4} \text{ s}^{-1}$ ; reach 13,  $1.0 \times 10^{-4} \text{ s}^{-1}$ ) for OTIS simulations. The resulting calibrated model exhibited a good fit with measured instream conditions (fig. 24). The limited distribution and magnitude of removal coefficients indicate that reactive processes are operating only to a minimal extent in the study reach. Throughout much of the study reach, the streambed is relatively free from iron, aluminum, and manganese flocculent material. The limited amount of iron, aluminum, and manganese phases available in the water column and on the streambed relative to other areas limits sorption reactions. In addition, the near-neutral pH of the Animas River in the study reach limits mobility of many solutes (for example, iron and aluminum), so that if they do enter the river in acidic tributary inflow, they are quickly removed to the streambed. Near-neutral pH in the upper Animas River is a result of a large proportion of propylitically altered rocks in the basin that generated water having near-neutral pH and some buffering capacity compared to conditions in the Cement Creek basin, where a larger proportion of rocks have been affected by acid alteration and thus generate acid waters (fig. 1; Bove and others, this volume).

### Remediation Simulations

Two remediation scenarios were evaluated for the Howardsville to Silverton study reach. The first remediation scenario examined the effects of remediating contributions from historical and active mills at Howardsville (model reach 3). This model reach accounted for 9 percent of the zinc load in the study reach (Paschke and others, 2005). The second remediation scenario evaluated the effect of remediating

<sup>3</sup>The pipe contained water from Arrastra Creek that was diverted from the creek to supply process water to the Mayflower Mill when it was operating. At the time of the study, the water flowed from Arrastra Creek through the pipeline to the mill and back to the Animas River. It was not used or altered at the mill.

**Table 11.** Animas River, Howardsville to Silverton, reach number, distance at end of reach, and description of reaches used in OTIS modeling of synoptic samples (September 1997).

[Distance is downstream from arbitrary stream datum; m, meters. Reach numbers correspond to those in figures 22–25]

Model reach	Distance (m)	Brief description of reach and significant inflows
1	595	Animas River downstream from tracer-injection site.
2	955	Animas River upstream from Howardsville.
3	1,059	Animas River downstream from Howardsville.
4	1,135	Animas River downstream from Cunningham Creek.
5	2,800	Animas River at 2,800 meters.
6	4,166	Animas River upstream from Arrastra Creek.
7	4,310	Animas River downstream from Arrastra Creek.
8	4,916	Animas River downstream from right bank acid inflows and upstream from Boulder Gulch.
9	5,131	Animas River downstream from Boulder Gulch.
10	5,536	Animas River downstream from Blair Gulch.
11	6,038	Animas River at 6,038 m.
12	6,288	Animas River downstream from zinc concentration increase.
13	7,283	Animas River downstream from zinc loss.
14	7,858	Animas River at end of study reach.
15	7,958	Animas River at downstream OTIS boundary.

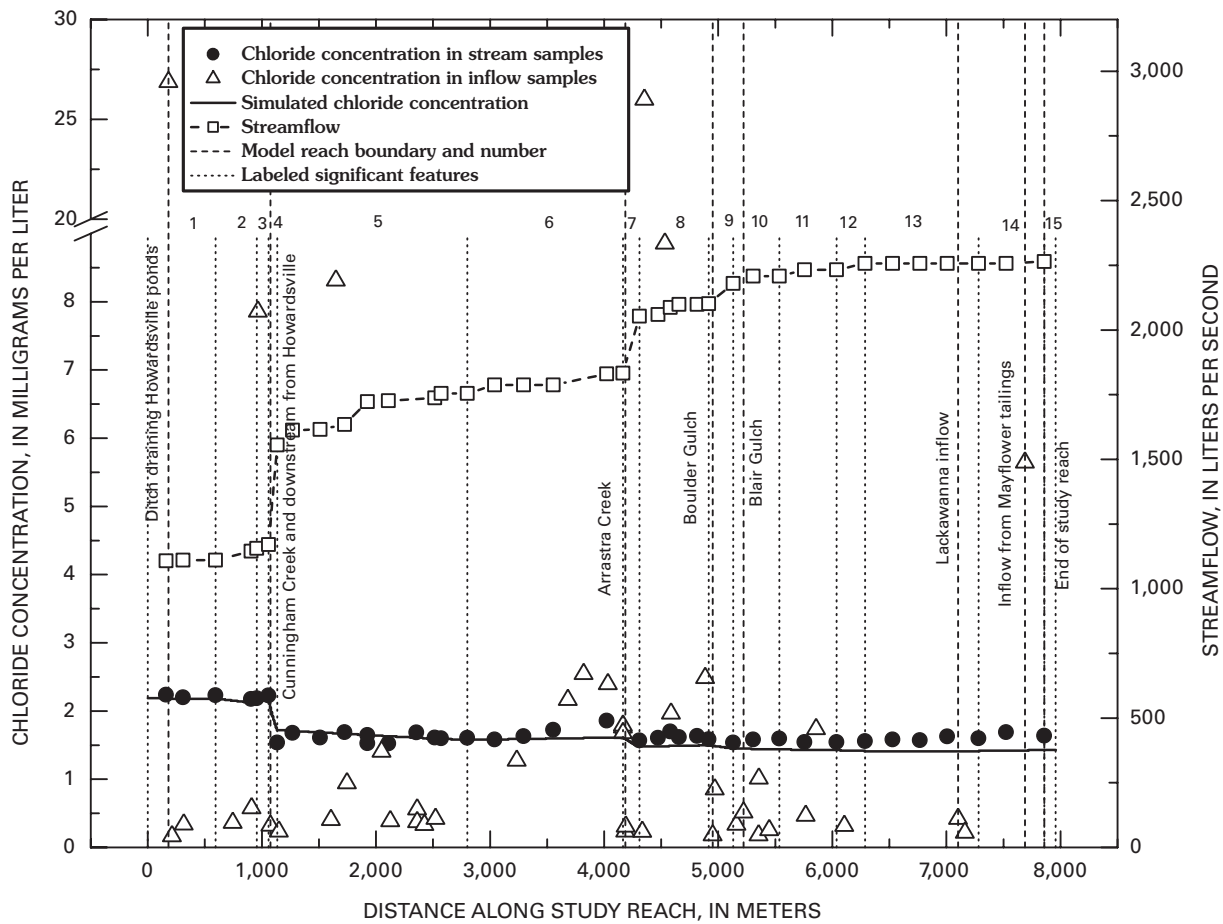


**Figure 22.** Variation in chloride concentration, streamflow, and simulated chloride concentration with distance, showing location of OTIS model reaches and significant features, Animas River, Howardsville to Silverton mass-loading study (September 1997) and OTIS solute-transport model.

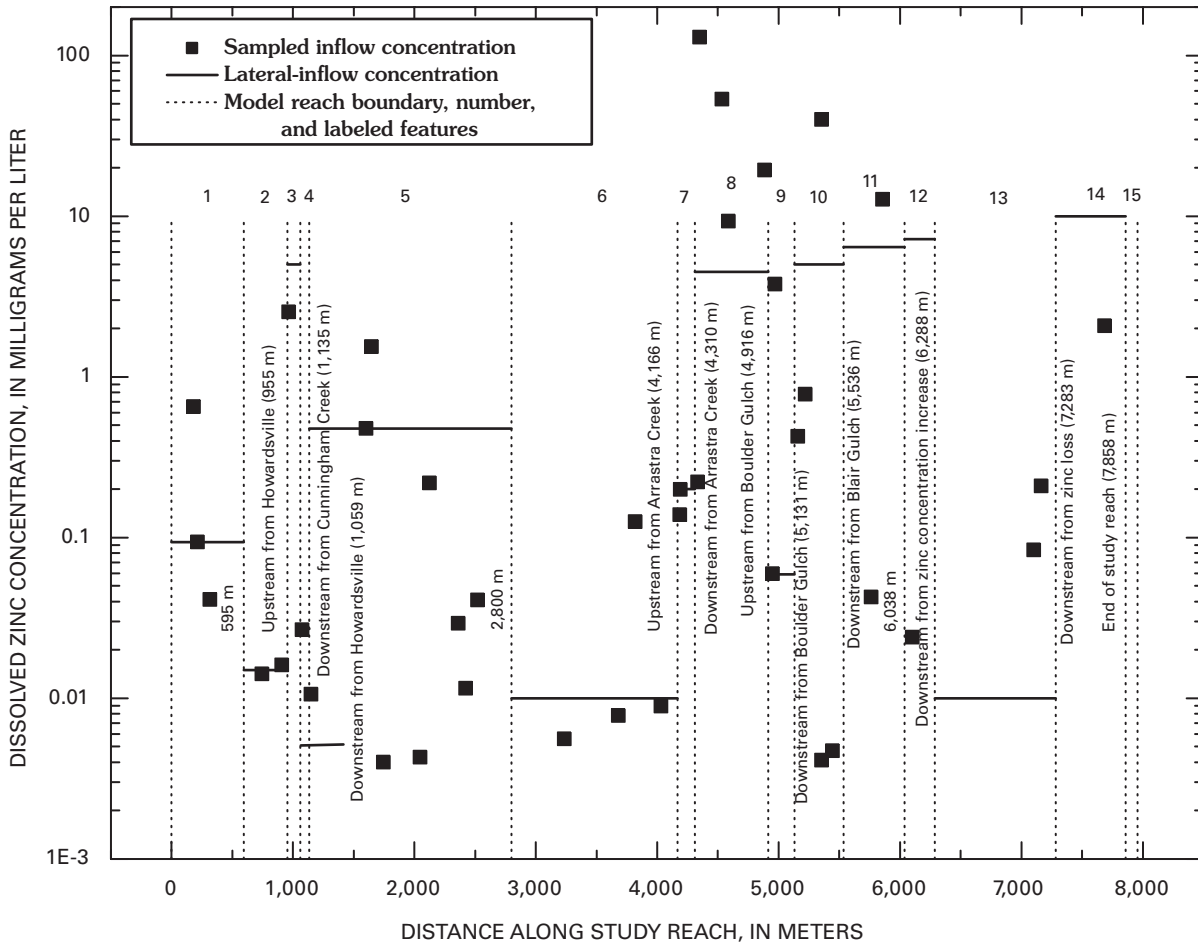


**Figure 23.** Variation in dissolved zinc calibrated lateral-inflow concentrations and observed inflow concentrations (September 1997) with distance and OTIS model reach, Animas River, Howardsville to Silverton OTIS model.

contribution from the mills at Howardsville and from the Mayflower Mill (model reaches 3 and 12). Model reach 12 contributed 15 percent of the total zinc load observed throughout the Howardsville to Silverton study reach during the 1997 synoptic study (Paschke and others, 2005).<sup>4</sup> Remediation simulations were accomplished through the assumption that remediation would reduce zinc concentrations in the inflows by 75 percent. In addition, both of these remediation scenarios were implemented with the assumption that upstream remediation (Eureka to Howardsville section) had already been accomplished. The upstream zinc load accounted for 26 percent of the load in the study reach (Paschke and others, 2005). Accordingly, for both remediation simulations, the upstream

<sup>4</sup>Note that zinc concentrations increased along model reach 12 and remained elevated downstream (fig. 24). However, no inflows having high zinc concentrations were sampled in the reach, which indicates that unsampled inflows contributed zinc load to the stream (Paschke and others, 2005). When load increases along a stream reach having no sampled inflows to account for the load increase, the increased loads are generally attributed to unsampled ground-water discharge along the reach (Kimball and others, 2002).

boundary concentration was reduced from 0.28 to 0.19 mg/L, which represented the simulated zinc concentration upstream from the inflow at Howardsville and reflects 75 percent reduction in the zinc load from the vicinity of the Forest Queen mine (including unsampled inflow at 1,940 m in the 1998 Eureka to Howardsville study) and Kittimack tailings inflows from our previous results (fig. 20).

The first remediation scenario is similar to remediation scenario 1 completed for the Eureka to Howardsville 1998 study. It is repeated here for the 1997 data set to examine the effects of remediation on stream reaches downstream from Howardsville. The simulation result (fig. 25) indicates that downstream from the Kittimack tailings to upstream from Arrastra Creek instream zinc concentrations would approach 0.18 mg/L if zinc concentrations were reduced by 75 percent in the inflows to the stream reaches containing the Forest Queen mine, the Kittimack tailings, and the mills downstream from Howardsville. An instream zinc concentration of 0.18 mg/L is the upper limit of acute toxicity for some sensitive aquatic species (Besser and Brumbaugh, this volume). State of Colorado hardness-based acute and chronic

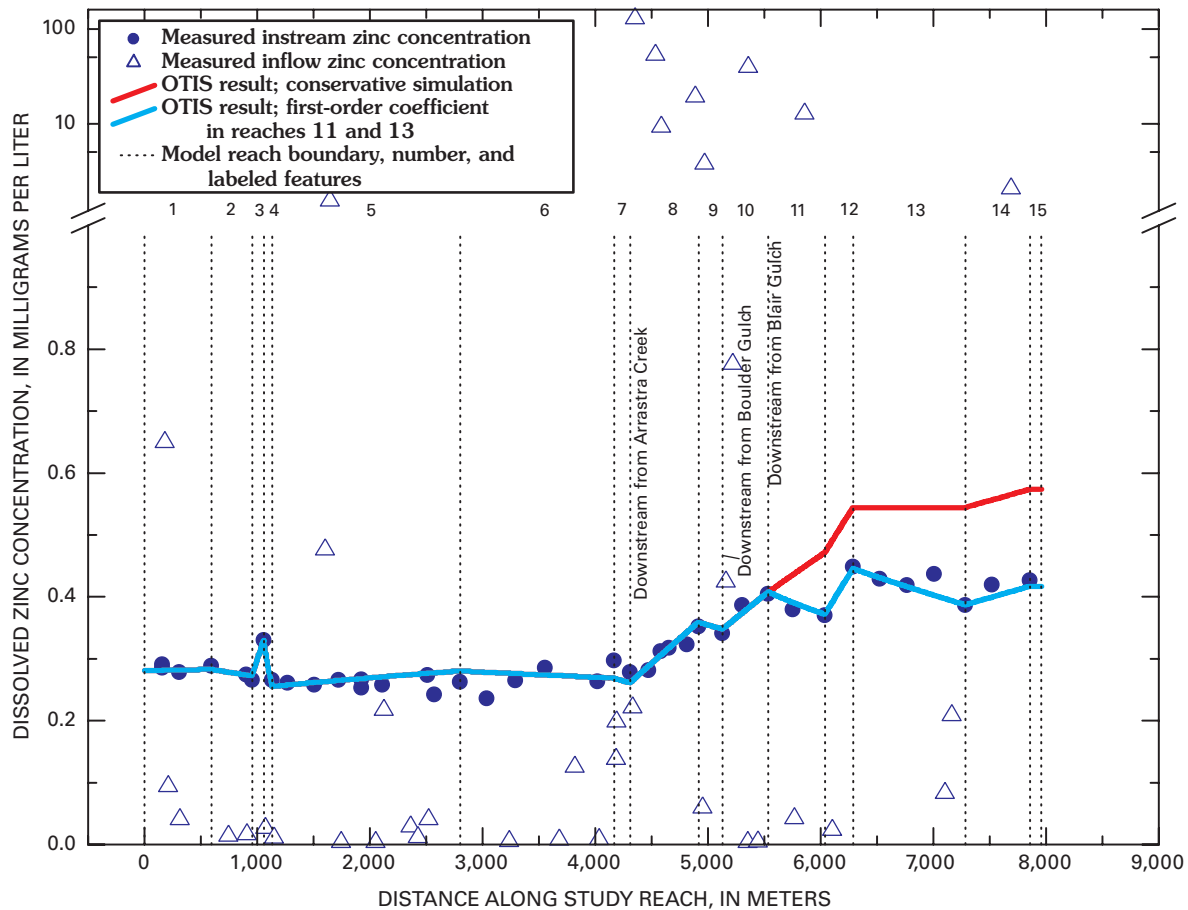


**Figure 24.** Variation in dissolved zinc concentrations with distance in stream and inflow samples (September 1997) and in OTIS conservative and calibrated reactive simulations, showing model reach and number and location of significant features, Animas River, Howardsville to Silverton.

zinc toxicity standards are less than 0.13 mg/L throughout the study reach (Paschke and others, 2005). However, as the zinc-rich inflows downstream from Arrastra Creek (including some near the Mayflower Mill) contributed to the Animas River, instream concentrations increased to greater than 0.18 mg/L.

For the second remediation scenario, the effects of remediating inflow to the reach containing the Mayflower Mill and tailings (model reach 12) in addition to the upstream model reaches were evaluated. Remediation of these inflows was represented using an upstream boundary condition of 0.19 mg/L zinc, and 75 percent reductions in zinc lateral-inflow concentration ( $C_L$ ) for model reaches 3 and 12. These simulations represented the effects of remediating inflow from the Forest Queen mine, Kittimack tailings, inflow downstream from Howardsville, and presumed ground-water discharge to the stream in model reach 12. Simulation results are shown in figure 25 and indicate that instream zinc concentrations remained higher than 0.30 mg/L downstream from Arrastra Creek due to sampled and unsampled inflows having elevated zinc concentrations in the lower portion of the study reach (for example, model reaches 8, 10, 12, and 14, fig. 24).

### Significance of Metal Removal Processes in Cement Creek and the Upper Animas River

The first-order removal coefficients ( $\lambda$ ) estimated by the model are a measure of the rate of metal removal and may be compared across model reaches in each model, or between modeled streams. The comparison can be instructive, but it is necessary to also compare the metal-removal rates (first-order removal coefficients) to the residence time of water in each model reach to assess where removal reactions are most important. Using a method similar to that presented in Kimball and others (1994), we calculated a reaction half-life ( $t_r$ , the amount of time the reaction used to consume half of the metal present in the water column) for each first-order removal coefficient ( $\lambda$ ):

$$t_r = \frac{\ln 2}{\lambda} \tag{4}$$

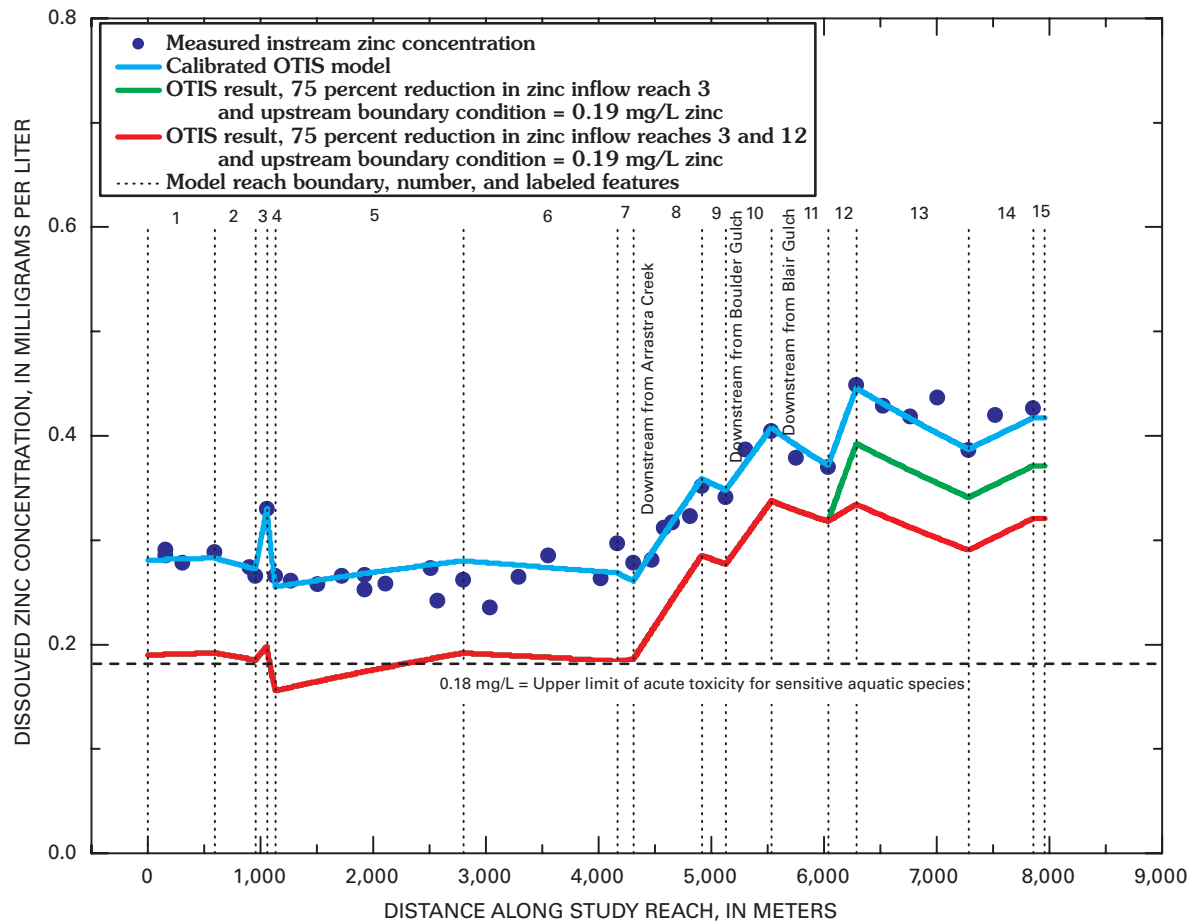


**Figure 25.** Variation in dissolved zinc concentrations with distance in calibrated OTIS model and in simulations of two remediation scenarios, showing model reach and number and location of some significant features, Animas River, Howardsville to Silverton.

In addition, a convective travel time ( $t_c$ ) can be calculated for each reach:

$$t_c = \frac{L}{u} \tag{5}$$

where  $L$  is the reach length in meters and  $u$  is the velocity (m/s) in the reach determined by dividing streamflow by stream cross-sectional area ( $A$ ). A dimensionless parameter, the Damkohler number (Bahr and Rubin, 1987; Kimball and others, 1994), relates travel time to the half-reaction time:

$$D_n = \frac{t_c}{t_r} \tag{6}$$

If the travel time is large compared to the half-reaction time ( $D_n > 1$ ), stream water resides in the model reach long enough for more than half of the solutes to be removed from the water column by the reaction. Conversely, if the travel time is less than the half-reaction time ( $D_n < 1$ ), less than half of the solutes are removed by the reaction during transport through the model reach. The larger the value of  $D_n$ , the more complete the removal reaction.

Damkohler numbers for the OTIS model reaches were greater than 1 only in the upstream model reaches of Cement Creek (table 12). Elsewhere,  $D_n$  was less than 1, indicating that travel times through the reaches were fast relative to the half-reaction rates: reactions progressed less than halfway to completion. In many cases,  $D_n$  was less than 0.10: reactions removed less than 5 percent of the solute from the water column and were not very significant.

If removal reactions were not significant, how can we account for streambed metal concentrations for some metals that exceed 1,500 parts per million (Church and others, 1997) in some reaches of the upper Animas River and Cement Creek? Although the reactions may not appear significant on the time scale of the OTIS solute-transport model, when integrated through time by the continuous flow of the streams, the total amount of metal transferred from the water column to the streambed by removal reactions can be large. Using data from the OTIS model for the upper Animas River, Howardsville to Silverton reach, we can calculate the magnitude of daily metal removal. For instance, the difference in zinc concentrations between the conservative and reactive OTIS models at the downstream end of the upper Animas River, Howardsville to Silverton study reach was 0.15 mg/L (fig. 24). This

**Table 12.** Damkohler number ( $D_n$ ) for upper Animas River OTIS solute-transport study reaches that have first-order removal coefficients.

[Leaders (--), model reaches and constituents not having a first-order removal coefficient ( $\lambda$ )]

Model reach number	Copper	Iron	Zinc
Upper Cement Creek			
1	3.9	130	0.15
2	12	400	0.46
3	2.1	72	0.69
10	--	1.2	--
11	--	0.06	--
12	--	0.08	--
14	--	0.49	--
15	--	0.74	--
Lower Cement Creek			
3	0.2	0.22	--
7	0.12	0.16	0.01
8	--	0.02	0.06
9	0.04	0.02	--
10	0.03	0.03	--
11	--	0.25	--
12	--	0.04	0.06
15	--	0.05	--
18	0.03	0.03	0.01
19	0.01	0.005	0.09
22	0.16	0.15	0.23
24	0.16	0.03	0.24
30	0.08	0.13	0.25
Upper Animas River, Eureka to Howardsville			
3	--	--	0.18
5	--	--	0.05
8	--	--	0.17
13	--	--	0.24
Upper Animas River, Howardsville to Silverton			
11	--	--	0.41
13	--	--	0.31

concentration difference represented a load of 29 kg/d removed by instream processes. Kimball and others (this volume) report removal of 17 kg/d zinc in this reach. The difference between the two removal estimates arises from the different calculation methods—Kimball and others (this volume) integrated net decreases in load between each stream site and the next in the Animas River along the entire study reach to estimate the total amount of zinc removed. This method can underestimate load losses, because in some reaches a net gain in load may be the result of a larger gain offset by some loss. The net calculation misses this smaller loss. In contrast, within OTIS, individual model reaches can experience a gain in load through contribution from inflow in the model reach, and a loss in load through implementation of a first-order removal coefficient. The gain in load is recorded at the end of the reach in the conservative simulation. The loss in load and the net change are recorded in the reactive simulation. The difference between the two simulations approximates metal removal through the entire

modeled reach and provides a different estimate of the net loss than the mass-balance calculation used by Kimball and others (this volume). Nevertheless, the estimates of zinc removed throughout the extent of the reach differ only by a factor of 2 between the solute-transport model presented herein and the mass-balance calculations of Kimball and others (this volume) and indicate that, although zinc transport may be considered relatively conservative based on the Damkohler numbers, metal removal is substantial when integrated through time. The amount of metal stored on streambed sediment (Church and others, 1997) is consistent with the results of the OTIS solute-transport simulations.

### Comparison of Remediation Using OTIS and a Mass-Loading Model

A comparison of concentrations resulting from remediation at the end of the OTIS model reaches with concentrations estimated by the same remediation using a mass-loading model is also instructive. The mass-loading calculations were estimated by reducing the load of each remediated inflow by the amount of the hypothetical remediation. The load of each inflow was the load estimated by environmental sampling of the inflow which was different than the load estimated by the OTIS model for those inflow reaches where calibrated lateral-inflow concentrations differed from observed-inflow concentrations. The load at the end of the study reach was reduced by the amount of load reduction caused by remediation of the inflows. The resulting concentration at the end of the study reach was calculated by dividing the resulting load by streamflow.

Differences in concentrations ensuing from remediation estimated using OTIS and using a simple mass-loading model increase with the amount of load reduction caused by remediation (table 13). The mass-loading model estimated a zinc concentration 100 percent greater than the OTIS model in upper Cement Creek, and 23 percent greater than the OTIS model in the upper Animas River, Eureka to Howardsville study reach (table 13). In contrast, in lower Cement Creek and in the upper Animas River, Howardsville to Silverton reach, the mass-loading and OTIS models estimated comparable zinc concentrations at the end of the study reaches (table 13). The differences between the OTIS and mass-loading models arise because (1) lateral-inflow concentrations used for some reaches of the OTIS model were different than ambient (observed) concentrations and (2) first-order removal reactions that occurred downstream from remediation in the OTIS model may change instream concentrations. For constituents where inflow concentrations are representative of the load increase occurring in the stream, and where reactive removal is trivial, there may be no advantage to using OTIS. However, one may need to go through construction of an OTIS model or a detailed loading analysis such as presented in Kimball and others (this volume) before knowing which model will be more applicable and expedient for the situation at hand.

**Table 13.** Summary of maximum simulated reductions in zinc load for all four study areas using OTIS and using a simple mass-loading model.

[Concentration values in milligrams per liter. Mass-loading model remediation estimates used the same percentage reductions and the same inflow sites as used in the OTIS model remediation simulations. Data for the mass-loading calculations from Sole and others (this volume)]

Study reach	Calibrated zinc concentration at downstream end of study reach	Simulated remediated zinc concentration at downstream end of study reach, using maximum remediation possible and OTIS model	Percent reduction (OTIS model versus ambient conditions)	Simulated remediated zinc concentration at downstream end of study reach, using maximum remediation possible and mass-loading model	Percent difference (OTIS model versus mass-loading model)
Upper Cement Creek	4.52	0.83	82	1.69	104
Lower Cement Creek	0.793	0.727	8.3	0.715	2
Upper Animas River, Eureka to Howardsville.	0.295	0.191	35	0.235	23
Upper Animas River, Howardsville to Silverton.	0.417	0.321	23	0.330	3

## Summary and Conclusions

The solute-transport model OTIS was used to simulate ambient conditions in four study reaches in the Animas River watershed study area and to simulate a variety of remediation scenarios for the study reaches. Lateral-inflow concentrations ( $C_L$ ) and first-order removal coefficients ( $\lambda$ ) used in the models were consistent with geochemical conditions observed in the four modeled reaches. Simulations for lower Cement Creek indicated that the model was successful in simulating increases in concentration at the mouth of the stream that have resulted from increased loading from the Mogul mine (# 13) after plugging of the American tunnel (# 96) in 1996. Except for some model reaches in upper Cement Creek, comparison of first-order removal coefficients with travel time indicated that removal reactions do not proceed to completion on the time scale of the OTIS simulations. However, when integrated through time, reactions that remove metal from the water column to the streambed explain observed elevated concentrations of metals in streambed sediment in the Animas River and Cement Creek (Church and others, 1997).

The results of the simulations reemphasize some of the conclusions from the mass-loading analysis (Kimball and others, this volume).

1. Remediation likely will be more successful in reducing instream concentrations of metals where metal loading is dominated by a few large sources.
2. Loading from diffuse seepage and ground-water inflow along some streams sustains and elevates metal concentrations and loads along some stream reaches.
3. In streams where metal concentrations and pH are not extreme, remediation may decrease metal concentrations sufficient to improve water quality and support more aquatic biota.

The largest percent reductions from remediation were achieved where a small number of distinct sources dominated loading for a particular metal, as, for example, in upper Cement Creek, where three mining sources (combined inflow from the Queen Anne and Grand Mogul mines, the Mogul mine, and North Fork Cement Creek) dominated the loading for copper and zinc. Simulation of complete remediation of these three sources achieved 90 and 82 percent reductions in copper and zinc concentrations. In contrast, lower Cement Creek has more distinct and diffuse sources of metal loads, and remediation of three of the larger point sources of mining-related metal loading achieved only 17 and 8.3 percent reduction in copper and zinc loads at the mouth of the creek. In lower Cement Creek, more than 50 percent of the copper and zinc loads were from unsampled ground-water discharge that occurred along the study reach (Kimball and others, this volume; Smith and others, this volume). The model results agree with loading analyses that indicate that remediation will be less effective in streams where ground-water sources of metal loading contribute a significant proportion of the metal loading to the stream.

Loading from diffuse seepage and ground water along the study reaches sustains elevated metal concentrations (and load) along some study reaches. This pattern is evident in the remediation simulations where concentrations increase in some nonremediated model reaches. Examples are copper and zinc concentrations in the Mogul mine to North Fork Cement Creek reach of upper Cement Creek; copper, iron, and zinc concentrations in the reaches just upstream from Prospect Gulch and in the lower bog area in lower Cement Creek; zinc in model reach 13 in the Animas River, Eureka to Howardsville study reach; and zinc in model reaches 8, 10, and 14 in the Animas River, Howardsville to Silverton study reach. Remediation of these reaches is not considered because most of this seepage results from the weathering of exposed hydrothermally altered rock and is not related to mining

activity. However, if some of the seepage were traced to mining activity (such as the presumed ground-water discharge in model reach 12 of the upper Animas River, Howardsville to Silverton OTIS model), remediation is likely to be cost prohibitive considering current (2004) available technologies. Although much of the diffuse seepage contributing to water-quality degradation is likely related to non-mining affected weathering (as opposed to weathering accelerated by mining activities) of acid-generating mineral assemblages, locations of diffuse seepage that may be mining related represent opportunities to explore innovative and emerging treatment technologies such as reactive barriers or sulfate-reducing injection systems (Benner and others, 1999; Saunders and others, 2001).

Streams containing lower initial metal concentrations and higher pH values probably represent the best targets for remediation. In spite of the large percent reductions simulated by the most extensive hypothetical remediation in upper Cement Creek, the simulated post-remediation zinc concentration was still much greater than concentrations that were simulated with remediation in both Animas River study reaches. In the upper Animas River, the simulated post-remediation concentrations approached concentrations that might promote improvement in conditions for aquatic life. Therefore, remediation seems more likely to improve the aquatic ecosystem in streams like the Animas River, than in streams that initially contain low pH and high metal concentrations such as Cement Creek. The pH and metal concentrations in Cement Creek, however, represent challenges that can be studied to increase our understanding of the natural processes that operate in such systems, and the limits of remediation in watersheds where non-mining affected weathering of acid-generating mineral assemblages degrades water quality.

## References Cited

- Allison, J.D., Brown, D.S., and Novo-Gradac, K.J., 1991, MINTEQA2/PRODEFA2, A geochemical assessment model for environmental systems; Version 3.0 User's Manual: U.S. Environmental Protection Agency Report EPA/600/3-91/021.
- Bahr, J.M., and Rubin, Jacob, 1987, Direct comparison of kinetic and local equilibrium formulations for solute transport affected by surface reactions: *Water Resources Research*, v. 23, p. 438–452.
- Ball, J.D., and Nordstrom, D.K., 1991, User's manual for WATEQ4F, with revised thermodynamic data base and test cases for calculating speciation of major, trace, and redox elements in natural waters: U.S. Geological Survey Open-File Report 91-183, 192 p.
- Bencala, K.E., and McKnight, D.M., 1987, Identifying in-stream variability—Sampling iron in an acidic stream, *in* Averett, R.C., and McKnight, D.M., eds., *Chemical quality of water and the hydrologic cycle*: Chelsea, Mich., Lewis Publishers, Inc., p. 255–269.
- Benner, S.G., Blowes, D.W., Gould, W.D., Herbert, R.B., Jr., and Ptacek, C.J., 1999, Geochemistry of a permeable reactive barrier for metals and acid mine drainage: *Environmental Science and Technology*, v. 22, p. 2793–2799.
- Blair, R.W., Jr., Yager, D.B., and Church, S.E., 2002, Surficial geologic maps along the riparian zone of the Animas River and its headwater tributaries, Silverton to Durango, Colorado with upper Animas River watershed gradient profiles: U.S. Geological Survey Digital Data Series, DDS-71. One CD-ROM.
- Broshears, R.E., Bencala, K.E., Kimball, B.A., and McKnight, D.M., 1993, Tracer-dilution experiments and solute-transport simulations for a mountain stream, Saint Kevin Gulch, Colorado: U.S. Geological Survey Water-Resources Investigations Report 92-4081, 18 p.
- Church, S.E., Kimball, B.A., Fey, D.L., Ferderer, D.A., Yager, T.J., and Vaughn, R.B., 1997, Source, transport, and partitioning of metals between water, colloids, and bed sediments of the Animas River, Colorado: U.S. Geological Survey Open-File Report 97-151, 135 p.
- Crawford, C.G., Slack, J.R., and Hirsch, R.M., 1983, Non-parametric tests for trends in water-quality data using the statistical analysis system: U.S. Geological Survey Open-File Report 83-550, p. 11–12.
- Crowfoot, R.W., Boulger, R.W., and O'Neill, G.B., 2002, Water resources data water year 2001—Volume 2, Colorado River basin: U.S. Geological Survey Water-Data Report CO-01-2, 559 p.
- Crowfoot, R.W., Bruce, N.L., Unruh, J.W., Steinheimer, J.T., Ritz, G.F., Smith, M.E., Jenkins, R.A., and O'Neill, G.B., 1999, Water resources data water year 1998—Volume 2, Colorado River basin: U.S. Geological Survey Water-Data Report CO-98-2, 569 p.
- Crowfoot, R.W., Paillet, A.W., Ritz, G.F., Smith, M.E., Jenkins, R.A., and O'Neill, G.B., 1997, Water resources data water year 1996—Volume 2, Colorado River basin: U.S. Geological Survey Water-Data Report CO-96-2, 551 p.

- Crowfoot, R.W., Paillet, A.W., Ritz, G.F., Smith, M.E., Jenkins, R.A., and O'Neill, G.B., 1998, Water resources data water year 1997—Volume 2, Colorado River basin: U.S. Geological Survey Water-Data Report CO-97-2, 565 p.
- Crowfoot, R.W., Unruh, J.W., Boulger, R.W., and O'Neill, G.B., 2001, Water resources data water year 2000—Volume 2, Colorado River basin: U.S. Geological Survey Water-Data Report CO-00-2, 596 p.
- Crowfoot, R.W., Unruh, J.W., Ritz, G.F., Boulger, R.W., and O'Neill, G.B., 2000, Water resources data water year 1999—Volume 2, Colorado River basin: U.S. Geological Survey Water-Data Report CO-99-2, 492 p.
- Desborough, G.A., Leinz, Reinhard, Sutley, Stephen, Briggs, Paul, Swayze, P.A., Smith, K.S., and Breit, George, 2000, Leaching studies of schwertmannite-rich precipitates from the Animas River headwaters, Colorado, and Boulder River headwaters, Montana: U.S. Geological Survey Open-File Report 00-004, 16 p.
- Harvey, J.W., and Fuller, C.C., 1998, Effect of enhanced manganese oxidation in the hyporheic zone on basin-scale geochemical mass balance: *Water Resources Research*, v. 34, p. 623–636.
- Kilpatrick, F.A., and Cobb, E.D., 1985, Measurement of discharge using tracers: U.S. Geological Survey Techniques of Water-Resources Investigations Book 3, Chapter A16, 52 p.
- Kimball, B.A., Runkel, R.L., Walton-Day, Katherine, and Bencala, K.E., 2002, Assessment of metal loads in watersheds affected by acid mine drainage by using tracer injection and synoptic sampling; Cement Creek, Colorado, U.S.A.: *Applied Geochemistry*, v. 17, p. 1183–1207.
- Kimball, B.A., 1997, Use of tracer injections and synoptic sampling to measure metal loading from acid mine drainage: U.S. Geological Survey Fact Sheet FS-245-96, 4 p.
- Kimball, B.A., Broshears, R.E., Bencala, K.E., and McKnight, D.M., 1994, Coupling of hydrologic transport and chemical reactions in a stream affected by acid mine drainage: *Environment Science and Technology*, v. 28, p. 2065–2073.
- Leib, K.J., Mast, M.A., and Wright, W.G., 2003, Using water-quality profiles to characterize seasonal water quality and loading in the upper Animas River basin, southwestern Colorado: U.S. Geological Survey Water-Resources Investigations Report 02-4230, 43 p.
- Mast, M.A., Evans, J.B., Leib, K.J., and Wright, W.G., 2000, Hydrologic and water-quality data at selected sites in the upper Animas River watershed, Southwestern Colorado, 1997–99: U.S. Geological Survey Open-File Report 00-53, 20 p. plus Appendix and 1 plate.
- Paschke, S.S., Kimball, B.A., and Runkel, R.L., 2005, Quantification and simulation of metal loading to the upper Animas River, Eureka to Silverton, San Juan County, Colorado, September 1997 and August 1998: U.S. Geological Survey Scientific Investigations Report 2005-5054, 82 p.
- Runkel, R.L., 1998, One-dimensional transport with inflow and storage (OTIS)—A solute transport model for streams and rivers: U.S. Geological Survey Water-Resources Investigations Report 98-4018, 73 p. At URL <http://co.water.usgs.gov/otis>.
- Runkel, R.L., and Kimball, B.A., 2002, Evaluating remedial alternatives for an acid mine drainage stream—Application of a reactive transport model: *Environmental Science and Technology*, v. 36, p. 1093–1101.
- Saunders, J.A., Lee, M.K., Whitmer, J.M., and Thomas, R.C., 2001, In situ bioremediation of metals-contaminated groundwater using sulfate-reducing bacteria—A case history, *in* Leeson, A., Peyton, B.M., Means, J.L., and Magar, V.S., eds., *Bioremediation of inorganic compounds*, v. 6, no. 9: Battelle Press, p. 105–112.
- Walton-Day, Katherine, Runkel, R.L., Kimball, B.A., and Bencala, K.E., 1999, Application of the solute-transport models OTIS and OTEQ and implications for remediation in a watershed affected by acid mine drainage, Cement Creek, Animas River Basin, Colorado, *in* Morganwalp, D.W., and Buxton, H.T., eds., U.S. Geological Survey Toxic Substances Hydrology Program—Proceedings of the technical meeting, Charleston, South Carolina, March 8–12, 1999—Volume 1 of 3, Contamination from hardrock mining: U.S. Geological Survey Water-Resources Investigations Report 99-4018A, p. 37–46.
- Wirt, Laurie, Leib, K.J., Melick, Roger, and Bove, D.J., 2001, Metal loading assessment of a small mountainous sub-basin characterized by acid drainage—Prospect Gulch, Upper Animas River watershed, Colorado: U.S. Geological Survey Open-File Report 01-0258, online version 1.1, 36 p. URL <http://pubs.usgs.gov/of/2001/ofr-01-0258/>.
- Zellweger, G.W., Bencala, K.E., McKnight, D.M., Hirsch, R.M., and Kimball, B.A., 1988, Practical aspects of tracer experiments in acidic, metal enriched streams, *in* Mallard, G.E., ed., U.S. Geological Survey Toxic Substances Hydrology Program—Surface-Water Contamination—Proceedings of the technical meeting, Denver, Colo., February 2–4, 1987: U.S. Geological Survey Open-File Report 87-764, p. 125–130.

## Appendix. Calibration of the Solute-Transport Model OTIS

Calibration of the solute transport model OTIS involved three steps:

- Determination of physical parameters
- Model calibration for conservative solutes
- Model calibration for reactive solutes.

The preceding text provided a general overview of how to accomplish these steps. This appendix provides step-by-step details of model construction and calibration for the interested reader.

### Determination of Physical Parameters

Steps 1a through 1e (fig. 26) were used to determine physical parameters (dispersion ( $D$ ) and stream cross-sectional area ( $A$ )) for OTIS unless otherwise noted in the chapter. First, the average concentration value of samples collected during the plateau period (fig. 2) was calculated to represent the plateau concentrations (step 1a, fig. 26). Streamflow ( $Q$ , step 1b, fig. 26) at each transport site was calculated by dividing the constant and known mass flux of the injected tracer by the plateau concentration of the tracer at a transport site (Kimball and others, this volume). Arrival time ( $t_{50}$ ) at a site (step 1c, fig. 26) is defined as the time at which the instream tracer concentration reaches one-half of the plateau concentration ( $C_{50}$ ) (Zellweger and others, 1988). Travel time ( $t_t$ ) between two sites is simply the difference in arrival times between two transport sites (fig. 2). Stream cross-sectional area ( $A$ ) (step 1d, fig. 26) was initially calculated from:

$$A = \frac{\text{streamflow}}{\text{velocity}} = \frac{(Q_i + Q_{i-1})/2}{(x_i - x_{i-1})/t_t} \quad (7)$$

where

$Q_i$  and  $Q_{i-1}$  are streamflow ( $\text{m}^3/\text{s}$ ) between two transport sites

and

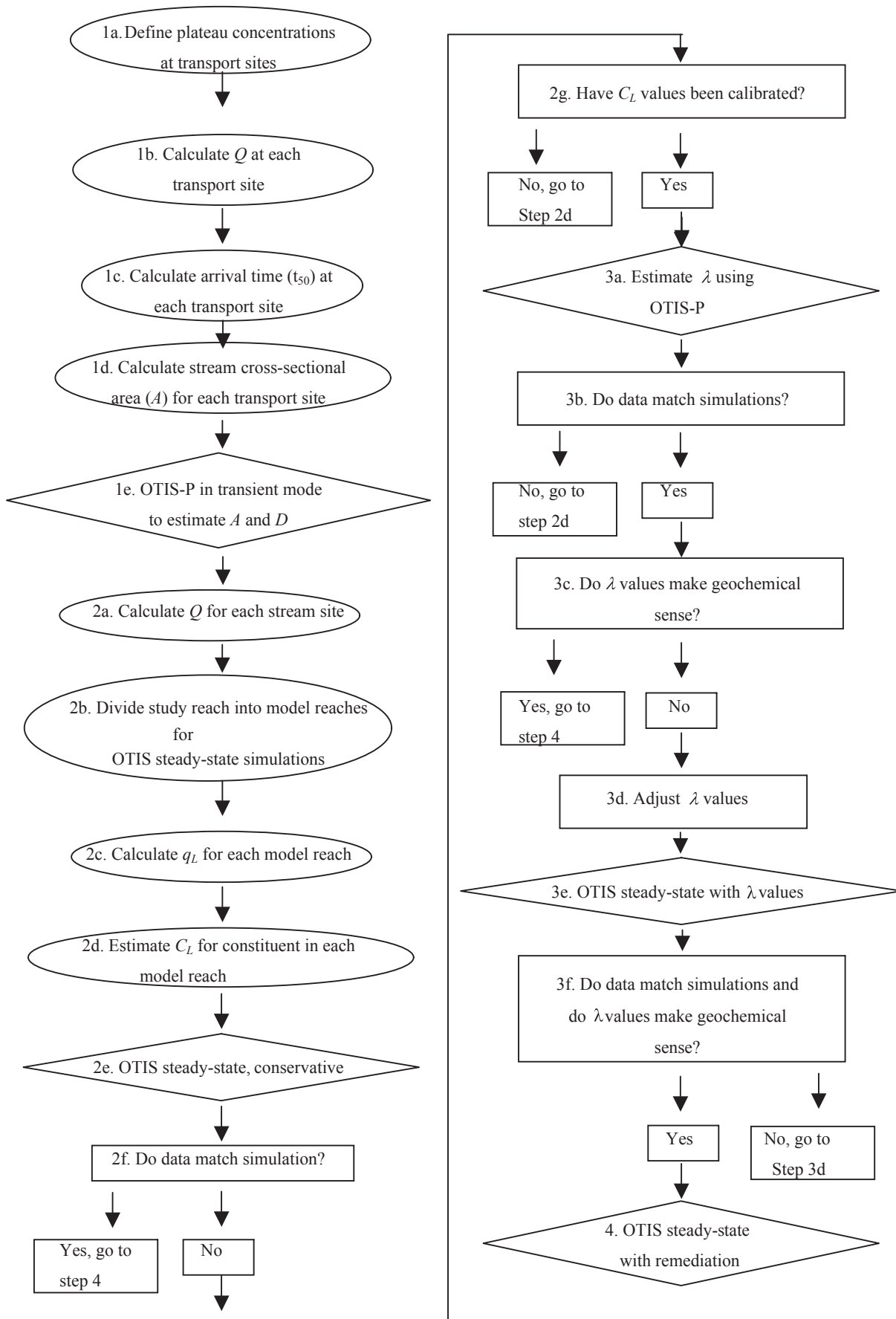
$x_i$  and  $x_{i-1}$  are the distances (m) of the transport sites downstream from an arbitrary stream reference point.

This initial estimate of stream cross-sectional area was later refined using OTIS-P (step 1e, fig. 26). The remaining parameter (dispersion ( $D$ )) needed to simulate ambient conditions at each transport site was adjusted to obtain a best-fit of simulated conditions to the data using the model OTIS-P in transient mode (step 1e, fig. 26). Once the physical parameters were determined, the next step was to calibrate the model in hydrological steady-state (where streamflow and constituent concentration are constant at each site through time) for each constituent of interest using data from the synoptic sampling (steps 2a–3f, fig. 26). There were two types of calibration: one for conservative constituents (steps 2a–2g, fig. 26), and one for reactive constituents (steps 2a–3f, fig. 26).

### Model Calibration for Conservative Solutes

The first step in model calibration for conservative solutes was to use OTIS to simulate the tracer concentration to verify that the simulation matched the data and that lateral-inflow values ( $q_L$ ) were correct. To accomplish this task (step 2a, fig. 26), the streamflow was calculated for each stream site using the tracer concentrations measured in the synoptic sample collected at each site. This process can be somewhat involved, and is described in detail in Kimball and others (this volume). But, briefly, streamflow at each site was calculated by dividing the constant and known mass flux of the injected tracer by the concentration of tracer in the synoptic sample, after first adjusting for ambient concentration of the tracer. Next (step 2b, fig. 26), the study reach was divided into subreaches (known as model reaches) chosen on the basis of knowledge of the major physical and chemical inflows to the stream derived from the loading calculations (Kimball and others, this volume). Model reaches were chosen to bracket the major surface- and groundwater inflows to the stream, including locations of mine drainage such as inflow from adits or tributaries. An effort was made to minimize the total number of model reaches to expedite parameter estimation and model computation times but still have a sufficient number of model reaches to accommodate the variations in constituent profiles. Lateral inflow ( $q_L$ ) was then calculated for each model reach (step 2c, fig. 26). Lateral inflow ( $q_L$ ) has units of  $\text{m}^2/\text{s}$ , and was calculated as the difference in flow between the downstream ends of adjacent model reaches divided by the distance between the downstream ends of the model reaches. Lateral inflow ( $q_L$ ) does not have units of volume per time as expected for a variable that relates to flow, but rather units of area per time because the inflow is distributed along the length of a model reach.

Next, preliminary estimates of lateral-inflow concentrations ( $C_L$ ) were made for each model reach (step 2d, fig. 26). For some tracers (such as lithium and bromide), these concentrations typically were negligible. For other tracers (such as sodium and chloride) and other constituents, several methods were used to assign lateral-inflow concentrations ( $C_L$ ). If there was no gain in flow or load along a model reach, the lateral-inflow concentration ( $C_L$ ) and the lateral inflow ( $q_L$ ) used in the model were zero. For model reaches that contained inflow, three potential situations exist: (1) No visible inflows were observed or no inflow samples were collected. (2) The model reach contained one sampled inflow. (3) The model reach contained several sampled inflows. In case (1), inflow concentrations from an adjacent model reach can be used, or an effective inflow concentration, that was calculated from the change in load observed along the model reach, was used (equation 2). Effective inflow concentration may actually be lower than an actual inflow concentration because the calculated effective inflow concentration incorporates reactions that may have occurred between the two sites and removed solute from the water column.



In case (2), the chemistry of the sampled inflow was used as a first estimate for lateral-inflow concentration ( $C_L$ ). In case (3), the flow-weighted average value of inflow concentrations or the value from one of the inflows judged to be most representative of the inflows in that model reach was used as a first estimate for lateral-inflow concentration ( $C_L$ ).

After the model is constructed and constituent profiles produced by the model are examined (step 2e, fig. 26), first estimates of lateral-inflow concentration ( $C_L$ ) may not produce a simulation that fits the measured data (answer to step 2f is “no”). At this point two potential actions exist: lateral-inflow concentrations ( $C_L$ ) either have or have not been calibrated. If lateral-inflow concentrations ( $C_L$ ) have been calibrated, then move to step 3a (fig. 26) to begin estimation of first-order removal coefficients ( $\lambda$ ). If lateral-inflow concentrations have not been calibrated, then calibration proceeds as follows. Calibration of lateral-inflow concentrations ( $C_L$ ) uses an iterative approach (steps 2d–2g, fig. 26) wherein representative concentrations are used as the initial values for lateral-inflow concentrations ( $C_L$ ). Starting from the upstream end of the study section and working in a downstream direction, if the change in load within a model reach is underestimated using the representative concentration, then effective inflow concentration (equation 2) is used to attempt to increase the change in load. In some cases, a value less than the effective inflow concentration was used if the effective inflow concentration seemed much greater than sampled inflow concentrations. This procedure was continued for each model reach working in a downstream direction until the simulation either generally fit the observed data (conservative solute) or yielded greater concentrations than the observed data (reactive solute) at which point the lateral-inflow concentrations ( $C_L$ ) have been calibrated. Then, in the case of a reactive solute, the answer to step 2f (fig. 26) is “no” (the simulation does not fit the data), but the answer to step 2g (fig. 26) is “yes” (lateral-inflow concentrations ( $C_L$ ) have been calibrated), and the next step is to estimate first-order removal coefficients ( $\lambda$ ).

## Model Calibration for Reactive Solutes

Calibration of the model for reactive solutes requires all of the previous steps noted for conservative solutes (steps 2a–2g, fig. 26). The distinction between conservative and reactive solutes becomes important during calibration of lateral-inflow concentration ( $C_L$ ). For a conservative solute, when appropriate lateral-inflow concentrations ( $C_L$ ) have been chosen, the simulation matches the data. For a reactive solute, the simulation will overestimate the data. To use lateral-inflow concentrations ( $C_L$ ) that cause the simulations to overestimate

the data seems somewhat counterintuitive. However, during the iterative process used in steps 2d–2g (fig. 26), it sometimes becomes apparent that the elevated lateral-inflow concentrations ( $C_L$ ) needed to match large, incremental increases in stream concentration in some model reaches must be offset by removal in downstream model reaches where all possible choices for lateral-inflow concentrations ( $C_L$ ) (sometimes including  $C_L = 0$ ) result in simulations that overestimate the observed data.

First-order removal coefficients ( $\lambda$ ) are used to offset the large concentration increases in certain model reaches. First-order removal coefficients ( $\lambda$ ) are estimated using OTIS-P (step 3a, fig. 26) (Runkel, 1998). Simulations resulting from initial estimates of first-order removal coefficients ( $\lambda$ ) were compared to the data. Generally, good agreement between simulations and data was quickly obtained. However, an examination of the distribution of first-order removal coefficients ( $\lambda$ ) is instructive in light of the general geochemistry of the stream and coincident behavior of other solutes. For example, if first-order removal coefficients ( $\lambda$ ) are large in one model reach for zinc only, and pH values are not sufficiently high to indicate removal of zinc by formation of zinc minerals, then a likely mechanism for zinc removal is sorption to or coprecipitation with iron or manganese minerals. However, if there is no first-order removal coefficient ( $\lambda$ ) for iron or manganese in that model reach, then the removal of zinc may need to be transferred to an adjacent or nearby model reach where iron or manganese removal is occurring. Therefore, if the estimated first-order removal coefficients ( $\lambda$ ) do not relate to the geochemistry of the stream, then an iterative approach is recommended for determining first-order removal coefficients ( $\lambda$ ) whereby the values are adjusted model reach by model reach moving in a downstream direction (fig. 26, steps 3b–3f). Generally, first-order removal coefficients ( $\lambda$ ) for iron and (or) manganese are estimated first. Then solutes that might sorb to or coprecipitate with iron or manganese, such as copper or zinc, are estimated so that the resulting model simulates their removal in reaches having favorable geochemical conditions (that is, coincident removal of either iron or manganese).

## Physical Parameters for OTIS Models

In the upper Cement Creek study reach, a dispersion coefficient of 0.6 was used for the simulations. Values for stream cross-sectional area ( $A$ ) were calculated from the time-variant tracer data collected at sites T1 (501 m), T2 (2,885 m), and T3 (3,844 m) as previously described (fig. 2). The change in cross-sectional area between T1 and T2 was large. Therefore, cross-sectional area for model reaches between the two sites was calculated dividing the average velocity of T1 and T2 into the streamflow value determined using the tracer for the site at the end of each model reach. The cross-sectional area for T3 was used for all modeled reaches between T2 and T3, and downstream from T3. Values of  $A$ ,  $D$ , and  $q_L$  are shown in table 14. Physical parameters used for the OTIS models for lower Cement Creek are in table 15.

**Figure 26 (facing page).** Actions necessary to calibrate OTIS solute transport model.  $Q$ , streamflow;  $D$ , dispersion coefficient;  $q_L$ , lateral inflow;  $C_L$ , lateral-inflow concentration;  $\lambda$ , first-order removal coefficient. Oval shapes indicate actions or calculations. Diamond shapes indicate execution of the OTIS or OTIS-P model. Rectangular shapes indicate decision points.

**Table 14.** Model reaches, reach lengths, and hydraulic parameters for upper Cement Creek OTIS simulations.

[m, meters; m<sup>2</sup>, square meters; m<sup>2</sup>/s, square meters per second; m<sup>3</sup>/s-m, cubic meters per second per meter]

Model reach number	Distance from injection site (m)	Model reach length (m)	Dispersion coefficient (D) (m <sup>2</sup> /s)	Stream cross-sectional area (A) (m <sup>2</sup> )	Lateral inflow (q <sub>L</sub> ) (m <sup>3</sup> /s-m)
1	41	41	0.6	0.195	0.00
2	259	218	0.6	0.195	3.25×10 <sup>-5</sup>
3	345	86	0.6	0.195	2.24×10 <sup>-4</sup>
4	827	482	0.6	0.198	6.91×10 <sup>-6</sup>
5	927	100	0.6	0.199	2.99×10 <sup>-6</sup>
6	1,142	215	0.6	0.212	1.17×10 <sup>-5</sup>
7	1,292	150	0.6	0.231	2.46×10 <sup>-5</sup>
8	1,315	23	0.6	0.27	3.31×10 <sup>-4</sup>
9	1,367	52	0.6	0.314	1.64×10 <sup>-4</sup>
10	2,885	1,518	0.6	0.437	1.69×10 <sup>-5</sup>
11	2,976	91	0.6	0.455	2.21×10 <sup>-5</sup>
12	3,107	131	0.6	0.455	5.15×10 <sup>-5</sup>
13	3,844	737	0.6	0.455	7.78×10 <sup>-6</sup>
14	3,931	87	0.6	0.455	5.24×10 <sup>-4</sup>
15	4,200	269	0.6	0.455	5.67×10 <sup>-4</sup>

**Table 15.** Model reaches, reach lengths, and hydraulic parameters for lower Cement Creek OTIS simulations.

[m, meters; m<sup>2</sup>, square meters; m<sup>2</sup>/s, square meters per second; m<sup>3</sup>/s-m, cubic meters per second per meter]

Model reach number	Distance from arbitrary datum (m)	Model reach length (m)	Dispersion coefficient (D) (m <sup>2</sup> /s)	Stream cross-sectional area (A) (m <sup>2</sup> )	Lateral inflow (q <sub>L</sub> ) (m <sup>3</sup> /s-m)
1	1,050	58	1.0	0.212	0.00
2	1,106	56	1.0	0.301	2.63×10 <sup>-3</sup>
3	2,425	1,319	1.0	0.620	1.11×10 <sup>-5</sup>
4	2,785	360	1.0	0.620	7.28×10 <sup>-5</sup>
5	2,970	185	1.0	0.620	5.23×10 <sup>-5</sup>
6	3,125	155	1.0	0.620	1.27×10 <sup>-4</sup>
7	3,317	192	1.0	0.620	1.07×10 <sup>-4</sup>
8	3,655	338	1.0	0.620	3.43×10 <sup>-5</sup>
9	3,893	238	1.0	0.827	8.14×10 <sup>-5</sup>
10	4,260	367	1.0	0.827	1.92×10 <sup>-5</sup>
11	4,483	223	1.0	0.827	0.00
12	4,586	103	1.0	0.827	1.47×10 <sup>-4</sup>
13	5,050	464	1.0	0.827	6.55×10 <sup>-5</sup>
14	5,215	165	1.0	0.827	2.92×10 <sup>-5</sup>
15	5,365	150	1.0	0.827	1.02×10 <sup>-4</sup>
16	5,652	287	1.0	0.827	9.93×10 <sup>-5</sup>
17	5,767	115	1.0	0.827	1.68×10 <sup>-4</sup>
18	5,897	130	1.0	1.051	1.07×10 <sup>-4</sup>
19	5,957	60	1.0	1.051	3.78×10 <sup>-4</sup>
20	6,447	490	1.0	1.051	5.13×10 <sup>-5</sup>
21	6,907	460	1.0	1.051	6.09×10 <sup>-5</sup>
22	7,131	224	1.0	1.051	2.33×10 <sup>-4</sup>
23	7,331	200	1.0	1.051	4.26×10 <sup>-5</sup>
24	7,501	170	1.0	1.051	3.67×10 <sup>-5</sup>
25	7,698	197	1.0	1.277	6.55×10 <sup>-5</sup>
26	9,060	1,362	1.0	1.277	3.11×10 <sup>-5</sup>
27	9,360	300	1.0	1.277	4.00×10 <sup>-5</sup>
28	9,905	545	1.0	1.277	6.79×10 <sup>-5</sup>
29	10,130	225	1.0	1.277	0.00
30	11,743	1,613	1.0	1.277	1.26×10 <sup>-5</sup>